Stability of Mixed Finite Element Methods with Anisotropic Meshes

by

Randrianarivony H. Maharavo.

Master's Thesis

Presented to the Mathematics Faculty of
the Technische Universität Chemnitz in
Partial Fulfillment of the Requirements for the Degree
Master of Science.
Advisor: Dr. Thomas Apel.

TECHNISCHE UNIVERSITÄT CHEMNITZ
April 30, 2001

ABSTRACT

The investigation of element pairs features one of the main difficulties in the finite element analysis of mixed problems. In this document, the stability of various well known finite element pairs is taken into consideration with special emphasis in anisotropic meshes. The model problem describes the incompressible Stokes equation which is frequently met in numerical flow analysis. The most important theoretical tool that will be used is the macroelement technique which will be detailed precisely. A couple of macroelement approaches are proved and formulated in a succinct fashion which facilitates their subsequent use. Outcomes from numerical tests which analyze different anisotropic meshes are also reported in order to confirm the theoretical results. Some counterexamples provide the evidence of pairs which are isotropically stable but which become unstable in anisotropic discretizations.

ACKNOWLEDGMENTS

I would like to express my sincere thanks to Prof. Tröltzsch who has helped me, in various ways, to pursue my studies at the Technische Universität Chemnitz.

I have been feeling also fortunate to have the helps of Dr. Apel who has assisted me to overcome many hardships. Moreover, I especially thank him for having reviewed this document and for his special remarks and corrections which have really improved it.

Furthermore, I would like to thank the staff of the mathematics faculty for having made it a special place to acquire valuable knowledges.

Last, but definitely not the least, I am indebted to the mathematics computing center for having let me access its computing materials which have allowed me to perform all the numerical tests and to type this document.

Contents

Important notations:

1. The following notations concern the domain:

Ω	:	it is a bounded open simply connected subset of $\mathbf{R}^d$ whose properties are specified in each section
$\Gamma = \partial\Omega$	:	it is the boundary of Ω
d	:	dimension of Ω, $d = 2$ or $d = 3$
T	:	a finite element
K	:	a macroelement composed of finite elements.

2. The following ones deal with polynomials:

$\mathcal{P}_k$	:	set of all polynomials $p(x,y) = \sum_{0\leq i+j\leq k} a_{ij}x^i y^j$
$\mathcal{Q}_k$	:	set of all polynomials $p(x,y) = \sum_{0\leq i,j\leq k} a_{ij}x^i y^j$
$\mathcal{Q}_{r,s}$	:	set of all polynomials $p(x,y) = \sum_{\substack{0\leq i\leq r \\ 0\leq j\leq s}} a_{ij}x^i y^j$
λ_i	:	the i-th barycentric coordinate with respect to the apices of a given triangle $(\mathbf{a}_1, \mathbf{a}_2, \mathbf{a}_3)$ and which is given by $\lambda_i \in \mathcal{P}_1$ and $\lambda_i(\mathbf{a}_j) = \delta_{ij}$

3. The following ones deal with function spaces:

$\mathcal{C}(\Omega)$	:	set of all continuous functions in Ω
$L^2(\Omega)$	:	set of all square integrable functions in Ω
$L^2_0(\Omega)$	:	set of functions in $L^2(\Omega)$ whose integrals are vanishing
$H^1(\Omega)$	:	the Sobolev space of order one which is the space of all square integrable functions f such that $\|f\|_{1,\Omega} < \infty$
$H^1_0(\Omega)$	:	set of all functions in $H^1(\Omega)$ with vanishing boundary trace
$H^{\frac{1}{2}}(\Gamma)$	:	set of all functions in $L^2(\Gamma)$ that are boundary values of functions in $H^1(\Omega)$
$H^{-1}(\Omega)$	:	the dual space of $H^1_0(\Omega)$
$H^{\frac{1}{2}}_{00}(\Gamma_i)$	:	set of functions in $H^{\frac{1}{2}}(\Gamma_i)$ whose zero extensions to all Γ belong to $H^{\frac{1}{2}}(\Gamma)$.

4. The following ones are for general purpose:

X^*	:	the dual of X
$X^\perp$	:	the orthogonal complement of X
X^o	:	the polar of X
Ran (A)	:	the range of the operator A
ker (A)	:	the kernel of the operator A

5. The following ones concern norms, seminorms and scalar products:

$$
\begin{array}{lcl}
\|f\|^2_{0,X} & = & \int_X |f(\mathbf{x})|^2 d\mathbf{x} \\
\|f\|^2_{1,X} & = & \|f\|^2_{0,X} + \sum_{i=1,\ldots,d} \|\frac{\partial f}{\partial x_i}\|^2_{0,X} \\
|f|^2_{1,X} & = & \sum_{i=1,\ldots,d} \|\frac{\partial f}{\partial x_i}\|^2_{0,X} \\
\|f\|_{\frac{1}{2},\Gamma} & = & \inf\{\|g\|_{1,\Omega} : g \in H^1(\Omega),\, g|_\Gamma = f\} \\
\|v\|^2_{\frac{1}{2},00,\Gamma_i} & = & \|v\|^2_{\frac{1}{2},\Gamma_i} + \int_{\Gamma_i} \frac{|v|^2}{\rho} ds \\
(\cdot,\cdot)_{0,\Omega} & = & \text{scalar product in } L^2(\Omega) \\
<\cdot,\cdot>_{\mathbf{R}^N} & = & \text{scalar product in } \mathbf{R}^N
\end{array}
$$

Chapter 1

Introduction

1.1 Preliminary ideas

The analyses and applications of anisotropic grids have developed tremendously since the eighties and they are still in the range of ongoing research topics nowadays (see for example [Ape99], [SSS97]), [ANS99], [Kun97], [ANS00]). In this preliminary chapter, we are going to introduce what an anisotropic mesh is. To that end, we recall briefly the concept of the classical finite element partitioning. We will see afterwards that anisotropic meshes are very useful in various flow simulations and mechanical problems. We will see also in this introductory chapter many interesting properties which are useful both in the theoretical and in the numerical viewpoints. Before going any further, it should be noticed that the goal of this document is not at all to simulate mechanical problems, but rather to analyze in a rigorous fashion the stability of several element pairs in anisotropic grids.

1.1.1 Recall of a standard FE-mesh

Let Ω be a bounded polygonal (resp. polyhedral) domain of $\mathbf{R}^2$ (resp. $\mathbf{R}^3$). A discretization $\mathcal{T}_h$ of Ω is called admissible if the following four conditions are fulfilled:

(C0) $\overline{\Omega}$ is the union of all closures of the elements of $\mathcal{T}_h$, i. e.

$$\overline{\Omega} = \bigcup_{T \in \mathcal{T}_h} \overline{T}. \tag{1.1}$$

(C1) The elements of $\mathcal{T}_h$ are disjoint, i. e.

$$T_i \cap T_j = \emptyset \quad \text{for two distinct elements } T_i,\, T_j \in \mathcal{T}_h. \tag{1.2}$$

(C2) Every edge (resp. face) of any element $T_i \in \mathcal{T}_h$ is *either* a part of the boundary $\partial\Omega$ *or* an edge (resp. a face) of another element T_j of $\mathcal{T}_h$.

(C3) If for any $T \in \mathcal{T}_h$, we define:

$$\begin{aligned} h(T) &:= \operatorname{diam}(T) = \max\{\|\mathbf{x}-\mathbf{y}\|_{\mathbf{R}^d},\, \mathbf{x},\mathbf{y} \in T\} \\ \rho(T) &:= \text{supremum of the diameters of all balls contained in } T \\ \sigma(T) &:= h(T)/\rho(T), \end{aligned}$$

then the classical FE-theory requires that there is a constant $\kappa > 0$ such that :

$$\sigma(T) \leq \kappa \quad \forall\, T \in \mathcal{T}_h, \tag{1.3}$$

where κ is independent of the chosen T and h.

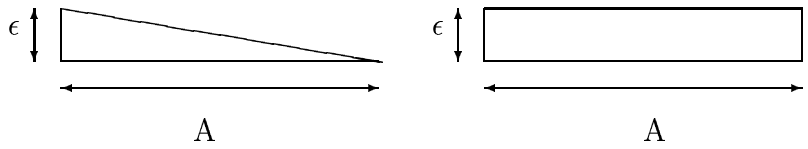

Figure 1.1: Very thin triangle and rectangle.

Roughly speaking, condition (C3) means that very thin triangles or rectangles (i. e. one edge is very long compared with another) are not allowed to belong to the mesh $\mathcal{T}_h$; in Figure 1.1, we can see a graphical illustration of such thin triangular or rectangular elements which can become anisotropic if $\epsilon \ll A$.

Unless otherwise stated, the quantity $\sigma(T)$ will be the aspect ratio of the element T. And the aspect ratio of the mesh $\mathcal{T}_h$ is the maximum of all $\sigma(T)$ i. e.

$$\sigma_h = \max_{T \in \mathcal{T}_h} \sigma(T).$$

1.1.2 Anisotropic FE-discretizations and some applications

An anisotropic FE-discretization still satisfies the previous conditions (C0), (C1) and (C2), but the condition (C3) is not any more required. In other

words, very stretched triangles like in Figure 1.1 can be present in the mesh.

In some mechanical or physical phenomena, some variable is varying significantly in one direction (for example in x-direction) compared with the variation in the other directions. That can be found for example in flows presenting boundary layers which are very well known in fluid mechanics. A boundary layer is an extremely thin region next to the boundary of a domain in which the value of the solution is increasing considerably. Such discussions can be found for example in [Zdr97]. Simulations of such problems invoke the use of anisotropic grids because the solution only changes significantly in one direction where we need a very fine discretization. And for the other directions, since the variation of the solution is comparatively very small, we can let the mesh be very stretched. The layers can sometimes also be located within the domain (not necessarily in the boundary), we have therefore the so-called internal layers. Such problems are certainly very appropriate to anisotropic meshes for the same reasons.

An illustration is the simulation of fluid flows past an airfoil (scientific word for the wing of an airplane) with very high Reynold number. There, a very thin domain in the proximity of the airfoil suffers from a very high variation of the solution. The phenomenon is predicted by the fact that the higher the Reynold number is, the thinner the layer is and also the more stretched the grid must be. We need therefore an anisotropic mesh in this case. For more information about engineering viewpoints of the application of anisotropic mesh in high Reynold number flow, we can read [Mav97]. We can think of still using standard FEM in such problems by refining the mesh in all directions but that would surely be very computationally expensive. For example imagine a refinement of magnitude 10^{-6} in all directions, then we would end up at a large number of grid points in order to treat isotropically problems having layers.

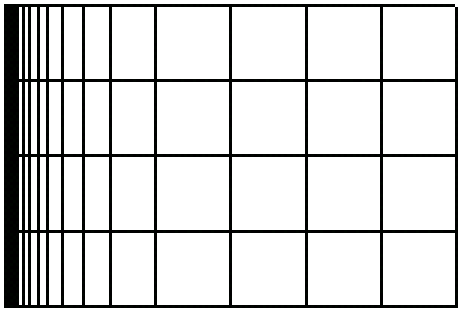

Figure 1.2: An example of anisotropic mesh for boundary layers.

As a simple graphical illustration, we can find in Figure 1.2 a discretization of a rectangle for problems having layers in the left boundary of the domain. As a matter of fact, we are in a situation of having a mesh refinement toward the left boundary. We can see clearly the presence of stretched elements next to the boundary. In the proximity of the boundary, rectangles are getting so thin that we see only a thick dark line.

1.2 Some paramount facts from Sobolev spaces

In this section, some well known results from the theory of Sobolev spaces are recalled since they will be of so much use later due to the fact that most of our stability analysis is partially based on them. Many of the theorems in this section are mentioned without proofs. It would take a large number of pages to repeat all their proofs in this document. If one wants to read the proofs, one can find them in many books which contain sufficiently large descriptions about Sobolev spaces like [Gri85].

Let $\Omega \subset \mathbf{R}^d$ be a domain whose boundary Γ is supposed to be sufficiently regular. We recall that a measurable function $f \in L^2(\Omega)$ if

$$\|f\|_{0,\Omega}^2 := \int_\Omega |f(\mathbf{x})|^2 d\mathbf{x} < \infty \ .$$

The space that we will most frequently use is the Sobolev space $H^1(\Omega)$ which is precisely the set of all square integrable functions f with:

$$\|f\|_{1,\Omega}^2 := \|f\|_{0,\Omega}^2 + \sum_{i=1,\ldots,d} \left\| \frac{\partial f}{\partial x_i} \right\|_{0,\Omega}^2 < \infty \ .$$

We will repeatedly use also the seminorm in $H^1(\Omega)$ which is given by:

$$|f|_{1,\Omega}^2 := \sum_{i=1,\ldots,d} \left\| \frac{\partial f}{\partial x_i} \right\|_{0,\Omega}^2 .$$

Now we should be able to introduce the boundary spaces. Firstly, it is to be reminded that:

$$H^{\frac{1}{2}}(\Gamma) := \left\{ f \in L^2(\Gamma) |\ \exists g \in H^1(\Omega) :\ g|_\Gamma = f \right\} \ .$$

Its norm can be defined by:

$$\|f\|_{\frac{1}{2},\Gamma} := \inf_{\substack{g \in H^1(\Omega) \\ g|_\Gamma = f}} \|g\|_{1,\Omega} \ .$$

Second, let us recall a space defined on a boundary piece. For that purpose let us assume that $\Gamma = \overline{\Gamma_1 \cup \Gamma_2}$. We suppose furthermore that the boundary pieces Γ_i are of nonzero measures. Then we have

$$H_{00}^{\frac{1}{2}}(\Gamma_i) := \left\{ u \in H^{\frac{1}{2}}(\Gamma_i) : \text{the zero extension } \tilde{u} \text{ of } u \text{ to all } \Gamma \text{ is in } H^{\frac{1}{2}} \right\} .$$

The following theorem provides a characterization of the last space and it specifies also a norm thereof at the same time.

Theorem 1 If we denote

$$\rho(\mathbf{x}) := \text{dist}(\mathbf{x}, \partial\Gamma_i),$$

then we have the following characterization:

$$H_{00}^{\frac{1}{2}}(\Gamma_i) = \left\{ v \in H^{\frac{1}{2}}(\Gamma_i) : \rho^{-\frac{1}{2}} v \in L^2(\Gamma_i) \right\} .$$

This theorem permits us to introduce the following norm in $H_{00}^{\frac{1}{2}}(\Gamma_i)$:

$$\|v\|^2_{\frac{1}{2},00,\Gamma_i} := \|v\|^2_{\frac{1}{2},\Gamma_i} + \int_{\Gamma_i} \frac{|v|^2}{\rho} ds .$$

Now that we have met all the necessary definitions and introductions, it is time we recalled some important theorems from Sobolev space theory. The first one is the Poincaré-Friedrichs inequality.

Theorem 2 (Poincaré-Friedrichs inequality) Let Ω be a bounded domain. We suppose further that Ω has a Lipschitz boundary Γ. Then there exists a positive constant K which depends only on Ω such that:

$$\|v\|_{1,\Omega} \leq K |v|_{1,\Omega}$$

holds for all $v \in V := \{u \in H^1(\Omega) : u = 0 \text{ on } \Gamma_1\}$ where Γ_1 is a part of Γ with nonzero measure.

Theorem 3 (A trace theorem) Let $\Omega \subset \mathbf{R}^d$ be a bounded domain with Lipschitz boundary Γ. Then the trace mapping:

$$\begin{array}{rccc} t: & H^1(\Omega) & \longrightarrow & H^{\frac{1}{2}}(\Gamma) \\ & u & \rightarrow & u|_\Gamma \end{array}$$

is a continuous surjective operator.

1.3 Brief remark about the saddle point problem

Although this document deals mainly with the Stokes problem, some information about the general saddle point problem is worth being said in order to formulate well the unique solvability, the a-priori error analysis, and the eigenvalue problem related to the LBB-condition. Therefore the current section will focus briefly on it.

Let V and Q be two Hilbert spaces whose scalar products are $(\cdot,\cdot)_V$, $(\cdot,\cdot)_Q$ respectively and whose norms are $\|\cdot\|_V$, $\|\cdot\|_Q$ respectively. Let

$$a : V \times V \to \mathbf{R} \qquad b : V \times Q \to \mathbf{R}$$

be two continuous bilinear forms.

The general saddle point problem can be formulated as in the following equation: Let $f \in V^*$ and $g \in Q^*$ be given.

Search for $(u, q) \in V \times Q$ such that:

$$(P) \qquad \left\{ \begin{array}{lcl} a(u,v) + b(v,q) & = & < f, v > \ \forall\, v \in V \\ b(u,p) & = & < g, p > \ \forall\, p \in Q\ . \end{array} \right. \tag{1.4}$$

Two continuous operators $A : V \to V^*$ and $B : V \to Q^*$ can be defined with the help of the bilinear forms $a(\cdot,\cdot)$ and $b(\cdot,\cdot)$. The adjoint operator $B^*$of B can be deduced immediately. And we have in fact:

$$\begin{array}{rcll} < Au, v > & = & a(u,v) & \forall\, u, v \in V \\ < Bu, p > & = & b(u,p) & \forall\, u \in V,\ \forall\, p \in Q \\ < v, B^*p > & = & b(v,p) & \forall\, v \in V\ \forall\, p \in Q\ . \end{array}$$

We have:

$$\begin{array}{rcl} U := \ker(B) & = & \{u \in V : b(u,q) = 0\ \forall\, q \in Q\} \\ \ker(B^*) & = & \{p \in Q : b(u,q) = 0\ \forall\, u \in V\}\ . \end{array}$$

Before we go further let us recall the definition of the polar and the orthogonal complement of the closed subspace U:

$$\begin{array}{rcl} U^0 & := & \{l \in V^* :< l, v >= 0\ \forall v \in U\} \\ U^T & := & \{v \in V :\ (u,v)_V = 0\ \forall u \in U\}\ . \end{array}$$

The following lemma will be important in the proof of the existence and uniqueness of the continuous as well as the discrete problems.

Lemma 1 We have the equivalence of the following three statements:

1- $\exists\, \gamma > 0 \qquad \forall\, p \in Q$

$$\sup_{u \in V} \frac{b(u,p)}{\|u\|_V} \geq \gamma \|p\|_Q, \tag{1.5}$$

2- $B : U^{\perp} \to Q^*$ is an isomorphism and :

$$\|Bv\|_{Q^*} \geq \gamma \|v\|_V \quad \forall v \in U^{\perp},$$

3- $B^* : Q \to U^0$ is an isomorphism and :

$$\|B^* p\|_{V^*} \geq \gamma \|p\|_Q \quad \forall p \in Q. \tag{1.6}$$

Proof

Part 1: Let us prove that (1.5) and the inequality (1.6) are equivalent. Suppose first that (1.5) is true. By using the operator notations, we have for all p in Q:

$$\|B^* p\|_{V^*} = \sup_{0 \neq u \in V} \frac{< B^* p, u >}{\|u\|_V} = \sup_{0 \neq u \in V} \frac{b(u,p)}{\|u\|_V} \geq \|p\|_Q.$$

Thus, (1.6) is proved.

The converse can certainly be proved in a very similar fashion.

Part 2: Now, let us prove that the inequality (1.6) implies that B^* is an isomorphism from Q onto U^0. From (1.6), we can deduce that

$$\ker\,(B^*) = \{0\}\ .$$

That means that B^* is a 1-to-1 mapping. It follows then that B^* is bijective from Q onto $\mathrm{Ran}(B^*)$. It remains therefore to see that

$$\mathrm{Ran}(B^*) = U^0\ . \tag{1.7}$$

The inequality (1.6) implies in particular that the operator B^* has a continuous inverse so that $\mathrm{Ran}(B^*)$ is a closed subspace of V^*. According to the closed range theorem then we have

$$\mathrm{Ran}(B^*) = (\ker\,(B))^0\ ,$$

which gives (1.7).

Part 3: The equivalence of 2- and 3- can be clearly seen by noting that U^0 can be identified with $(U^\perp)^*$.

Theorem 4 (Existence and Uniqueness) Suppose $a(\cdot,\cdot)$ is coercive on $\ker(B)$. That is:

$$\exists \gamma > 0 : \ a(u,u) \geq \gamma \|u\|_V^2, \ \forall\, u \in \ker(B).$$

Suppose furthermore that the inf-sup condition is satisfied, i.e.:

$$\inf_{0 \neq p \in Q} \sup_{0 \neq u \in V} \frac{b(u,p)}{\|u\|_Q \|p\|_Q} \geq \gamma \ . \tag{1.8}$$

Then problem (P) in (1.4) has a unique solution.

Proof

Because g belongs to Q^*, Lemma 1 ensures the existence of a unique $u_0 \in U^\perp$ such that $Bu_0 = g$.

Let us first introduce an auxiliary problem (Q):

Search for $u \in U(g) := \{v \in V : b(v,p) =< g,p > \quad \forall p \in Q\}$ with

$$(Q) \qquad a(u,v) =< f,v > \quad \forall v \in U. \tag{1.9}$$

According to Lax-Milgram's theorem, there exists a unique $w \in U$ with:

$$a(w,v) =< (f - Au_0), v > \quad \forall v \in U \ .$$

That means that the problem (Q) has a unique solution which is:

$$u := u_0 + w \in U(g).$$

(because any solution of (Q) gives a solution of the latter problem, and vice versa).

As a consequence, $(f - Au) \in U^0$ because for any $v \in U$,

$$< f - Au, v >=< f,v > - a(u,v) = 0.$$

According to Lemma 1 again, there exists a unique $p \in Q$ such that

$$B^* p = f - Au,$$

or equivalently,

$$b(v,p) =< f,v > - a(u,v) \quad \forall v \in V. \tag{1.10}$$

On the other hand, since $u \in U(g)$, we have:

$$b(u,q) =< g,q > \quad \forall q \in Q. \tag{1.11}$$

The combination of (1.10) and (1.11) then gives the desired result.

1.4 The Stokes problem

The Stokes equation is one of the most exciting applications of the general abstract saddle point problem stated earlier. We consider for our analysis a bounded connected domain Ω which is a subset of $\mathbf{R}^d$. The purpose of the investigation is to search for the velocity $\mathbf{u} = (u_1, ..., u_d)$ and the pressure p such that:

$$\left\{ \begin{array}{rcll} -\nu\Delta\mathbf{u} + \mathbf{grad}\, p &=& \mathbf{f} & \text{in } \Omega \\ \operatorname{div}\mathbf{u} &=& 0 & \text{in } \Omega \\ \mathbf{u} &=& \mathbf{0} & \text{on } \partial\Omega\ , \end{array} \right.$$

where

$$\Delta\,\mathbf{u} = \sum_{i=1}^{d} \frac{\partial^2 \mathbf{u}}{\partial x_i \partial x_i}\ , \tag{1.12}$$

$$\mathbf{grad}\, p = \left(\frac{\partial p}{\partial x_1}, ..., \frac{\partial p}{\partial x_d} \right)^T\ , \tag{1.13}$$

$$\operatorname{div}\mathbf{u} = \sum_{i=1}^{d} \frac{\partial u_i}{\partial x_i}\ . \tag{1.14}$$

The quantity ν has a mechanical interpretation: it is effectively the kinematic viscosity which is the inverse of the Reynold number of the flow. But mathematically speaking, it is considered as no more than a constant.

Multiplying this equation by appropriate functions and integrating by part gives the following variational formulation: Find $(\mathbf{u}, p) \in H_0^1(\Omega)^d \times L_0^2(\Omega)$ such that:

$$\left\{ \begin{array}{rcll} \nu(\nabla\mathbf{u}, \nabla\mathbf{v}) - (\operatorname{div}\mathbf{v}, p) &=& (\mathbf{f}, \mathbf{v}), & \forall \mathbf{v} \in H_0^1(\Omega)^d \\ (\operatorname{div}\mathbf{u}, q) &=& 0 & \forall q \in L_0^2(\Omega), \end{array} \right. \tag{1.15}$$

where $(\cdot, \cdot)$ denotes the inner product in $L^2(\Omega)$.

It can be seen that it has a form of a saddle point problem with: $V = H_0^1(\Omega)^d$, $Q = L_0^2(\Omega)$ and the bilinear forms are given by:

$$a(\mathbf{u}, \mathbf{v}) = \nu(\nabla\mathbf{u}, \nabla\mathbf{v}) = \nu \int_\Omega \sum_{i,j} \frac{\partial u_i}{\partial x_j} \frac{\partial v_i}{\partial x_j}, \tag{1.16}$$

$$b(\mathbf{u}, p) = -\int_\Omega \operatorname{div}\mathbf{v}\, q\ . \tag{1.17}$$

We are going to apply the preceeding theory about the abstract saddle point problem in order to see the unique solvability of the Stokes problem. But before doing that, we ought to specify the ker (B) of the latter. We can verify that it is in fact given by:

$$\ker(B) = \left\{ \mathbf{u} \in H_0^1(\Omega)^d : \operatorname{div} \mathbf{u} = 0 \text{ in } L^2(\Omega) \right\}.$$

We only need to show the coercivity of $a(\cdot,\cdot)$ on ker (B) and the stability of $b(\cdot,\cdot)$. The coercivity is a one line proof, since by the Poincaré-Friedrich inequality (see Theorem 2), we have:

$$a(\mathbf{u},\mathbf{u}) = \nu |\mathbf{u}|_{1,\Omega}^2 > C\nu \|\mathbf{u}\|_{1,\Omega}^2.$$

The most difficult point is then to prove the stability (1.8) which is equivalent, in the case of Stokes problem, to:

$$\inf_{0 \neq p \in L_0^2(\Omega)} \sup_{0 \neq u \in H_0^1(\Omega)^d} \frac{(\operatorname{div} \mathbf{u}, p)}{|\mathbf{u}|_1 \|p\|_0} \geq \theta. \tag{1.18}$$

This last relation is referred to as the continuous inf-sup condition.

The proof of the continuous inf-sup condition uses the following lemma whose proof could be found in [GR86] on page 24.

Lemma 2 Denote by

$$\begin{aligned} U &= \{\mathbf{v} \in H_0^1(\Omega)^d : \operatorname{div} \mathbf{v} = 0\} \\ U^0 &= \{y \in H^{-1}(\Omega)^d :< y, \phi >= 0 \ \forall \phi \in U\}. \end{aligned}$$

Then we have:

i) The operator **grad** is an isomorphism of $L_0^2(\Omega)$ onto U^0;

ii) The operator div is an isomorphism of $U^\perp$ onto $L_0^2(\Omega)$.

Theorem 5 (continuous inf-sup condition) For the Stokes problem, the continuous inf-sup condition in (1.18) holds.

Proof

Let q be an arbitrary pressure function in $L_0^2(\Omega)$. The preceeding lemma ensures the existence of some $\mathbf{v} \in U^\perp$ such that:

$$\operatorname{div} \mathbf{v} = q \quad \text{and } |\mathbf{v}|_1 \leq C\|q\|_0.$$

Consequently:

$$\frac{(q, \operatorname{div} \mathbf{v})}{|\mathbf{v}|_1} = \frac{\|q\|_0^2}{|\mathbf{v}|_1} \geq \left(\frac{1}{C}\right) \|q\|_0.$$

We can deduce the continuous inf-sup condition (1.18) with $\theta = \frac{1}{C}$.

Remark 1 The contributions of Ladyzhenskaya, Babuska and Brezzi to the analysis of the inf-sup condition (1.18) were very remarkable. Therefore, it is often referred to as the LBB condition. It is however to be noted that it has a lot of other names. Among others, it is called divergence stability condition, stability condition, Babuska-Brezzi condition, BB condition, inf-sup condition.

1.5 FE-approximation and the LBB-condition

This section will contain the FE-discretization of the continuous problem. That is to say, it will ensure the existence and uniqueness of the solution of the discrete problem for each mesh size h. We will see as well the error analysis, that is, the estimation of the error of the approximated solution from the exact solution. And finally we will see the importance of the LBB condition in order to have a nice approximation.

1.5.1 Abstract finite element discretization

The finite element discretization consists mainly of considering two finite dimensional subspaces $V_h \subset V$ and $Q_h \subset Q$. The discrete problem deals then with searching for $(\mathbf{u_h}, p_h) \in V_h \times Q_h$ such that:

$$(\mathcal{P}_h) \quad \left\{ \begin{array}{lllll} a(\mathbf{u}_h, \mathbf{v}_h) & +b(\mathbf{v}_h, p_h) & = & < f, \mathbf{v}_h > & \forall \mathbf{v}_h \in V_h \\ b(\mathbf{u}_h, q_h) & & = & < g, q_h > & \forall q_h \in Q_h. \end{array} \right. \tag{1.19}$$

Like in the case of the continuous problem, we can also introduce the following discrete continuous operators:

$$\begin{array}{rcll} < A_h u_h, v_h > & = & a(u_h, v_h) & \forall\, u_h, v_h \in V_h \\ < B_h u_h, p_h > & = & b(u_h, p_h) & \forall\, p_h \in Q_h, \forall\, u_h \in V_h. \end{array}$$

Similarly to the continuous problem, we have the following uniqueness and existence result of the FE-approximation problem $(\mathcal{P}_h)$. Define:

$$U_h := \{v_h \in V_h : b(v_h, p_h) = 0 \quad \forall p_h \in Q_h\}.$$

Theorem 6 Suppose we have coercivity on U_h, i. e.

$$\exists \alpha^* > 0 : \; a(v_h, v_h) \geq \alpha^* \|v_h\|_V^2 \quad \forall v_h \in U_h.$$

Suppose further that we have the following discrete LBB condition: There exists $\gamma^* > 0$:

$$\inf_{p_h \in Q_h} \sup_{u \in V_h} \frac{b(u,p)}{\|u\|_V \|p\|_Q} \geq \gamma^*. \tag{1.20}$$

Then the problem $\mathcal{P}_h$ in (1.19) has a unique solution.

Proof

It is the equivalent of Theorem 4 for the discrete problem.

Lemma 3 (Fortin's Lemma) Assume that the continuous inf-sup condition (1.8) is satisfied.

The discrete inf-sup condition (1.20) holds with a constant γ^* independent of h if and only if there exists a continuous linear operator $\pi_h \in \mathcal{L}(V, V_h)$ satisfying:

(A1) $b(v - \pi_h v, p_h) = 0 \quad \forall p_h \in Q_h \, \forall v \in V$, and

(A2) $\|\pi_h v\|_V \leq C \|v\|_V \quad \forall v \in V$

with a constant $C > 0$ independent of h

Proof

Part 1:

First, suppose we have an operator $\pi_h \in \mathcal{L}(V, V_h)$ satisfying the assumptions (A1) and (A2). Let us prove that the discrete inf-sup condition (1.20) follows. Let p_h be an arbitrary element of Q_h. We have:

$$\sup_{v_h \in V_h} \frac{b(v_h, p_h)}{\|v_h\|_V} \geq \sup_{v \in V} \frac{b(\pi_h v, p_h)}{\|\pi_h v\|_V} \quad \text{because } \mathrm{Im}(\pi_h) \subset V_h$$

According to the assumption (A1), we have therefore:

$$\sup_{v_h \in V_h} \frac{b(v_h, p_h)}{\|v_h\|_V} \geq \sup_{v \in V} \frac{b(v, p_h)}{\|\pi_h v\|_V}.$$

Applying (A2) implies consequently:

$$\sup_{v_h \in V_h} \frac{b(v_h, p_h)}{\|v_h\|_V} \geq \frac{1}{C} \sup_{v \in V} \frac{b(v, p_h)}{\|v\|_V}.$$

Now, we can use the continuous inf-sup condition in order to have:

$$\sup_{v_h \in V_h} \frac{b(v_h, p_h)}{\|v_h\|_V} \geq \frac{\gamma}{C} \|p_h\|_Q.$$

That means that the discrete inf-sup condition (1.20) is satisfied.

Part 2:

Now let us suppose that the discrete inf-sup condition (1.20) is satisfied and let us prove that we have an operator $\pi_h \in \mathcal{L}(V, V_h)$ having the properties (A1) and (A2).

We need to apply Lemma 1 to the discrete operator B_h. For each $v \in V$, we have $B_h v \in Q^*$. Since B_h is an isomorphism from $V_h^\perp$ onto Q_h^*, there exists a unique element of $V_h^\perp$ that we denote by $\pi_h v$ such that:

$$B_h(\pi_h v) = B_h v.$$

That means simply that: $b(\pi_h v, p_h) = b(v, p_h) \quad \forall p_h \in Q_h$. Lemma 1, applied to the discrete operators, implies also in particular that

$$\gamma^* \|\pi_h v\|_V \leq \|B_h(\pi_h v)\|_{Q^*},$$

which implies that:

$$\|\pi_h v\|_V \leq \frac{1}{\gamma^*} \|B_h v\|_{Q^*} \leq \frac{\|b\|}{\gamma^*} \|v\|_V,$$

where

$$\|b\| = \sup_{\substack{0 \neq v \in V \\ 0 \neq p \in Q}} \frac{b(v, p)}{\|v\|_V \|p\|_Q}.$$

is a finite number because b is a continuous bilinear form.

1.5.2 Error estimation for the Stokes approximation

The preceding result of the abstract FE-discretization of the saddle point problem can certainly be applied to the Stokes problem. In this subsection,

we are estimating the error between $(\mathbf{u}_h, p_h)$ and $(\mathbf{u}, p)$. That is precisely the purpose of the next theorem which summerizes our error estimation result for the Stokes problem. V_h and Q_h are finite dimensional subspaces of $H_0^1(\Omega)^d$ and $L_0^2(\Omega)$

Theorem 7 Let V_h and Q_h be discrete finite dimensional subspaces for the velocity and for the pressure respectively. Moreover we suppose that those subspaces satisfy:

$$\inf_{0\neq p_h\in Q_h}\sup_{0\neq \mathbf{u}_h\in V_h}\frac{\int_\Omega \operatorname{div}\mathbf{u}_h\, p_h}{|\mathbf{u}|_{1,\Omega}\|p_h\|_{0,\Omega}}=\gamma_h \quad \text{with}\,\gamma_h>0. \tag{1.21}$$

Then we can estimate the error as:

$$\|\mathbf{u}-\mathbf{u}_h\|_{1,\Omega}\leq \frac{C}{\gamma_h}\inf_{\mathbf{v}_h\in V_h}\|\mathbf{u}-\mathbf{v}_h\|_{1,\Omega}+C\inf_{q_h\in Q_h}\|p-q_h\|_{0,\Omega}. \tag{1.22}$$

$$\|p-p_h\|_{0,\Omega}\leq \frac{C}{\gamma_h^2}\inf_{\mathbf{v}_h\in V_h}\|\mathbf{u}-\mathbf{v}_h\|_{1,\Omega}+\frac{C}{\gamma_h}\inf_{q_h\in Q_h}\|p-q_h\|_{0,\Omega}\ , \tag{1.23}$$

where C depends only upon Ω.

Proof See [BF91].

Remark 2 In the preceding theorem it can be very well noticed that the velocity and the pressure errors depend mainly on γ_h^{-1} and γ_h^{-2} respectively. The first remark that should be pointed out is that the velocity is better approximated than the pressure because (1.23) has a γ_h^{-1} more factor than (1.22).

It is to be noticed as well that if γ_h is tending to zero then we have a very bad estimate for the velocity and the pressure estimate is even still worse because γ_h^{-1} is tending to infinity. It is therefore of overwhelming importance to have γ_h independent of h or equivalently to have some $\gamma>0$ with $\gamma_h>\gamma$ for all h. That means simply:

$$\inf_{0\neq p_h\in Q_h}\sup_{0\neq \mathbf{u}_h\in V_h}\frac{\int_\Omega \operatorname{div}\mathbf{u}_h\, p_h}{|\mathbf{u}|_{1,\Omega}\|p_h\|_{0,\Omega}}\geq\gamma\ .$$

1.6 Numerical evaluations of LBB-constants

In this section, a couple of approaches for the computation of inf-sup quantities are detailed.

1.6.1 First approach

In this first approach, a generalized eigenvalue problem is invoked. The relationship between the eigenvalue problem and the inf-sup constant can be seen in [Mal81] where the author gives full details about this topic. But it can also be found in many other documents like [BF91], [BIC00], [CB93]. In the following discussion, we will review this eigenproblem in order to evaluate the inf-sup constants.

Eigenproblem pertaining to the discrete inf-sup constant

Let V_h and Q_h be finite dimensional subspaces of $H_0^1(\Omega)^d$ and $L_0^2(\Omega)$ respectively. We are interested in computing, for all mesh width h, the discrete inf-sup constant which is given by:

$$\inf_{p_h \in Q_h} \sup_{\mathbf{v_h} \in V_h} \frac{\int_\Omega p_h \operatorname{div} \mathbf{v_h}}{|\mathbf{v_h}|_{1,\Omega} \|p_h\|_{0,\Omega}} \ . \tag{1.24}$$

Let us first formulate the discrete problem in vector and matrix forms. Because we are dealing with finite dimensional spaces, the functions $\mathbf{v_h}$ and q_h can be written as:

$$\mathbf{v_h} = \sum_{i=1}^{N} \alpha_i \phi_i \qquad p_h = \sum_{i=1}^{M} \beta_i \psi_i \ ,$$

where $\{\phi_i\}_{i=1}^N$ and $\{\psi_i\}_{i=1}^M$ are bases in V_h and Q_h respectively.

We can define immediately the following vectors:

$$\underline{v} = \{\alpha_i\}_{i=1,\ldots,N} \quad \underline{p} = \{\beta_i\}_{i=1,\ldots,M}.$$

The introduction of the following matrices K, B, M is of capital importance.

$$\begin{aligned} b(\mathbf{v_h}, p_h) &= < B\underline{v}, \underline{p} >_{\mathbf{R}^M} = < \underline{v}, B^T \underline{p} >_{\mathbf{R}^N} \\ |\mathbf{v_h}|_{1,\Omega}^2 &= < K\underline{v}, \underline{v} >_{\mathbf{R}^N} \\ \|p_h\|_{0,\Omega}^2 &= < M\underline{p}, \underline{p} >_{\mathbf{R}^M} \ . \end{aligned}$$

The discrete problem can in fact be formulated with the help of those matrices as:

$$\begin{pmatrix} \nu K & \vdots & B^T \\ \cdots & & \cdots \\ B & \vdots & 0 \end{pmatrix} \begin{pmatrix} \underline{v} \\ \cdots \\ \underline{p} \end{pmatrix} = \begin{pmatrix} F \\ \cdots \\ 0 \end{pmatrix} .$$

Those diverse definitions permit us to observe right away that the square of the initial inf-sup constant (1.24) is given by:

$$\inf_{\underline{p}} \left\{ \sup_{\underline{v}} \frac{(\underline{p}^T B \bar{v})^2}{(\underline{v}^T K \underline{v})(\underline{p}^T M \underline{p})} \right\}.$$

If we make Cholesky factorizations $K = LL^T, \quad M = GG^T$ then it is equal to:

$$\inf_{\underline{p}} \left\{ \sup_{\underline{v}} \frac{(\underline{p}^T B \underline{v})^2}{[(L^T \underline{v})^T (L^T \underline{v})][(G^T \underline{p})^T (G^T \underline{p})]} \right\}.$$

After putting $\underline{w} = L^T \underline{v}$ and $\underline{q} = G^T \underline{p}$, we obtain:

$$\inf_{\underline{q}} \left\{ \frac{1}{\underline{q}^T \underline{q}} \sup_{\underline{w}} \frac{(\underline{w}^T L^{-1} B^T G^{-T} \underline{q})^2}{\underline{w}^T \underline{w}} \right\} = \inf_{\underline{q}} \left\{ \frac{1}{\underline{q}^T \underline{q}} (L^{-1} B^T G^{-T} \underline{q})^T (L^{-1} B^T G^{-T} \underline{q}) \right\}$$

$$= \inf_{\underline{q}} \left\{ \frac{1}{\underline{q}^T \underline{q}} \underline{q}^T G^{-1} (B K^{-1} B^T) G^{-T} \underline{q} \right\} = \lambda_{min} \left[G^{-1} (B K^{-1} B^T) G^{-T} \right].$$

And the eigenvalues of this last matrix are the generalized eigenvalues of

$$(B K^{-1} B^T) \underline{p} = \lambda M \underline{p} \,. \tag{1.25}$$

because $\left[G^{-1} (B K^{-1} B^T) G^{-T} \right] \underline{q} = \lambda \underline{q}$ implies:

$$(B K^{-1} B^T) \underline{p} = \lambda G G^T \underline{p} = \lambda M \underline{p} \,,$$

where $\underline{p} = G^{-T} \underline{q}$.
We have therefore the following property:

Property 1 Let us consider the following generalized eigenvalue problem:

$$(B K^{-1} B^T) \underline{p} = \lambda M \underline{p} \,. \tag{1.26}$$

If γ_h^2 is the smallest eigenvalue of this generalized eigenproblem, then

$$\gamma_h = \inf_{q_h \in Q_h} \sup_{\mathbf{v}_h \in V_h} \frac{\int_\Omega q_h \operatorname{div} \mathbf{v}_h}{|\mathbf{v}_h|_{1,\Omega} \|q_h\|_{0,\Omega}} \,.$$

Remark 3 In practical point of view, it is very difficult to find a basis $\{\psi_i\}$ of the space $Q_h \subset L^2_0(\Omega)$ because it demands that every function of $L^2_0(\Omega)$ has zero integral over Ω. Therefore, one consider a basis $\{\tilde{\psi}_i\}$ of $\tilde{Q}_h \subset L^2(\Omega)$, where

$$\tilde{Q}_h \cap L^2_0(\Omega) = Q_h \ .$$

Of course, every function in Q_h can be written as linear combination of $\{\tilde{\psi}_i\}$ because Q_h is a subspace of $\tilde{Q}_h$. In this situation, the inf-sup constant is the square root of the smallest nonzero eigenvalue. This property has been discussed in [Mal81], [BF91], [BIC00], [CB93].

Algorithm

We can implement a numerical computation of inf-sup quantities by using facts which are based on the previous eigenvalue theory.

1. Generate the mesh whose inf-sup constant is to be computed,

2. Assemble the matrices K, B, M which were defined in the preceding section,

3. Determine the smallest (nonzero) eigenvalue γ_{min} of:

$$(BK^{-1}B^T)\underline{p} = \lambda M\underline{p},$$

4. The wanted inf-sup constant is $\sqrt{\gamma_{min}}$.

1.6.2 Second approach

As for the second approach, it invokes theory from constrained nonlinear optimization. Before giving numerical instructions of how to compute our inf-sup constants, some further definitions and notations are necessary. Let us pick for example finite dimensional subspaces

$$\begin{aligned} \tilde{Q}_h &\subset L^2(\Omega) \ , \\ V_h &\subset H^1_0(\Omega)^d \ . \end{aligned}$$

Let us consider again the problem of computing the following inf-sup constant:

$$\gamma_h = \inf_{0 \neq p_h \in Q_h} \sup_{0 \neq \mathbf{v}_h \in V_h} \frac{b(\mathbf{v}_h, p_h)}{|\mathbf{v}_h|_{1,\Omega} \|p\|_{0,\Omega}} \ ,$$

where $Q_h = \tilde{Q}_h \cap L^2_0(\Omega)$.

In the our present discussion, we adopt the following dimensionalities:

$$\begin{aligned} N &= \dim \tilde{Q}_h \\ M &= \dim V_h \ . \end{aligned}$$

We denote by $\{\psi_i\}_{i=1,...,N}$ a basis of $\tilde{Q}_h$. If we define

$$a_i = \int_\Omega \psi_i d\mathbf{x} \quad \text{and} \qquad \underline{a} = (a_1, ..., a_N) \ ,$$

and if we introduce the following hyperplane in $\mathbf{R}^N$ by:

$$\mathcal{H} = \left\{ (q_1, ..., q_N) \in \mathbf{R}^N : \sum_{i=1}^N q_i a_i = 0 \right\} \ ,$$

then we can obtain the following characterization of Q_h from $\tilde{Q}_h$:

$$\sum_{i=1}^N q_i \psi_i \in Q_h \iff (q_1, ..., q_N) \in \mathcal{H} \ .$$

Now we are able to reformulate our inf-sup constant in matrix-vector form. It gives in fact:

$$\gamma_h = \inf_{\substack{0 \neq \underline{q} \in \mathbf{R}^N \\ \underline{q} \in \mathcal{H}}} \sup_{0 \neq \underline{v} \in \mathbf{R}^M} \frac{\underline{v}^T B^T \underline{q}}{\sqrt{\underline{v}^T K \underline{v}} \sqrt{\underline{q}^T M \underline{q}}}.$$

Or equivalently:

$$\text{For all } \underline{q} \in \mathbf{R}^N \setminus \{\mathbf{0}\}, \underline{q} \in \mathcal{H} \qquad \sup_{0 \neq \underline{v} \in \mathbf{R}^M} \frac{\underline{v}^T B^T \underline{q}}{\sqrt{\underline{v}^T K \underline{v}}} \geq \gamma_h \sqrt{\underline{q}^T M \underline{q}} \ .$$

Now we can perform a Cholesky factorization of $K = LL^T$ and so we can simply obtain:

$$\underline{v}^T K \underline{v} = (L^T \underline{v})^T (L^T \underline{v}) \ .$$

And by replacing $\underline{w} = L^T \underline{v}$, we should obtain:

$$\sup_{0 \neq \underline{w} \in \mathbf{R}^M} \frac{\underline{w}^T L^{-1} B^T \underline{q}}{\sqrt{\underline{w}^T \underline{w}}} \geq \gamma_h \sqrt{\underline{q}^T M \underline{q}}.$$

And we should notice that the left hand side is nothing else but $\|L^{-1}B^T\underline{q}\|_{\mathbf{R}^M}$ where $\|\cdot\|_{\mathbf{R}^M}$ denotes the usual Euclidian norm in $\mathbf{R}^M$. Our initial inf-sup constant is finally equivalent to:

$$\gamma_h = \inf_{\substack{0\neq\underline{q}\in\mathbf{R}^N \\ \underline{q}\in\mathcal{H}}} \frac{\|L^{-1}B^T\underline{q}\|_{\mathbf{R}^M}}{\sqrt{\underline{q}^T M\underline{q}}} \ .$$

In other words, we have to solve the following constrained nonlinear optimization problem:

Let us first denote by $F(\underline{q}) = \frac{\|L^{-1}B^T\underline{q}\|_{\mathbf{R}^M}}{\sqrt{\underline{q}^T M\underline{q}}}$.

Our problem is then:

$$\begin{cases} F(\underline{q}) \longrightarrow \min \\ \text{subject to } \underline{q}\in\mathcal{H}. \end{cases} \tag{1.27}$$

There are efficient numerical algorithms to minimize such a problem of nonlinear programming. You can find below one of them. The following algorithm is commonly known as Gradient Projection Method (Gradientenprojektionsverfahren or GPV in German literature).

A preliminary remark will be established before we give a description of the algorithm: since $\mathcal{H}$ is a convex set in $\mathbf{R}^N$, let us denote by $P_{\mathcal{H}}$ the orthogonal projection in $\mathcal{H}$, i.e.:

$$\|\underline{q} - P_{\mathcal{H}}\underline{q}\|_{\mathbf{R}^N} = \min_{\underline{p}\in\mathcal{H}} \|\underline{q} - \underline{p}\|_{\mathbf{R}^N}. \tag{1.28}$$

Now, the Gradient Projection Method consists of performing the next steps:

Step 0. Choose an arbitrary initial guess $\underline{q}_0 \in \mathcal{H}$ and set $k = 0$,

Step 1. For the point $\underline{q}_k$ and the direction $\underline{d}_k := -\nabla F(\underline{q}_k)$, we compute a line search for the following *unconstrained* problem:

$$\begin{cases} F(\underline{q}) \longrightarrow \min \\ \underline{q}\in\mathbf{R}^N, \end{cases}$$

in order to obtain a step length α_k,

Step 2. Establish the projection $P_{\mathcal{H}}(\underline{q}_k + \alpha_k\underline{d}_k)$,

Step 3. In the case $P_{\mathcal{H}}(\underline{q}_k + \alpha_k \underline{d}_k) = \underline{q}_k$, we terminate, otherwise the new iterate is

$$\underline{q}_{k+1} = P_{\mathcal{H}}(\underline{q}_k + \alpha_k \underline{d}_k) \ ,$$

and we come back to step 1. with the incrementation $k := k + 1$.

A further remark ought to be mentioned about step 2: since the definition (1.28) of the orthogonal projection on the hyperplane $\mathcal{H}$ does not seem to be easy in computational aspect, a practical formula for its evaluation is found below:

$$P_{\mathcal{H}}(\underline{q}) = \underline{q} - \frac{< \underline{a}, \underline{q} >_{\mathbf{R}^N} - \alpha}{\|\underline{a}\|^2_{\mathbf{R}^N}} \cdot \underline{a}^T \ ,$$

where $\alpha =< \underline{a}, \underline{r} >$ with $\underline{r}$ an arbitrary vector belonging to $\mathcal{H}$.

One can therefore follow the following direction if one is interested in the second approach:

1. Generate the mesh whose inf-sup constant is to be computed,
2. Assemble the matrix K, B, M which were defined in the previous section,
3. Compute a Cholesky factorization of $K = LL^T$,
4. Establish the function of N-variables F,
5. Establish the coefficients a_i defining the hyperplane $\mathcal{H}$,
6. Solve the nonlinear programming (1.27) subject to the hyperplane constraint.

1.6.3 Comparison

For the sake of comparison, I have computed once the inf-sup constant of a certain mesh both with this current method and the one in the preceding section and the results agree very well. It is however to be noticed that this algorithm of Gradient Projection Method has the disadvantage of being extremely slow, in particular if accurate results are needed. It is however to be mentioned that many improvements of this algorithms are in existence. There are other very efficient algorithms of such a nonlinear optimization. This is however not the place to give details of these methods because the main purpose of our analysis is presently to investigate FE-stabilities. Readers who are interested in such an approach is well advised to browse existing documents in constrained nonlinear programming such as [NW99].

Chapter 2

Macroelement approaches

2.1 Arbitrary macroelement partitioning

Another possibility to prove the divergence stability is to use macroelement partitioning. The following idea was used first by Boland & Nicolaides but it can also be found in some other document like [GR86]. The technique consists in fact in partitioning the domain into subdomains and having some local stability besides a reduced macrowise stability which imply the stability of the initial pair of spaces. Therefore, instead of proving the stability, we have two smaller problems which should be easier to prove. We should see in this section the detailed description of it because it will be of much use later on. A similar technique can also be found in [Ste84] and [Ste90]. Before telling the results, let us first introduce some notations:

We suppose that we have a partitioning of the initial domain Ω into a finite number of disjoint subsets. That is:

$$\overline{\Omega} = \bigcup_{r=1}^{R} \overline{K}_r \ ,$$

where K_r is a Lipschitz continuous open subset with boundary Γ_r.

Now let us introduce the following subspaces

$$\begin{array}{rl} V_h & \text{is a finite dimensional subspace of } H_0^1(\Omega)^d \ , \\ \tilde{Q}_h & \text{is a finite dimensional subspace of } L^2(\Omega) \ , \\ Q_h & := \tilde{Q}_h \cap L_0^2(\Omega) \ . \end{array}$$

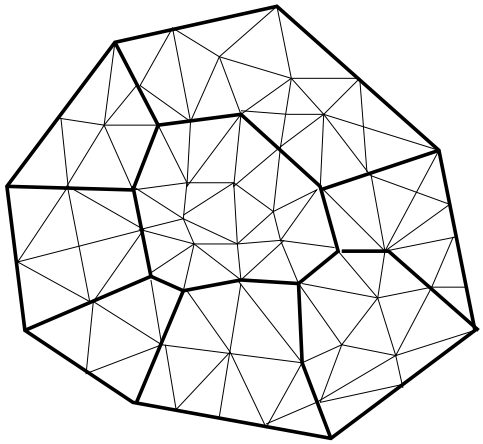

Figure 2.1: Macroelement partitioning.

We suppose furthermore that $\tilde{Q}_h$ contains all the constant functions, i.e.

$$\underline{\mathbf{R}} \subset \tilde{Q}_h \ ,$$

where $\underline{\mathbf{R}}$ is the set of all constant functions in Ω.

The partitioning is graphically illustrated in Figure 2.1. Please note that the macroelement boundaries are indicated by bold lines.

Now, we are in a position of introducing the local spaces. These are those which are related to each macroelement. For each $r \in \{1, ..., R\}$, let us define the following:

$$\begin{aligned} V_h(K_r) &:= \{\mathbf{v} \in V_h : \mathbf{v} = 0 \,\text{in}\, \Omega \setminus K_r\} \ , \\ \tilde{Q}_h(K_r) &:= \{p|_{K_r} \,;\, p \in \tilde{Q}_h\} \ , \\ Q_h(K_r) &:= \tilde{Q}_h(K_r) \cap L_0^2(K_r) \ . \end{aligned}$$

Remark 4 Note that in this chapter and in the following ones, elements are denoted by T and macroelements are denoted by K which may have some indices.

Remark 5 The macroelement partitioning must fulfill the condition that an element must belong to one and only one macroelement. In other words, every element must be located in one macroelement and no element should be shared by two or more macroelements.

We have then the following theorem which is the most important result in this section. Only a sketch of the proof will be given here, readers who are interested in seeing the proof in full detail are advised to read Theorem 1.12 of [GR86].

Theorem 8 Suppose we have the following assumptions:

(A1) *Local stability:*

There is a positive constant α such that for all $p_h \in Q_h(K_r)$ we have:

$$\sup_{\mathbf{v}_h \in V_h(K_r)} \frac{1}{|\mathbf{v}_h|_{1,K_r}} \int_{K_r} p_h \mathrm{div}\, \mathbf{v}_h \geq \alpha \|p_h\|_{0,K_r} \quad \forall r \in \{1, ..., R\}, \tag{2.1}$$

where α is independent of h and r.

(A2) *Reduced global stability:*

We define $\bar{Q}_h$ to be the macrowise constant space, i.e.:

$$\bar{Q}_h = \{p \in L_0^2(\Omega) : \ p|_{K_r} \text{is constant}, 1 \leq r \leq R\}.$$

Suppose there is a subspace $\bar{V}_h$ of V_h for which:

$$\sup_{\mathbf{v}_h \in \bar{V}_h} \frac{1}{|\mathbf{v}_h|_{1,\Omega}} \int_{\Omega} p_h \mathrm{div}\, \mathbf{v}_h \geq \beta \|p_h\|_{0,\Omega} \quad \forall p_h \in \bar{Q}_h, \tag{2.2}$$

where β is a constant independent of h.

Under the assumptions (A1) and (A2), we have then stability for the initial pair of spaces (V_h, Q_h), i.e. there exists $\gamma > 0$ such that:

$$\sup_{\mathbf{v}_h \in V_h} \frac{1}{|\mathbf{v}_h|_{1,\Omega}} \int_{\Omega} p_h \mathrm{div}\, \mathbf{v}_h \geq \gamma \|p_h\|_{0,\Omega} \quad \forall p_h \in Q_h,$$

where γ depends only on α, β and the dimension d of Ω ($d = 2, 3$).

Proof (Sketch)

For each $p_r \in \tilde{Q}_h(K_r)$, there exists $(\tilde{p}_r, p_r^*) \in Q_h(K_r) \times \underline{\mathbf{R}}$ such that $p_r = \tilde{p}_r + p_r^*$.

Indeed, we can take:

$$\begin{aligned} p_r^* &= \frac{1}{\mathrm{meas}(K_r)} \int_{K_r} p_r \\ \tilde{p}_r &= p_r - p_r^*. \end{aligned}$$

Furthermore, $Q_h(K_r) \cap \underline{\mathbf{R}} = \{0\}$.

Hence, we have the following direct sum:

$$\tilde{Q}_h(K_r) = Q_h(K_r) \oplus \underline{\mathbf{R}}. \tag{2.3}$$

The relation (2.3) is even an orthogonal decomposition since

$$(p_h, c)_{K_r} = 0 \quad \forall p_h \in Q_h(K_r) \quad \forall c \in \underline{\mathbf{R}}.$$

Let us consider now an arbitrary function $q_h \in Q_h$. It can then be written as:

$$q_h = \tilde{q}_h + \bar{q}_h,$$

where $\tilde{q}_h|_{K_r} \in Q_h(K_r)$ and $\bar{q}_h \in \bar{Q}_h$.

By the orthogonality (2.3), we have moreover:

$$\|q_h\|^2_{0,\Omega} = \|\tilde{q}_h\|^2_{0,\Omega} + \|\bar{q}_h\|^2_{0,\Omega}. \tag{2.4}$$

Define now the function $q_r := \tilde{q}_h|_{K_r}$.

By the local stability (2.1), there exists a function $\tilde{\mathbf{v}}_r \in V_h(K_r)$ with:

$$\begin{cases} \int_{K_r} q_r \mathrm{div}\, \mathbf{v}_r dx = \|q_r\|^2_{0,K_r} \\ |\mathbf{v}_r|_{1,K_r} \leq \frac{1}{\alpha}\|q_r\|_{0,K_r}. \end{cases} \tag{2.5}$$

Similarly, the reduced global stability (2.2) ensures the existence of a function $\bar{\mathbf{v}}_h \in \bar{V}_h$ with:

$$\begin{cases} \int_{\Omega} \bar{q}_h \mathrm{div}\, \bar{\mathbf{v}}_h dx = \|\bar{q}_h\|^2_{0,\Omega} \\ |\bar{\mathbf{v}}_h|_{1,\Omega} \leq \frac{1}{\beta}\|\bar{q}_h\|_{0,\Omega}. \end{cases} \tag{2.6}$$

Let us define $\tilde{\mathbf{v}}_h \in V_h$ to be the function whose restriction in K_r is coinciding to $\tilde{\mathbf{v}}_r$.

The velocity associated with q_h will be then:

$$\mathbf{v}_h := \tilde{\mathbf{v}}_h + \delta \bar{\mathbf{v}}_h.$$

The coefficient $\delta > 0$ will be appropriately chosen later on. We have the following relation:

$$(q_h, \mathrm{div}\, \mathbf{v}_h) = (\tilde{q}_h, \mathrm{div}\, \tilde{\mathbf{v}}_h) + (\bar{q}_h, \mathrm{div}\, \tilde{\mathbf{v}}_h) + \delta(\tilde{q}_h, \mathrm{div}\, \bar{\mathbf{v}}_h) + \delta(\bar{q}_h, \mathrm{div}\, \bar{\mathbf{v}}_h).$$

If we combine this last relation with (2.5) and (2.6), we obtain after some calculations:

$$(q_h, \operatorname{div} \mathbf{v}_h) \geq \frac{1}{2}\|\tilde{q}_h\|_{0,\Omega}^2 + \delta\left(1 - \frac{\delta d}{2\beta^2}\right)\|\bar{q}_h\|_{0,\Omega}^2.$$

This last inequality is true for any δ, now if we take $\delta = \frac{\beta^2}{d}$, we obtain:

$$(q_h, \operatorname{div} \mathbf{v}_h) \geq \frac{1}{2}\|\tilde{q}_h\|_{0,\Omega}^2 + \frac{\beta^2}{2d}\|\bar{q}_h\|_{0,\Omega}^2.$$

And we have therefore:

$$(q_h, \operatorname{div} \mathbf{v}_h) \geq \min\left(\frac{1}{2}, \frac{\beta^2}{2d}\right)\left(\|\tilde{q}_h\|_{0,\Omega}^2 + \|\bar{q}_h\|_{0,\Omega}^2\right).$$

As for the estimation of $|\mathbf{v}_h|_{1,\Omega}$, we have with the help of (2.5),(2.6) and (2.4):

$$\begin{aligned} |\mathbf{v}_h|_{1,\Omega} &\leq |\tilde{\mathbf{v}}_h|_{1,\Omega} + \delta|\bar{\mathbf{v}}_h|_{1,\Omega} \\ &\leq \sqrt{2}\left[\frac{1}{\alpha^2} + \left(\frac{\beta}{d}\right)^2\right]^{1/2}\|q_h\|_{0,\Omega}. \end{aligned}$$

We have then:

$$\frac{1}{|\mathbf{v}_h|_{1,\Omega}}(q_h, \operatorname{div} \mathbf{v}_h) \geq \frac{\min\left(\frac{1}{2}, \frac{\beta^2}{2d}\right)}{\sqrt{2}\left[\frac{1}{\alpha^2} + \left(\frac{\beta}{d}\right)^2\right]^{1/2}}\|q_h\|_{0,\Omega}.$$

The stability of the pair (V_h, Q_h) is then obtained with an inf-sup constant $\gamma > 0$ which is only depending on α, β, d.

Remark 6 In Theorem 8, we should note that the final inf-sup constant γ is independent of the number of the macroelement R.

Remark 7 It must be remarked that this method is a very general one because in the proof the uniformity of the mesh is nowhere involved.

2.2 Uniform macroelement partitioning

In this section, we do not demand the macroelement partitioning to be quite arbitrary. We will give a detail here of how the foregoing section can be simplified if the macroelement partitioning is κ-uniform. It is not at all a restrictive assumption because a lot of meshes can be treated that way. We can even still deal with anisotropic meshes because the triangulation within each macroelement can be arbitrary and every element there are allowed to have arbitrary high aspect ratio. Before introducing the main result in this section, let us first see some further definitions and notations.

2.2.1 The considered macroelement

The properties of our future meshing are as follows. We will take into consideration a κ-uniform macroelement partitioning $\mathcal{T}_m$. That means that for every macroelement K of $\mathcal{T}_m$,

$$\frac{h(K)}{\rho(K)} \leq \kappa < \infty. \tag{2.7}$$

We want also that every macroelement $K \in \mathcal{T}_m$ are affine images of a reference domain $\hat{K}$. That means simply that :

$$K = F_K(\hat{K}), \quad \text{where } F_K : \hat{K} \to K \text{ affine mapping .}$$

2.2.2 The meshes on each macroelement

Let $\mathcal{F}$ stand for a family of meshes on the reference macroelement $\hat{K}$. An illustration will be given when sufficient definitions are introduced. Any mesh on a macroelement K will be an affine image of a mesh belonging to $\mathcal{F}$. In other words, a mesh $\mathcal{T}_K$ inside a macroelement K is given by:

$$\mathcal{T}_K = F_K(\hat{\mathcal{T}}) \qquad \text{for some } \hat{\mathcal{T}} \in \mathcal{F}.$$

The mesh $\mathcal{T}$ on the whole domain Ω is then the union of all $\mathcal{T}_K$, K macroelement. Or similarly, the restriction of $\mathcal{T}$ to K is the mesh $\mathcal{T}_K$.

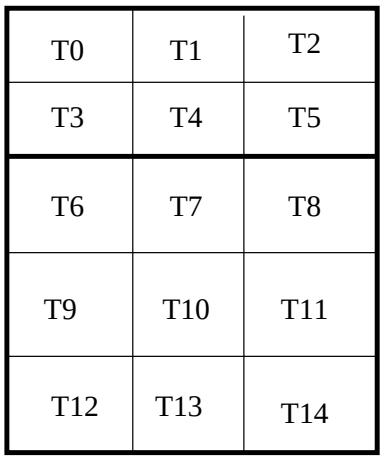

Figure 2.2: Illustration.

2.2.3 Illustration

As an illustration, let us consider a two dimensional rectangular domain Ω and the reference domain will be $\hat{K} = (0,1)^2$. $\mathcal{F}$ will be the set of all tensor product mesh on the reference macroelement $\hat{K}$. In Figure 2.2, we can see an example of rectangular domain Ω composed of two macroelements and each macroelement is subdivided into tensor product meshes. The discretization of the domain Ω is therefore $\mathcal{T} = \{T_i : i = 0, ..., 14\}$.

2.2.4 Discrete spaces

The following discrete spaces are important for the formulation of the next theorem. We will adopt these notations in this section. The initial abstract pair of spaces whose stability is to be established is (V_h, Q_h) where:

$$\begin{aligned} V_h &:= \{\mathbf{u} = (u_1, ..., u_d) \in H_0^1(\Omega)^d : u_i|_T \circ F_T \in R_{k_1,k_2}(\hat{K}) \ \forall T \in \mathcal{T}\} \\ Q_h &:= \{p \in L_0^2(\Omega) : p|_T \circ F_T \in R_{k_1',k_2'}(\hat{K}) \ \forall T \in \mathcal{T}\} \ , \end{aligned}$$

where R_{k_1,k_2} and $R_{k_1',k_2'}$ are some space of polynomials whose degrees are related to some constant parameters k_1, k_2 and k_1', k_2'. In practice, they will be $\mathcal{P}_k$, $\mathcal{Q}_k$ or $\mathcal{Q}_{r,s}$ or some such matter. But for our abstract analysis, we let them to be very general.

The next notations are for local purposes:

$$\begin{aligned} V(\hat{K}) &:= \left[R_{k_1,k_2}(\hat{K}) \cap H_0^1(\hat{K})\right]^d \\ Q(\hat{K}) &:= R_{k_1',k_2'}(\hat{K}) \cap L_0^2(\hat{K}). \end{aligned}$$

And for any $\hat{\mathcal{T}} \in \mathcal{F}$, we define:

$$\begin{aligned} V(\hat{\mathcal{T}}) &:= \{\mathbf{u} = (u_1, ..., u_d) \in H_0^1(\hat{K}) : u_i|_T \circ F_T \in R_{k_1,k_2}(\hat{K}) \ \forall T \in \hat{\mathcal{T}}\} \\ Q(\hat{\mathcal{T}}) &:= \{p \in L_0^2(\hat{K}) : p|_T \circ F_T \in R_{k_1',k_2'}(\hat{K}) \ \forall T \in \hat{\mathcal{T}}\}. \end{aligned}$$

We should remark that for the mesh $\hat{\mathcal{T}}_0$ consisting of only one element which is $\hat{K}$ itself, we have:

$$\begin{aligned} V(\hat{\mathcal{T}}_0) &= V(\hat{K}) \\ Q(\hat{\mathcal{T}}_0) &= Q(\hat{K}). \end{aligned}$$

Finally, for a macroelement K, we introduce:

$$\begin{aligned} V(K, \mathcal{T}_K) &:= \{\mathbf{u} = (u_1, ..., u_d) \in H_0^1(K) : u_i|_T \circ F_T \in R_{k_1,k_2}(\hat{K}) \ \forall T \in \mathcal{T}_K\}, \\ Q(K, \mathcal{T}_K) &:= \{p \in L_0^2(K) : p|_T \circ F_T \in R_{k_1',k_2'}(\hat{K}) \ \forall T \in \mathcal{T}_K\}. \end{aligned}$$

2.2.5 Main result

In this subsection, we will give the relationship of the stabilities of the preceding discrete spaces. It will be noted that the analysis of the initial stability can then be reduced in three easier and independent stability analyses. The next theorem will contain in detail that statement.

Theorem 9 We suppose first that the underlying macroelement partitioning $\mathcal{T}_m$ is κ-uniform. We suppose furthermore the following assumptions:

(B1) *Reduced global stability:*

We define again $\bar{Q}_h$ to be the macrowise constant space, i.e.:

$$\bar{Q}_h := \{p \in L_0^2(\Omega) : \ p|_K \text{ is constant}, \forall K \in \mathcal{T}_m\} .$$

Suppose there is a subspace $\bar{V}_h$ of V_h for which:

$$\sup_{\mathbf{v}_h \in \bar{V}_h} \frac{1}{|\mathbf{v}_h|_{1,\Omega}} \int_\Omega p_h \operatorname{div} \mathbf{v}_h \geq C_1 \|p_h\|_{0,\Omega} \quad \forall p_h \in \bar{Q}_h \ , \tag{2.8}$$

where C_1 is a positive constant which is independent of h and which is allowed to depend on κ.

(B2) *Reference stability:*

$$\sup_{\mathbf{v}\in V(\hat{K})} \frac{1}{|\mathbf{v}|_{1,\hat{K}}} \int_{\hat{K}} p \operatorname{div} \mathbf{v} \geq C_2 \|p\|_{0,\hat{K}} \quad \forall p \in Q(\hat{K}) \ . \tag{2.9}$$

(B3) *$\mathcal{F}$-uniform reference stability:*

$$\sup_{\mathbf{v}_h\in V(\hat{\mathcal{T}})} \frac{1}{|\mathbf{v}_h|_{1,\hat{K}}} \int_{\hat{K}} p_h \operatorname{div} \mathbf{v}_h \geq C_3 \|p_h\|_{0,\hat{K}} \quad \forall p_h \in Q(\hat{\mathcal{T}}), \tag{2.10}$$

where C_3 is a positive constant which is independent of h and the mesh $\hat{\mathcal{T}} \in \mathcal{F}$.

Under those hypotheses, we have stability of the initial pair (V_h, Q_h). In other words, there exists some positive constant C_4 for which:

$$\sup_{\mathbf{v}_h\in V_h} \frac{1}{|\mathbf{v}_h|_{1,\Omega}} \int_{\Omega} p_h \operatorname{div} \mathbf{v}_h dx \geq C_4 \|p_h\|_{0,\Omega} \quad \forall p_h \in Q_h, \tag{2.11}$$

where C_4 does not depend on the number of macroelements in $\mathcal{T}_m$; it depends only on $C_1(\kappa), C_2, C_3$.

Remark 8 Although this second macroelement technique seems to be a little bit restrictive compared to the first one, it can treat a lot of practical problems. But in the analytical aspect, it is easier to verify since we need to handle only a κ-uniform global smaller problem and problems on the reference domain. Note that the constant C_4 does not depend on the anisotropy of the mesh inside the macroelements. We will see application of this theorem in the subsequent section when we treat realistic spaces. This technique can be found namely in [SSS97].

Proof

The proof uses the Piola transform by exploiting the uniformity property.

Let $q_h \in V_h$. First, we do a similar decomposition as in the previous proof:

$$q_h = q^* + q_m.$$

This decomposition has the property that: $q_m \in \bar{Q}_h$ and $q_K^* := q^*|_K$ belong to $Q(K, \mathcal{T}_K)$ for all macroelement $K \in \mathcal{T}_m$. The idea is to report q_K^* to

the reference domain $\hat{K}$ and apply the known hypothesis on this reference domain.

Consider a macroelement K, we define:

$$q^*_{\hat{K}} := q^*_K \circ F_K \ .$$

The reduced global stability (2.8) ensures the existence of $\mathbf{v}_m \in \bar{V}_h$ such that:

$$\begin{cases} (\operatorname{div} \mathbf{v}_m, q_m)_\Omega \geq C_1 \|q_m\|^2_{0,\Omega} \\ |\mathbf{v}_m|_{1,\Omega} \leq \|q_m\|_{0,\Omega} \ . \end{cases}$$

We have $\mathcal{T}_K = F_K(\hat{\mathcal{T}})$ for some $\hat{\mathcal{T}} \in \mathcal{F}$ if K has more than one element; and $\mathcal{T}_K = F_K(\hat{\mathcal{T}})$ with $\hat{\mathcal{T}} = \hat{K}$ if the macroelement K is only composed of one element which is K itself (refer to previous subsection 2.2.2 for the definition of $\mathcal{T}_K$).

The relations (2.9) and (2.10) imply then the local existence of $\mathbf{v}^*_{\hat{K}} \in V(\hat{\mathcal{T}})$ so that:

$$\begin{cases} (\operatorname{div} \mathbf{v}^*_{\hat{K}}, q^*_{\hat{K}})_{\hat{K}} \geq \tilde{C} \|q^*_{\hat{K}}\|^2_{0,\hat{K}} \\ |\mathbf{v}^*_{\hat{K}}|_{1,\hat{K}} \leq \|q^*_{\hat{K}}\|_{0,\hat{K}} \ . \end{cases} \tag{2.12}$$

Let $\mathbf{v}^*_K$ be the Piola transform of $\mathbf{v}^*_{\hat{K}}$. That means:

$$\mathbf{v}^*_K := |J_K|^{-1} J_K \mathbf{v}^*_{\hat{K}} \circ F_K^{-1},$$

where J_K is the Jacobian of F_K and $|J_K|$ is its determinant. Since J_K is constant, $\mathbf{v}^*_K$ belong to $V(K, \mathcal{T}_K)$.

A property of Piola transforms gives (see Lemma 1.5 of [BF91]):

$$(\operatorname{div} \mathbf{v}^*_{\hat{K}}, q^*_{\hat{K}})_{\hat{K}} = (\operatorname{div} \mathbf{v}^*_K, q^*_K)_K.$$

Consequently, we have the following inequality thanks to the relation (2.12):

$$(\operatorname{div} \mathbf{v}^*_K, q^*_K)_K \geq \tilde{C} \|q^*_{\hat{K}}\|^2_{0,\hat{K}} \geq \frac{C}{h(K)^d} \tilde{C} \|q^*_K\|^2_{0,K}, \tag{2.13}$$

where C is a constant which does not depend on any parameter ($C = 1$ in the case $\hat{K} = (0,1)^2$ and K is a rectangle).

An analogous application of the scaling argument to the Piola transform provides:

$$|\mathbf{v}_K^*|_{1,K} \leq C_2 \frac{h(K)}{\rho(K)^{1+\frac{d}{2}}} |\mathbf{v}_{\hat{K}}^*|_{1,\hat{K}} \leq C_2 \frac{h(K)}{\rho(K)^{1+\frac{d}{2}}} \|q_{\hat{K}}^*\|_{0,\hat{K}} \leq C_2 \frac{h(K)}{\rho(K)^{1+d}} \|q_K^*\|_{0,K} \ . \tag{2.14}$$

If we define $\mathbf{u}_K^* \in V(K, \mathcal{T}_K)$ by the following scaling:

$$\mathbf{u}_K^* = \frac{\rho(K)^{1+d}}{C_2 h(K)} . \mathbf{v}_K^* \ ,$$

then relations (2.14) and (2.13) become:

$$(\operatorname{div} \mathbf{u}_K^*, q_K^*)_K \geq \frac{C}{C_2} \frac{\rho(K)^{1+d}}{h(K)^{1+d}} \|q_K^*\|_{0,K}^2 \quad \text{and} \quad |\mathbf{u}_K^*|_{1,K} \leq \|q_K^*\|_{0,K} \ .$$

Let us define $\gamma := \frac{C}{C_2} \frac{1}{\kappa^{1+d}}$. Therefore, the uniformity of the macroelement partitioning, that we have discussed in the relation (2.7), together with the last equations give:

$$(\operatorname{div} \mathbf{u}_K^*, q_K^*)_K \geq \gamma \|q_K^*\|_{0,K}^2 \quad \text{and} \quad |\mathbf{u}_K^*|_{1,K} \leq \|q_K^*\|_{0,K} \ .$$

Let us now introduce

$$\mathbf{v}^* := \sum_{K \in \mathcal{T}_m} \bar{\mathbf{u}}_K^* \ ,$$

where $\bar{\mathbf{u}}_K^*$ is the zero extension of $\mathbf{u}_K^*$ in the whole domain Ω.

We may note that $\mathbf{v}^*$ belongs to V_h. Besides, we have:

$$\begin{cases} (\operatorname{div} \mathbf{v}^*, q^*)_\Omega \geq \gamma \|q^*\|_{0,\Omega}^2 \\ |\mathbf{v}^*|_{1,\Omega} \leq \|q^*\|_{0,\Omega} \ . \end{cases}$$

The continuation of the proof is just like in the proof of the preceding theorem. That means, we define

$$\mathbf{v} = \mathbf{v}^* + \delta \mathbf{v}_m \ ,$$

where $\delta > 0$ will be suitably chosen in order to obtain:

$$\begin{cases} (\operatorname{div} \mathbf{v}, q)_\Omega \geq C_4 \|q\|_{0,\Omega}^2 \\ |\mathbf{v}|_{1,\Omega} \leq \|q\|_{0,\Omega} \ . \end{cases}$$

Chapter 3

The $Q_2 - Q_0$ pair

In this section, we approximate the velocity by functions whose components are piecewise Q_2 and we approximate the pressure by piecewise constant functions. For the isotropic case, the proof of the stability of this pair can be found in many documents (see [GR86],[BF91]). In the following discussion, we show that we still have stability for the anisotropic mesh in meshes which will be explained later on. To that end, we invoke the macroelement techniques. In the first section, we deal with stability on the reference domain with stripped mesh. The second section treats stability on the reference element with corner mesh. And in the last section, we collect everything with the help of the macroelement techniques in order to conclude the stability throughout the whole domain Ω.

3.1 Uniform reference stability on a stripped mesh

Definition

In the following analysis, we consider the domain $\hat{Q} = (-1,1)^2$. $\mathcal{T}_x$ is supposed to be an arbitrary discretization of $I = (-1,1)$. We define the grid $\mathcal{T}$ as the tensor product mesh (see Figure 3.1):

$$\mathcal{T} = \{T : T = T_x \times I, T_x \in \mathcal{T}_x\}.$$

We aim at establishing the inf-sup condition in $\hat{Q}$ independently of $\mathcal{T}_x$.

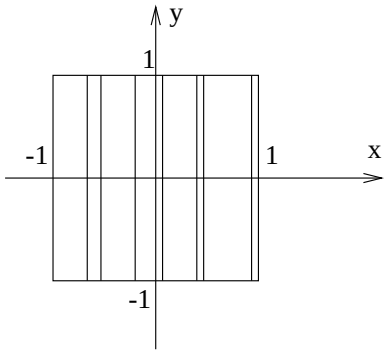

Figure 3.1: stripped mesh.

Theorem 10 Define the discrete velocity and pressure spaces as:

$$V = \{v \in H_0^1(\hat{Q}) : v|_T \circ F_T \in Q_2(\hat{Q}) \quad \forall T \in \mathcal{T}\}$$

$$Q = \{q \in L_0^2(\hat{Q}) : q|_T \circ F_T \in Q_0(\hat{Q}) \quad \forall T \in \mathcal{T}\},$$

where F_T is the affine mapping from $\hat{Q}$ to T.

Then the inf-sup condition holds with a constant which is independent of the discretization $\mathcal{T}_x$. That means:

$$\inf_{0 \neq p \in Q} \sup_{0 \neq \mathbf{v} \in V^2} \frac{(\operatorname{div} \mathbf{v}, p)}{|\mathbf{v}|_{1,\Omega} \|p\|_{0,\Omega}} \geq C, \tag{3.1}$$

where $C = C(\hat{Q})$.

We will prove this theorem when enough definitions and properties are introduced.

Definition

First we define the following space:

$$H(\hat{Q}) := \left\{ v \in H^1(\hat{Q}) : v|_{\Gamma_1} = v|_{\Gamma_3} = 0 \right\},$$

where Γ_1 and Γ_3 are the boundary sections given in:

$$\begin{aligned}
\Gamma_1 &:= \{(x,y) \in \mathbf{R}^2 : x \in (-1,1),\ y = -1\}, \\
\Gamma_2 &:= \{(x,y) \in \mathbf{R}^2 : x = 1,\ y \in (-1,1)\}, \\
\Gamma_3 &:= \{(x,y) \in \mathbf{R}^2 : x \in (-1,1),\ y = 1\}, \\
\Gamma_4 &:= \{(x,y) \in \mathbf{R}^2 : x = -1,\ y \in (-1,1)\}.
\end{aligned}$$

And let us introduce a projection $\pi^{\hat{Q}}$

$$\pi^{\hat{Q}} : H(\hat{Q}) \longrightarrow H(\hat{Q}) \cap Q_2(\hat{Q}), \text{ by:}$$

for $v \in H(\hat{Q})$, $\pi^{\hat{Q}} v$ is defined as the only function in $H(\hat{Q}) \cap Q_2(\hat{Q})$ satisfying:

$$(\pi^{\hat{Q}} v)(M_i) = 0 \qquad i = 1, 2, 3, 4 \tag{3.2}$$

$$\int_{\Gamma_i} (\pi^{\hat{Q}} v)(s) ds = \int_{\Gamma_i} v(s) ds \qquad i = 1, 2, 3, 4 \tag{3.3}$$

$$\int_{\hat{Q}} (\pi^{\hat{Q}} v)(\mathbf{x}) d\mathbf{x} = \int_{\hat{Q}} v(\mathbf{x}) d\mathbf{x} \tag{3.4}$$

where M_i are the four corner nodes:

$$M_1 = (-1, -1), \quad M_2 = (1, -1), \quad M_3 = (1, 1), \quad M_4 = (-1, 1).$$

Before we prove Theorem 10, we shall need to state the following lemma which gives some important properties of the projection $\pi^{\hat{Q}}$.

Lemma 4 There exists a constant C such that:

$$\begin{aligned} \|(\pi^{\hat{Q}} v)_{\hat{x}}\|^2_{0,\hat{Q}} &\leq C \|v_{\hat{x}}\|^2_{0,\hat{Q}} \\ \|(\pi^{\hat{Q}} v)_{\hat{y}}\|^2_{0,\hat{Q}} &\leq C (\|v_{\hat{y}}\|^2_{0,\hat{Q}} + \|v\|^2_{\frac{1}{2},00,\Gamma_2} + \|v\|^2_{\frac{1}{2},00,\Gamma_4}), \end{aligned}$$

for all $v \in H(\hat{Q})$.

Proof

The proof of this lemma is extremely long and it can be found for example in [SS97].

Definition For all elements T of $\mathcal{T}$, define:

$$\pi^T : H(T) \longrightarrow H(T) \cap Q_2(T)$$

$$\pi^T v := [\pi^{\hat{Q}}(v \circ F_T)] \circ F_T^{-1},$$

where

$$H(T) := \{v \in H^1(T) : v \circ F_T \in H(\hat{Q})\}.$$

Theorem 11 Consider an element $T \in \mathcal{T}$. There exists a constant $C > 0$ which does not depend upon T such that:

$$|\pi^T v|^2_{1,T} \leq C |v|^2_{1,T} \qquad \forall\, v \in H(T).$$

Proof

By using the continuity (Take $p = 2$ in the Theorem 1.5.2.3 of [Gri85] on page 43) of the trace operator

$$\begin{array}{rcl} \gamma : H(\hat{Q}) & \longrightarrow & H_{00}^{\frac{1}{2}}(\Gamma_2) \times H_{00}^{\frac{1}{2}}(\Gamma_4) \\ v & \rightarrow & (v|_{\Gamma_2}, v|_{\Gamma_4}), \end{array}$$

we can see the existence of some constant $C = C(\hat{Q}) > 0$ such that:

$$\|v\|^2_{\frac{1}{2},00,\Gamma_2} + \|v\|^2_{\frac{1}{2},00,\Gamma_4} \leq C|v|^2_{1,\hat{Q}} \quad \forall v \in H(\hat{Q}), \tag{3.5}$$

after applying the Poincaré inequality.

Due to Lemma 4 and the relation (3.5), we may write the following inequality:

$$\|(\pi^{\hat{Q}}v)_{\hat{y}}\|^2_{0,\hat{Q}} \leq C(\|v_{\hat{y}}\|^2_{0,\hat{Q}} + |v|^2_{1,\hat{Q}}) \quad \forall\, v \in H(\hat{Q}). \tag{3.6}$$

Consider now an element T of $\mathcal{T}$. It is consequently of the form

$$T = (x_1, x_2) \times (-1, 1) \qquad \text{with } -1 \leq x_1 < x_2 \leq 1.$$

Define $\delta := \frac{1}{2}(x_2 - x_1)$. As a result, it is seen that the affine mapping F_T is provided by:

$$\left\{ \begin{array}{rcl} x & = & \delta\hat{x} + \frac{1}{2}(x_1 + x_2) \\ y & = & \hat{y}. \end{array} \right.$$

By this change of variables, we can easily conclude in integration that:

$$\begin{array}{lll} \|(v \circ F_T)_{\hat{x}}\|^2_{0,\hat{Q}} = \delta\|v_x\|^2_{0,T} & , & \|(\pi^{\hat{Q}}[v \circ F_T])_{\hat{x}}\|^2_{0,\hat{Q}} = \delta\|(\pi^T v)_x\|^2_{0,T} \\ \|(v \circ F_T)_{\hat{y}}\|^2_{0,\hat{Q}} = \frac{1}{\delta}\|v_y\|^2_{0,T} & , & \|(\pi^{\hat{Q}}[v \circ F_T])_{\hat{y}}\|^2_{0,\hat{Q}} = \frac{1}{\delta}\|(\pi^T v)_y\|^2_{0,T}. \end{array}$$

Hence we have $|v \circ F_T|^2_{1,\hat{Q}} \leq \frac{1}{\delta}|v|^2_{1,T}$. Due to the previous lemma, we have:

$$\delta\|(\pi^T v)_x\|^2_{0,T} = \|(\pi^{\hat{Q}}[v \circ F_T])_{\hat{x}}\|^2_{0,\hat{Q}} \leq C\|(v \circ F_T)_{\hat{x}}\|^2_{0,\hat{Q}} = \delta C\|v_x\|^2_{0,T}\ .$$

Hence

$$\|(\pi^T v)_x\|^2_{0,T} \leq C\|v_x\|^2_{0,T}. \tag{3.7}$$

With the help of (3.6), we have:

$$\|(\pi^{\hat{Q}}[v \circ F_T])_{\hat{y}}\|^2_{0,\hat{Q}} \leq C(\|(v \circ F_T)_{\hat{y}}\|^2_{0,\hat{Q}} + |v \circ F_T|^2_{1,\hat{Q}}).$$

And so:

$$\frac{1}{\delta}\|(\pi^T v)_y\|^2_{0,T} \leq C(\frac{1}{\delta}\|v_y\|^2_{0,T} + \frac{1}{\delta}|v|^2_{1,T}).$$

Hence we obtain:

$$\|(\pi^T v)_y\|^2_{0,T} \leq C(\|v_y\|^2_{0,T} + |v|^2_{1,T}). \tag{3.8}$$

We can conclude from (3.7) and (3.8) that:

$$|\pi^T v|^2_{1,T} \leq C|v|^2_{1,T}.$$

Definition

For $\mathbf{v} = (v_1, v_2) \in [H(T)]^2$, we define

$$\Pi^T \mathbf{v} := (\pi^T v_1, \pi^T v_2).$$

Lemma 5 Consider an element T of $\mathcal{T}$ and $\mathbf{v} \in [H(T)]^2$. Then for all $p \in Q_0(T)$ (i. e. locally constant), we have:

$$(\operatorname{div} \mathbf{v}, p)_T = (\operatorname{div} \Pi^T \mathbf{v}, p)_T.$$

Proof

If we denote by $\mathbf{n}$ the unit exterior normal vector to ∂T, then the Green formula gives:

$$(\operatorname{div} \mathbf{v}, p)_T = \int_{\partial T} (\mathbf{v} \cdot \mathbf{n})\, p \quad \text{because } p \text{ is constant.}$$

For the considered T, its four edges $\Gamma_1(T)$, $\Gamma_2(T)$, $\Gamma_3(T)$, $\Gamma_4(T)$ will be defined in a similar way as in the definition of Γ_1, Γ_2, Γ_3, Γ_4.

In $\Gamma_1(T)$, $\mathbf{n} = \begin{pmatrix} 0 \\ -1 \end{pmatrix}$. In the continuation of the proof, $\mathbf{v}$ will be written componentwise as $\mathbf{v} = (v_1, v_2)$.

$$\begin{aligned}
\int_{\Gamma_1(T)} \mathbf{v}.\mathbf{n}\, p &= -\int_{\Gamma_1(T)} v_2\, p = -p \int_{\Gamma_1(T)} v_2(\mathbf{x}) d\mathbf{x} \\
&= -p \int_{\Gamma_1} v_2 \circ F_T(\hat{\mathbf{x}})\, \delta\, d\hat{\mathbf{x}} = -p \int_{\Gamma_1} \pi^{\hat{Q}}(v_2 \circ F_T)\, \delta\, d\hat{\mathbf{x}} \\
&= -p \int_{\Gamma_1(T)} [\pi^{\hat{Q}}(v_2 \circ F_T)] \circ F_T^{-1} d\mathbf{x} \\
&= -p \int_{\Gamma_1(T)} \pi^T v_2 d\mathbf{x} = \int_{\Gamma_1(T)} (\Pi^T \mathbf{v}).\mathbf{n}\, p\, d\mathbf{x}.
\end{aligned}$$

We can repeat the same thing for $\Gamma_2(T), \Gamma_3(T), \Gamma_4(T)$. And so we should obtain afterwards that:

$$\int_{\partial T} (\mathbf{v}.\mathbf{n})\, p = \int_{\partial T} ((\Pi^T \mathbf{v}).\, \mathbf{n})\, p \ .$$

Making use of the Green formula anew and taking into consideration the fact that p is constant we obtain:

$$\int_{\partial T} ((\Pi^T \mathbf{v}).\, \mathbf{n})\, p = (\mathrm{div}(\Pi^T \mathbf{v}),\, p)_T$$

And the lemma is consequently proved.

Proof of Theorem 10

With the help of the local projections Π^T, we can define element-wise a projection Π on the whole $[H_0^1(\hat{Q})]^2$:

$$\Pi : [H_0^1(\hat{Q})]^2 \longrightarrow V,$$

such that for $\mathbf{v} \in [H_0^1(\hat{Q})]^2$,

$$(\Pi \mathbf{v})|_T := \Pi^T(\mathbf{v}|_T), \quad \forall T \in \mathcal{T}$$

The continuity of $(\Pi \mathbf{v})$ across interelements is evident because of (3.2) and (3.3). According to Lemma 5 and Theorem 11, there is $C_1 = C_1(\hat{Q})$ with:

$$\begin{array}{rcll} (\mathrm{div}\, \mathbf{v}, p) & = & (\mathrm{div}\, \Pi \mathbf{v}, p) & \forall\, p \in\ Q, \\ |\Pi \mathbf{v}|_{1,\Omega} & \leq & C_1 |\mathbf{v}|. & \end{array}$$

On the other hand, we have the continuous inf-sup condition:

$$\inf_{0 \neq p \in L_0^2(\hat{Q})} \sup_{0 \neq \mathbf{v} \in [H_0^1(\hat{Q})]^2} \frac{(\mathrm{div}\, \mathbf{v}, p)}{|\mathbf{v}|_{1,\hat{Q}} \|p\|_{0,\hat{Q}}} \geq C_2(\hat{Q}) > 0.$$

According to Fortin's lemma (see Lemma 3), we conclude the evidence of the discrete inf-sup (3.1) with $C = \frac{C_2(\hat{Q})}{C_1(\hat{Q})}$.

And we conclude at the same time that C is a constant depending only on $\hat{Q}$.

3.2 How can corner problems be handled?

In this section it will be detailed how corner problems are handled. We will need the result from the first section here.

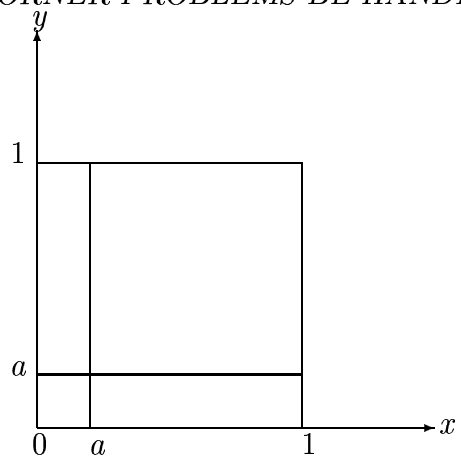

Figure 3.2: The examined domain and its grid.

3.2.1 Trouble with the corner

In a quite general mesh for a corner grid, we cannot expect any unconditional stability. The following very simple experiment that has been investigated in [SSS97] illustrates that fact.

We have done a program in C++ in order to reconstruct the inf-sup results which had been reported in [SSS97]. The generalized eigenvalue problem that we have discussed in Property 1 of section 1.6 was used in order to perform the numerical evaluations of LBB-constants. The mesh is explained graphically in Figure 3.2. The numerical experiment consists of varying the value of a and analyzing the inf-sup constants. The result of the numerical test is to be found in Figure 3.3. It can be very well seen that the inf-sup constants tend to zero as the mesh becomes anisotropic. And that fact shows precisely that the stability result is a function of the aspect ratio.

We need however to find some remedy for that problem, and that is the purpose of this section. We will see that we have stability on the reference element with a tensor product geometric mesh independently of the aspect ratio.

3.2.2 Stability on a geometric tensor product mesh

Explanation of $\Delta^2_{n,\sigma}$ and $\Delta_{n,\sigma}$

First, we need to explain the mesh for which we have stability. To that end, we need to take a real positive parameter $\sigma \in (0,1)$ which will be the

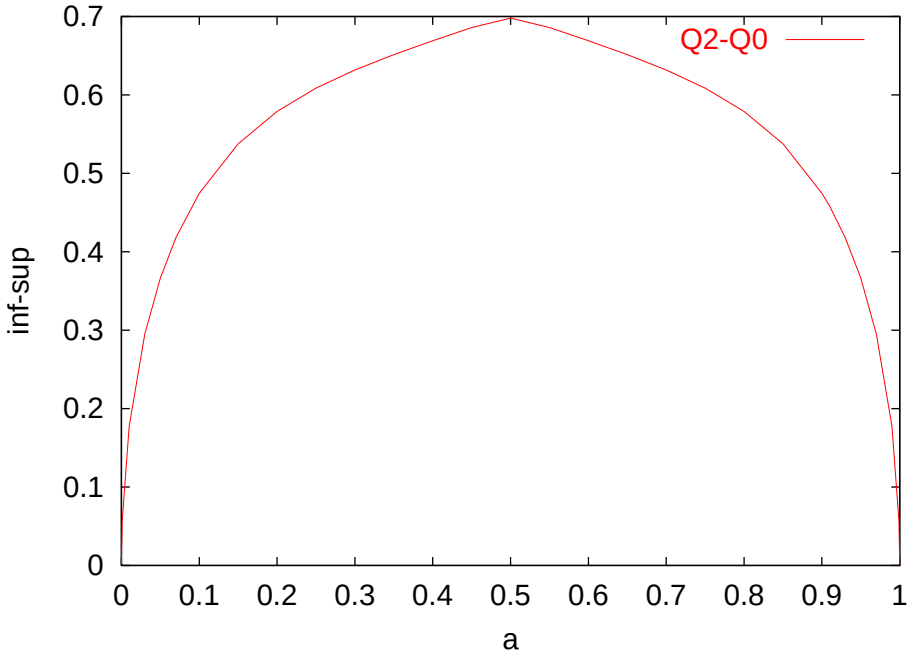

Figure 3.3: Inf-sup of $Q_2 - Q_0$ in function of a.

geometric grading factor. In this section the domain of study will always be the unit square $\hat{Q} = (0,1)^2$. Let us consider an integer parameter $n \in \mathbf{N}$. The x-unit interval $I_x = (0,1)$ will first be refined geometrically towards the origin 0. In other words, we subdivide it into subintervals $I_i = (x_{i-1}, x_i)$, $i = 1, ..., n+1$, with

$$\left\{ \begin{array}{rcl} x_0 & = & 0 \\ x_i & = & \sigma^{n+1-i}. \end{array} \right.$$

Afterwards, we do the same thing for the y-unit interval $I_y = (0,1)$. The mesh $\Delta^2_{n,\sigma}$ on $\hat{Q}$ will then be the tensor product of the resulting refinement along the x and the y axes. A graphical illustration can be found in the following figure (Figure 3.4) for the case $n = 4$ and the geometric grading factor is $\sigma = 0.5$. $\Delta^2_{n,\sigma}$ is displayed in the left mesh. To prove the stability on $\Delta^2_{n,\sigma}$, we want again the macroelement technique and the result from the stripped mesh.

The macroelement partitioning that we will consider then is the isotropic mesh $\Delta_{n,\sigma}$ which is drawn in solid line in right hand side of Figure 3.4. We need therefore a reduced stability on $\Delta_{n,\sigma}$. We cannot just apply the well

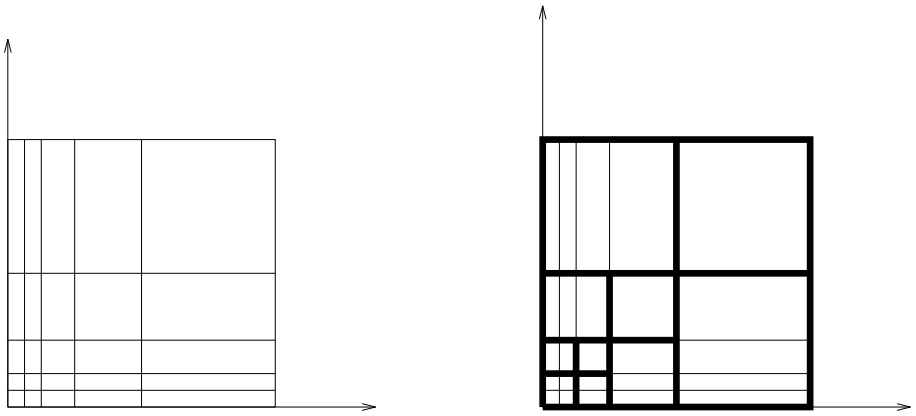

Figure 3.4: $\Delta^2_{n,\sigma}$ and the underlying macroelement.

known stability result from the standard isotropic analysis to $\Delta_{n,\sigma}$, because $\Delta_{n,\sigma}$ contains nonconforming nodes. In the next figure the scheme of $\Delta_{n,\sigma}$ without the mesh $\Delta^2_{n,\sigma}$ is reported in order to see that fact clearly. One can then find there the existence of a lot of hanging nodes.

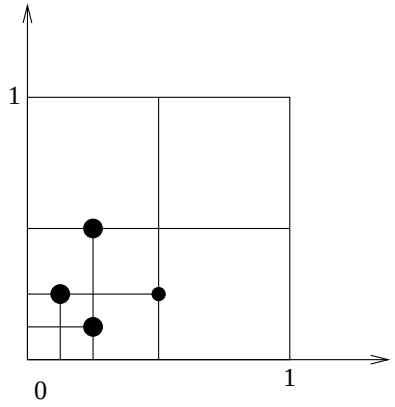

Figure 3.5: $\Delta_{n,\sigma}$ and its hanging nodes.

Statement of stability on $\Delta^2_{n,\sigma}$

We are now able to state the main result of divergence stability on the geometric tensor product mesh $\Delta^2_{n,\sigma}$. The following theorem states that fact precisely.

Theorem 12 Let us define

$$\begin{aligned} V_{h,\sigma} &= \{u \in H_0^1(\hat{Q}) : u|_T \in Q_2(T)\ \forall T \in \Delta_{n,\sigma}^2\} \\ Q_{h,\sigma} &= \{p \in L_0^2(\hat{Q}) : p|_T \in Q_0(T)\ \forall T \in \Delta_{n,\sigma}^2\}. \end{aligned}$$

Then we have stability, i.e. there exists a positive constant C for which:

$$\inf_{0 \neq p_h \in Q_{h,\sigma}} \sup_{0 \neq \mathbf{v}_h \in V_{h,\sigma}^2} \frac{(\operatorname{div} \mathbf{v}_h, p_h)}{|\mathbf{v}_h|_{1,\Omega} \|p_h\|_{0,\Omega}} \geq C, \tag{3.9}$$

where C is independent of n and the aspect ratio of each element. C depends only on $\hat{Q}$ and the geometric grading factor σ.

We will prove this theorem later on. But we need first to see a lot of preliminary results which will be the main purpose of the next two subsections.

3.2.3 Preliminary definitions and results

Introduction of the domains K_{ij} and the j-th layers

We label first the macroelements of $\Delta_{n,\sigma}$. More precisely, we adopt the following numbering:

$$\Delta_{n,\sigma} = \{K_{11}\} \cup \{K_{ij} : 1 \leq i \leq 3,\ 2 \leq j \leq n+1\}.$$

The numbering of K_{ij} are well explained in Figure 3.6. In the sequel, the reunion $K_{1j} \cup K_{2j} \cup K_{3j}$ will be referred to as the layer number j.

The space $S_{n,\sigma}$

Before going further, we want to introduce a space which is of extreme importance to the proof of the reduced global stability. For all macroelement $K \in \Delta_{n,\sigma}$, let us first define the local space $\mathcal{L}^1(K)$ which will be strictly located between the spaces $\mathcal{Q}_1^2$ and $\mathcal{Q}_2^2$. For any considered macroelement K of the mesh $\Delta_{n,\sigma}$ with vertices a_1, a_2, a_3 and $a_4 = a_0$, let f_i stand for the edge $[a_{i-1}, a_i]$. Furthermore, we will denote the outward normal to f_i by $\mathbf{n}_i$. We define $\hat{a}_i$, $\hat{f}_i$, $\hat{\mathbf{n}}_i$ similarly on the reference domain $\hat{Q}$.

Now we define first some reference polynomials:

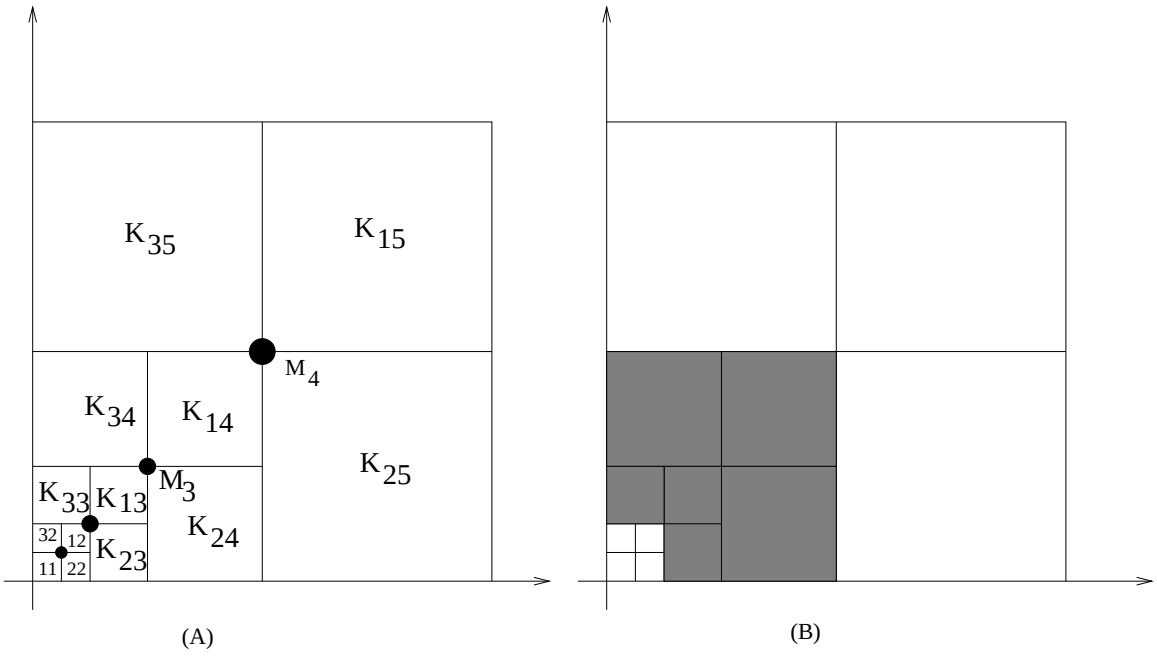

Figure 3.6: K_{ij} and the support of the basis function ϕ_i.

$$\begin{aligned}\hat{q}_1 &:= \hat{x}_2\hat{x}_3\hat{x}_4,\\ \hat{q}_2 &:= \hat{x}_1\hat{x}_3\hat{x}_4,\\ \hat{q}_3 &:= \hat{x}_1\hat{x}_2\hat{x}_4,\\ \hat{q}_4 &:= \hat{x}_1\hat{x}_2\hat{x}_3,\end{aligned}$$

where $\hat{x}_1, \hat{x}_2$ are the two basic reference variables and $\hat{x}_3$ and $\hat{x}_4$ are defined by:

$$\hat{x}_3 := 1 - \hat{x}_1, \quad \hat{x}_4 := 1 - \hat{x}_2.$$

The local space $\mathcal{L}^1(K)$ is then defined by:

$$\mathcal{L}^1(K) := \mathcal{Q}_1(K)^2 \oplus \text{span}(\mathbf{p}_1, \mathbf{p}_2, \mathbf{p}_3, \mathbf{p}_4),$$

where the functions $\mathbf{p}_i$ are the functions defined on K by:

$$\mathbf{p}_i = \mathbf{n}_i(\hat{q}_i \circ F_K^{-1}) \quad i = 1, ..., 4.$$

Finally, the space $S_{n,\sigma}$ will then be defined as:

$$S_{n,\sigma} = \{\mathbf{u} \in H_0^1(\hat{Q})^2 : \mathbf{u}|_K \in \mathcal{L}^1(K) \quad \forall K \in \Delta_{n,\sigma}\}.$$

A Clément type interpolant

In this part, we are going to discuss about an interpolation which acts similarly as the Clément interpolant on the mesh $\Delta_{n,\sigma}$. Given a function u in $H_0^1(\Omega)$, its interpolant Iu will belong to the following discrete space:

$$R_{n,\sigma} = \{u \in H_0^1(\hat{Q}) \cap \mathcal{C}(\hat{Q}) : \ u|_K \circ F_K \in \mathcal{Q}_1(\hat{K}) \quad \forall K \in \Delta_{n,\sigma}\}.$$

We should first remark that this space $R_{n,\sigma}$ has only degrees of freedom at the nodes M_i, $i = 1, .., n$ which have coordinates:

$$M_i = (\sigma^{n+1-i}, \sigma^{n+1-i}) \quad i = 1, 2, ..., n.$$

They are represented by solid points in Figure 3.6. We shall drop the index n sometimes in the sequel. The precise expression of the interpolant Iu is given by:

$$Iu := \sum_{i=1}^{n} \beta_i \phi_i,$$

where ϕ_i is the usual basis function at the node M_i, that is: $\phi_i \in R_{n,\sigma}$ and $\phi_i(M_j) = \delta_{ij}$. Besides, the coefficient β_i is given by the following expression:

$$\beta_i = \frac{1}{\text{meas}(\text{supp}(\phi_i))} \int_{\text{supp}(\phi_i)} u dx.$$

We note now that supp ϕ_i, the support of the function ϕ_i, is given by the reunion of the i-th and the $(i+1)$-th layers. It can be seen graphically in Figure 3.6. The following lemma will be stated but the proof will not be given here. Readers who are interested in knowing the proof are well advised to see the paper [SSS97].

Lemma 6 We have the following estimates for all u in $H_0^1(\Omega)$:

$$\sum_{K \in \Delta_{n,\sigma}} \frac{1}{h(K)^2} \|u - Iu\|_{0,K}^2 + \sum_{K \in \Delta_{n,\sigma}} |u - Iu|_{1,K}^2 + \sum_{e \in E_{n,\sigma}} \frac{1}{h_e} \|u - Iu\|_{0,e}^2 \leq C |u|_{1,\hat{Q}}^2, \tag{3.10}$$

and

$$\|Iu\|^2_{1,\hat{Q}} \leq C|u|^2_{1,\hat{Q}}, \tag{3.11}$$

where C is a positive constant which depends only on the mesh geometric grading factor σ. In the preceding estimate, we used the following notations:

$$\begin{array}{rcl} E_{n,\sigma} & = & \{e : e \text{ edge of} K,\ K \in \Delta_{n,\sigma}\} \\ h_e & := & \text{length of the edge } e \\ h(K) & := & \text{diameter of the macroelement } K. \end{array}$$

3.2.4 Proof of the stability on $\Delta^2_{n,\sigma}$

Reduced global stability on $S_{n,\sigma}$

In order to prove the stability in the mesh $\Delta^2_{n,\sigma}$, we need to see the reduced global stability on the macroelement partitioning which is $\Delta_{n,\sigma}$. That is precisely the purpose of Lemma 8 which we will prove carefully. Remember that we need only to see the stability on a subspace of the discrete velocity space.

Lemma 7 If we define the following local partitions:

$$\begin{array}{rcl} N_1 & := & K_{11} \cup K_{22} \cup K_{12} \cup K_{32} \\ N_j & := & \{K_{ik} : 1 \leq i \leq 3,\ j \leq k \leq j+1\}, \end{array}$$

and if we introduce the local spaces:

$$\begin{array}{rcl} R(N_j) & := & \{p \in L^2(N_j) : p|_K \in \mathcal{Q}_0(K)\ \forall K \subset N_j\} \\ L(N_j) & := & \{\mathbf{v} \in \mathcal{C}(N_j)^2 : \mathbf{v}|_K \in \mathcal{L}^1(K)\ \forall K \subset N_j\} \\ L_0(N_j) & := & L(N_j) \cap H^1_0(N_j)^2, \end{array}$$

then the following subspace is one-dimensional and consists of functions which are constant in N_j,

$$N_{N_j} := \{p \in R(N_j) : \ (\operatorname{div} \mathbf{v}, p)_{N_j} = 0 \quad \forall \mathbf{v} \in L_0(N_j)\}.$$

Proof of Lemma 7: See [SSS97].

Lemma 8 (reduced global stability on $S_{n,\sigma}$) On the mesh $\Delta_{n,\sigma}$, we have stability of the space $S_{n,\sigma}$ and the piecewise constant pressure with an inf-sup

constant which is independent of n and the aspect ratio and which depends solely on the mesh grading factor σ, i.e. we have:

$$\inf_{0\neq p_h\in R_h}\sup_{0\neq \mathbf{v}_h\in S_{n,\sigma}}\frac{(\operatorname{div}\mathbf{v}_h,p_h)}{|\mathbf{v}_h|_{1,\Omega}\|p_h\|_{0,\Omega}}\geq C\ , \tag{3.12}$$

where

$$R_h=\{p_h\in L^2_0(\Omega):\ p_h|_K \text{ is constant } \forall K\in\Delta_{n,\sigma}\}.$$

Proof of Lemma 8:

Let us consider a nonzero function $p\in R_h$. By virtue of the continuous inf-sup condition, we can find $\mathbf{v}=(v_1,v_2)\in H^1_0(\hat{Q})^2$ satisfying:

$$(\operatorname{div}\mathbf{v},p)_{\hat{Q}}\geq C_3\|p\|^2_{0,\hat{Q}}\quad |\mathbf{v}|_{1,\hat{Q}}\leq\|p\|_{0,\hat{Q}}, \tag{3.13}$$

where C_3 is a constant which depends only on $\hat{Q}$.

Let us define $\mathbf{v}_h=(Iv_1,Iv_2)\in R_{n,\sigma}$, where I is the Clément type interpolation defined earlier. We have therefore the following:

$$(\operatorname{div}\mathbf{v}_h,p)_{\hat{Q}}=(\operatorname{div}(\mathbf{v}_h-\mathbf{v}),p))_{\hat{Q}}+(\operatorname{div}\mathbf{v},p)_{\hat{Q}}. \tag{3.14}$$

We shall adopt the notation which was given in Lemma 7. Furthermore, we denote by $E(N_j)$ the set of all edges of N_j which are not on the boundary ∂N_j. Next, let us introduce:

$$E_0(N_j)=\{e\in E(N_j):\ e \text{ has no hanging node in the mid-point.}\}$$

$E(\Delta_{n,\sigma})$ and $E_0(\Delta_{n,\sigma})$ are defined similarly but with respect to the whole mesh $\Delta_{n,\sigma}$. We will also need the following quantities:

$$|p|^2_{N_j}:=\sum_{K\subset N_j}h(K)^2\|\mathbf{grad}\,p\|^2_{0,K}+\sum_{e\in E_0(N_j)}h_e\int_e|[p]_e|^2ds\quad\forall p\in R(N_j),$$

$$|p|^2_{h,\hat{Q}}:=\sum_{K\in\Delta_{n,\sigma}}h(K)^2\|\mathbf{grad}\,p\|^2_{0,K}+\sum_{e\in E_0(\Delta_{n,\sigma})}h_e\int_e|[p]_e|^2ds.$$

The latter is in fact a semi-norm in R_h. For an edge e of a macroelement K, $[p]_e$ stands for the jump of p across e. It is:

$$[p]_e(\mathbf{x})=\lim_{t\to0^+}p(\mathbf{x}+t\mathbf{n})-\lim_{t\to0^+}p(\mathbf{x}-t\mathbf{n})\quad\forall\mathbf{x}\in e,$$

where $\mathbf{n}$ is the unit normal pointing outward from K.

Applications of a partial integration, (3.13), and the Cauchy Schwarz inequality to the relation (3.14) yield:

$$(\operatorname{div}\mathbf{v}_h, p)_{\hat{Q}} \geq \sum_{K\in\Delta_{n,\sigma}} \int_K (\mathbf{v}-\mathbf{v}_h)\cdot\mathbf{grad}\, p + \sum_{e\in E_0(\Delta_{n,\sigma})} \int_e ((\mathbf{v}-\mathbf{v}_h)\cdot\mathbf{n})[p]_e ds + C_3\|p\|^2_{0,\hat{Q}} \tag{3.15}$$

$$\geq -\left\{ \sum_{K\in\Delta_{n,\sigma}} h(K)^{-2}\|\mathbf{v}_h-\mathbf{v}\|^2_{0,K} + \sum_{e\in E_0(\Delta_{n,\sigma})} h_e^{-1}\|\mathbf{v}_h-\mathbf{v}\|^2_{0,e} \right\}^{\frac{1}{2}} |p|_{h,\hat{Q}} + C_3\|p\|^2_{0,\hat{Q}}. \tag{3.16}$$

According to the property (3.10) of the Clément type interpolation, we have:

$$(\operatorname{div}\mathbf{v}_h, p) \geq -C_2|\mathbf{v}|_{1,\hat{Q}}|p|_{h,\hat{Q}} + C_3\|p\|^2_{0,\hat{Q}} \geq \|p\|^2_{0,\hat{Q}}\left(C_3 - C_2\frac{|p|_{h,\hat{Q}}}{\|p\|_{0,\hat{Q}}}\right),$$

because of (3.13). It is worth remarking that C_2 depends solely on σ.

An application of the Clément type interpolation property (3.11) gives $|\mathbf{v}_h|_{1,\hat{Q}} \leq C\|p\|_{0,\hat{Q}}$, with a constant C depending on σ. As a consequence, we have:

$$\frac{(\operatorname{div}\mathbf{v}_h, p)_{\hat{Q}}}{|\mathbf{v}_h|_{1,\hat{Q}}} \geq \|p\|_{0,\hat{Q}}\left(C_4 - C_5\frac{|p|_{h,\hat{Q}}}{\|p\|_{0,\hat{Q}}}\right). \tag{3.17}$$

On the other hand, we can have an orthogonal decomposition of $R(N_j)$ in $L^2(N_j)$:

$$R(N_j) = N_{N_j} \oplus W_{N_j}, \tag{3.18}$$

where W_{N_j} is the orthogonal complement of N_{N_j}.

According to Lemma 7, N_{N_j} is one dimensional and consists of functions which are constant in N_j.

Therefore Lemma 3.1 in [Ste84] implies

$$\sup_{\mathbf{0}\neq\mathbf{v}\in L_0(N_j)} \frac{(\operatorname{div}\mathbf{v}, p)_{N_j}}{|\mathbf{v}|_{1,N_j}|p|_{N_j}} \geq \gamma > 0 \quad \forall\, p \in W_{N_j}\setminus\{0\}, \tag{3.19}$$

where γ is independent of j but depending on σ.

Let us now denote by $p_j := p|_{N_j}$. Due to the decomposition (3.18), we have

$$p_j = c_j + q_j \quad \text{with } q_j \in W_{N_j}.$$

According to (3.19), there exists $\mathbf{v}_j \in L_0(N_j)$ such that :

$$(\operatorname{div} \mathbf{v}_j, q_j)_{N_j} \geq \gamma |q_j|^2_{N_j} \quad |\mathbf{v}_j|_{1,N_j} \leq |q_j|_{N_j}, \tag{3.20}$$

Since c_j is constant in N_j, $[p_j]_e = [q_j]_e$ and $\|\mathbf{grad}\, p_j\|^2_{0,K} = \|\mathbf{grad}\, q_j\|^2_{0,K}$ for all $K \subset N_j$ and $e \in E_0(N_j)$.

Therefore $|p_j|^2_{N_j}$ and $|q_j|^2_{N_j}$ are the same.

As a result, we have:

$$(\operatorname{div} \mathbf{v}_j, p_j)_{N_j} \geq \gamma |p_j|^2_{N_j} \quad |\mathbf{v}_j|_{1,N_j} \leq |p_j|_{N_j}, \tag{3.21}$$

Let $\mathbf{v} := \sum_{j=1}^{M} \mathbf{u}_j$, where $\mathbf{u}_j$ stands for the zero extension of $\mathbf{v}_j$ in the whole $\hat{Q}$. We have therefore:

$$(\operatorname{div} \mathbf{v}, p)_{\hat{Q}} = \sum_{j=1}^{M} (\operatorname{div} \mathbf{u}_j, p)_{\hat{Q}} = \sum_{j=1}^{M} (\operatorname{div} \mathbf{v}_j, p)_{N_j} \geq \gamma \sum_{j=1}^{M} |p_j|^2_{N_j} \geq C |p|^2_{h,\hat{Q}},$$

and

$$|\mathbf{v}|^2_{1,\hat{Q}} \leq \sum_{j=1}^{M} |\mathbf{v}_j|^2_{1,N_j} \leq \sum_{j=1}^{M} |p_j|^2_{N_j} \leq \tilde{C} |p|^2_{h,\hat{Q}}.$$

We have consequently a constant $C_1 > 0$ depending only on σ satisfying:

$$\sup_{\mathbf{0} \neq \mathbf{v} \in S_{n,\sigma}} \frac{(\operatorname{div} \mathbf{v}, p)_{\hat{Q}}}{|\mathbf{v}|_{1,\hat{Q}}} \geq C_1 |p|_{h,\hat{Q}} = C_1 \|p\|_{0,\hat{Q}} \frac{|p|_{h,\hat{Q}}}{\|p\|_{0,\hat{Q}}}. \tag{3.22}$$

Combining this last inequality with (3.17), we have:

$$\sup_{\mathbf{0} \neq \mathbf{v} \in S_{n,\sigma}} \frac{(\operatorname{div} \mathbf{v}, p)_{\hat{Q}}}{|\mathbf{v}|_{1,\hat{Q}}} \geq \|p\|_{0,\hat{Q}} \min_{t \geq 0} \max\{C_4 - C_5 t, C_1 t\} = \left(\frac{C_1 C_4}{C_1 + C_5} \right) \|p\|_{0,\hat{Q}}.$$

Proof of Theorem 12

Here the proof of the theorem about stability on $\Delta^2_{n,\sigma}$ will be given. It invokes the macroelement techniques. In fact, according to Lemma 8 on the macroelement partitioning $\Delta_{n,\sigma}$, the reduced global stability (2.8) is true. And by the theory which were detailed in Theorem 10, we have stability on the reference element independently of the chosen partititioning (i.e. on any stripped mesh). Thus, we have also the uniform reference stability (2.10). Therefore, we can deduce by virtue of a macroelement technique (see Theorem 9) the stability of the corner anisotropic mesh $\Delta^2_{n,\sigma}$. And therefore Theorem 12 is proved.

3.3 Main result

In the next discussion, we are giving details of the anisotropic stability on a two dimensional domain Ω by using the pair Q_2-Q_0. First, we are explaining how to obtain the mesh $\mathcal{T}_h$ of Ω. Let the macroelement decomposition $\mathcal{T}_m$ of Ω be κ-uniform, i. e. for every macroelement $K \in \mathcal{T}_m$,

$$\frac{h(K)}{\rho(K)} \leq \kappa < \infty \ .$$

We suppose also that every macroelement K is an affine image of a certain reference domain. In order to have the final mesh $\mathcal{T}_h$ of Ω, we suppose that each macroelement of $\mathcal{T}_m$ is further partitioned into a striped mesh (see first section of this chapter) or into a σ-geometric tensor product mesh (see second section of this chapter). Several samples of such a mesh can be found in the next figure (see Figure 3.7) which will be better explained in the next remark.

Theorem 13 For the following pair of spaces:

$$\begin{aligned} V_h &= \{v_h \in H^1_0(\Omega) : v_h|_T \circ F_T \in Q_2(\hat{Q}),\ \forall T \in \mathcal{T}_h\} \\ Q_h &= \{p_h \in L^2_0(\Omega) : p_h|_T \circ F_T \in Q_0(\hat{Q}),\ \forall T \in \mathcal{T}_h\}, \end{aligned}$$

we have stability, i.e.

$$\inf_{0 \neq p \in Q_h} \sup_{0 \neq \mathbf{v}_h \in V_h^2} \frac{(\operatorname{div} \mathbf{v}_h, p_h)}{|\mathbf{v}_h|_{1,\Omega} \|p_h\|_{0,\Omega}} \geq C,$$

where C is a positive constant which is independent of h and the mesh aspect ratio. C depends only on the uniformity parameter κ of the macroelement partitioning $\mathcal{T}_m$ and the geometric grading factor σ.

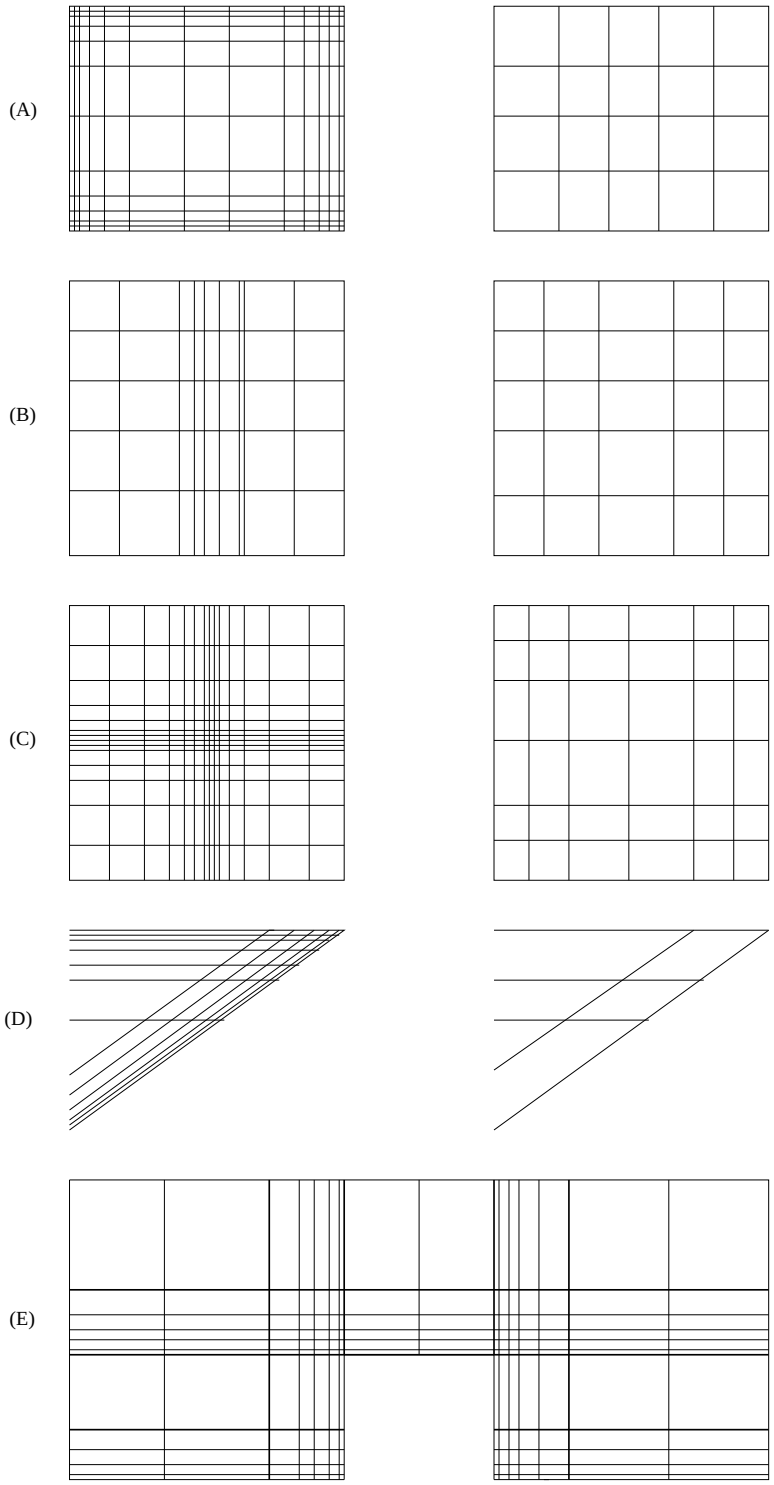

Figure 3.7: anisotropic meshes.

Proof

The first and second sections of this chapter ensure the uniform reference stability (2.10). Furthermore, the reduced global stability (2.8) and the reference stability (2.9) follow from the well known stability in ordinary isotropic meshes for $Q_2 - Q_0$ because the macroelement partitioning $\mathcal{T}_m$ is uniform. Theorem 13 is then an immediate consequence of the macroelement technique that was discussed in Theorem 9.

Remark 9 In Figure 3.7, you can find some examples of such a mesh. On the left hand side you can find the mesh $\mathcal{T}_h$ and on the right hand side the macroelement $\mathcal{T}_m$. For the last mesh (E), the macroelement decomposition is drawn in solid lines. You can find from those figures that each mesh within a macroelement is either a striped mesh or a geometric tensor product mesh. We can note that the meshes within macroelements can have high aspect ratio although the macroelement partitioning are required to be uniform. Note also in the mesh (D) that we use parallelogram elements. That is still allowed because parallelograms can be also an affine image of the reference element. These meshes are not the only possibilities, they show only that our case is not restrictive at all.

Chapter 4

The $Q_{k+1,k} - P_{k-1}$ pair

In this section we approximate the velocities by functions in $Q_{k+1,k}$ and use discontinuous pressures which are in P_{k-1}. It is to be remarked that we treat only the h-version. That means that the polynomial degree is fixed for all elements. We will only give very short comments about the p-version at the end. For the treatment of the hp-version, we can have a look at [AC00]. The pair $Q_k - P_{k-1}$ is a very appreciated one in the isotropic case but a simple test shows that it loses its stability as the mesh becomes anisotropic. Such a numerical test can be found later in the following section (Section 4.3). It should be mentioned at this beginning of this chapter that k will always be an integer parameter which is greater than or equal to 2.

The method that we will use here is again the macroelement technique. Since this method has already been used in the preceeding chapter about the $Q_2 - Q_0$ pair, we are only going to prove things which are new. In fact, we are only going to show how the reference stability on a stripped mesh can be proved. The rest of the theory is the same as before with very minor modifications. Again we will see that the corner macroelement still poses some problem in our case but we will see two remedies of how to overcome this problem.

4.1 Reference stability on a stripped mesh

4.1.1 Recall of results about Legendre polynomials

The Legendre polynomials can be defined with the help of the following formula:

$$L_n(x) = \frac{1}{n!2^n}\frac{d^n}{dx^n}[(x^2-1)^n], \quad x \in [-1,1],\ n = 0,1,2,3,....$$

These polynomials have a lot of interesting properties but we will only see those in which we are interested. For further detail about the properties of the Legendre polynomials, we can see [WG89].

Property 2 We have the following easy equalities:

$$\begin{array}{ll} L_0(x) = 1, & L_1(x) = x \\ L_n(1) = 1, & L_n(-1) = (-1)^n,\ n \geq 0. \end{array}$$

Property 3 (Orthogonality) If we define for all $i \in \mathbf{N} \cup \{0\}$ $\gamma_i = \frac{1}{2i+1}$, then we have the following orthogonality in $L_2([-1,1])$:

$$\int_{-1}^{1} L_i(x)L_j(x)dx = 2\gamma_i\delta_{ij}.$$

Definition 1 Let us define further $L_{-1}(x) = L_{-2}(x) = 0$, $\forall x \in [-1,1]$ and $\gamma_{-1} = 1$, then we can introduce the following polynomials:

$$U_i(x) := \gamma_{i-1}(L_i(x) - L_{i-2}(x)) \quad \forall x \in [-1,1] \quad i = 0,1,2,...$$

Property 4

$$\begin{aligned} U_0(x) &= 1, \quad U_1(x) = x, && (4.1)\\ U_i(x) &= \int_{-1}^{x} L_{i-1}(s)ds \quad i > 1, && (4.2)\\ U_i(\pm 1) &= 0 \quad i > 1\,, && (4.3)\\ U_i'(x) &= L_{i-1}(x) \quad i \geq 0, && (4.4) \end{aligned}$$

$\{U_i\}_{i=0,...,k}$build a basis of $P_k([-1,1])$.

It follows immediately that $\{U_i(x)U_j(y)\ \ i = 0,..,r,\ \ j = 0,...,s\}$ is a basis of $Q_{r,s}(\hat{Q})$, where $\hat{Q} = [-1,1]^2$.

Definition 2 Let us denote by Γ_1 and Γ_2 the following boundaries:

$$\begin{array}{rcl} \Gamma_1 & := & \{(x,y) \in \mathbf{R}^2 :\ x = -1,\ y \in (-1,1)\} \\ \Gamma_2 & := & \{(x,y) \in \mathbf{R}^2 :\ x = 1,\ y \in (-1,1)\}. \end{array}$$

And so we can also define the following space:

$$H := \{v \in H^1(\hat{Q}) : v = 0 \,\text{on}\, \Gamma_1, \Gamma_2\}.$$

Lemma 9 Let $v \in H^1(\hat{Q})$ which can be written as:

$$v(x,y) = \sum_{m=-1}^{\infty} \sum_{n=-1}^{\infty} v_{m,n} \frac{U_{m+1}(x)}{\gamma_m} \frac{U_{n+1}(y)}{\gamma_n}. \tag{4.5}$$

If $v \in H$, then $v_{-1,n} = v_{0,n} = 0 \ \forall n = -1, 0, 1, ...$

Proof

First of all we have

$$\frac{U_{m+1}(\pm 1)}{\gamma_m} = L_{m+1}(\pm 1) - L_{m-1}(\pm 1). \tag{4.6}$$

In the case that $m \geq 1$, the previous expression (4.6) is equal to:

$$(\pm 1)^{m+1} - (\pm 1)^{m-1} = 0.$$

In the case $m = 0$ and $m = -1$, (4.6) is respectively equal to:

$$\begin{aligned} L_1(\pm 1) - L_{-1}(\pm 1) &= \pm 1 \\ L_0(\pm 1) - L_{-2}(\pm 1) &= \pm 1. \end{aligned}$$

We have therefore the next relation:

$$0 = v(\pm 1, y) = \sum_{n=-1}^{\infty} \left\{ v_{-1,n} \frac{U_{n+1}(y)}{\gamma_n} \pm v_{0,n} \frac{U_{n+1}(y)}{\gamma_n} \right\}.$$

That means immediately that

$$\sum_{n=-1}^{\infty} (v_{-1,n} \pm v_{0,n}) \frac{U_{n+1}(y)}{\gamma_n} = 0.$$

Because the functions U_n form a basis, we have:

$(v_{-1,n} \pm v_{0,n}) = 0$. The sum and the difference are zero, so $v_{-1,n} = v_{0,n} = 0 \ \forall n = -1, 0, 1, 2, ...$

4.1.2 Preliminaries before the construction of a Fortin operator

Definition 3 Let us consider any continuous function $G : \mathbf{R}^2 \to [0,1]$. Fix an integer $k \geq 2$. For any function $v \in H$ which can be expressed as (4.5), we define:

$$v^*(x,y) = \sum_{m=-1}^{\infty} \sum_{n=-1}^{\infty} v^*_{m,n} \frac{U_{m+1}(x)}{\gamma_m} \frac{U_{n+1}(y)}{\gamma_n}, \tag{4.7}$$

where $v^*_{m,n} = G(\frac{m}{k}, \frac{n}{k}) v_{m,n}$.

Lemma 10 Let k be an integer which is greater or equal to 2. If the continuous function $G : \mathbf{R}^2 \to [0,1]$ satisfies:

$$G(a,b) = 0 \quad \text{if } (a,b) \in A, \tag{4.8}$$

where

$$A := \left\{ (x,y) \in \mathbf{R}^2 : x \geq 1 + \frac{1}{k} \text{ or } y \geq 1 \right\},$$

then $v^* \in Q_{k+1,k}$.

Proof

We have $v^*_{m,n} = 0$ if $m \geq k+1$ or $n \geq k$, according to the relation (4.8). That implies immediately that:

$$v^*(x,y) = \sum_{m=-1}^{k} \sum_{n=-1}^{k-1} v^*_{m,n} \frac{U_{m+1}(x)}{\gamma_m} \frac{U_{n+1}(y)}{\gamma_n},$$

which belongs to $Q_{k+1,k}$.

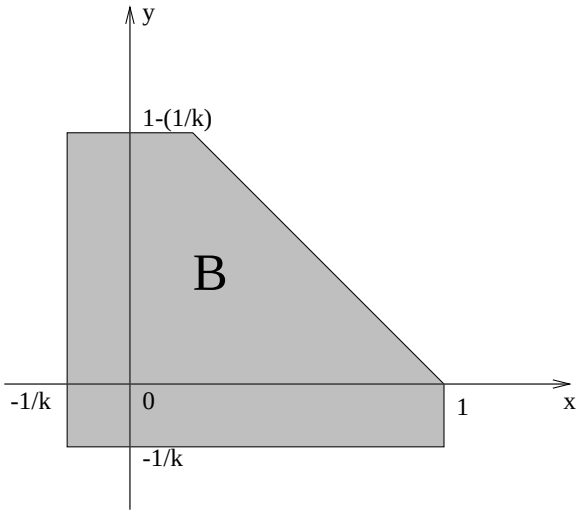

Figure 4.1: The region B.

Lemma 11 Suppose that the continuous function $G : \mathbf{R}^2 \to [0,1]$ satisfies (see Figure 4.1):

$$G(a,b) = 1 \quad \text{on } B := \left\{ (x,y) \in \left[-\frac{1}{k}, 1\right] \times \left[-\frac{1}{k}, 1 - \frac{1}{k}\right] : x + y \leq 1 \right\}.$$

Let v be as in (4.5),

then for all $q \in P_{k-1}(\hat{Q})$, we have:

$$\begin{cases} (\partial_x v^* - \partial_x v, q)_{\hat{Q}} = 0 \\ (\partial_y v^* - \partial_y v, q)_{\hat{Q}} = 0. \end{cases}$$

Proof

We need only to show the lemma for functions q such as $q(x,y) = L_i(x)L_j(y)$ with $i,j \geq 0$ and $i + j \leq k - 1$ because every function of $P_{k-1}(\hat{Q})$ can be written as linear combination of such functions. Due to the properties of the Legendre Polynomials that we have discussed earlier in Property 4, we have:

$$\partial_x v(x,y) = \sum_{m=0}^{\infty} \sum_{n=-1}^{\infty} \frac{1}{\gamma_m} v_{m,n} L_m(x) \frac{U_{n+1}(y)}{\gamma_n}.$$

According to the orthogonality of the Legendre polynomials that we have met in Property 3, we obtain the next relation:

$$(\partial_x v, q)_{\hat{Q}} = \sum_{n=-1}^{\infty} \frac{1}{\gamma_i} \frac{1}{\gamma_n} v_{i,n} 2\gamma_i (U_{n+1}, L_j) = 2 \sum_{n=-1}^{\infty} v_{i,n} [(L_{n+1}, L_j) - (L_{n-1}, L_j)]$$

$$= \quad 2\left[2v_{i,j-1}\gamma_j - 2v_{i,j+1}\gamma_j\right] = 4\gamma_j(v_{i,j-1} - v_{i,j+1}).$$

We can do the same calculations in order to see that

$$(\partial_x v^*, q)_{\hat{Q}} = 4\gamma_j(v^*_{i,j-1} - v^*_{i,j+1}) = 4\gamma_j\left[G\left(\frac{i}{k}, \frac{j-1}{k}\right)v_{i,j-1} - G\left(\frac{i}{k}, \frac{j+1}{k}\right)v_{i,j+1}\right].$$

For $i = -1,\ 0$, the coefficient v_{in} is zero (see Lemma 9) and so we can assume that $i \geq 1$.

Since $i + j \leq k - 1$, $\left(\frac{i}{k}, \frac{j-1}{k}\right) \in B$ and $\left(\frac{i}{k}, \frac{j+1}{k}\right) \in B$. Therefore

$$G\left(\frac{i}{k}, \frac{j-1}{k}\right) = G\left(\frac{i}{k}, \frac{j+1}{k}\right) = 1.$$

Consequently, $(\partial_x v^* - \partial_x v, q)_{\hat{Q}} = 0$. For the partial derivative with respect to y, we can act similarly.

Lemma 12 Let us consider a function v which can be written as in (4.5), then we have the following two equalities

$$\|\partial_x v\|^2_{0,\hat{Q}} = 4\sum_{m=0}^{\infty}\sum_{n=0}^{\infty}\frac{\gamma_n}{\gamma_m}(v_{m,n+1} - v_{m,n-1})^2,$$

and

$$\|\partial_y v\|^2_{0,\hat{Q}} = 4\sum_{m=0}^{\infty}\sum_{n=0}^{\infty}\frac{\gamma_m}{\gamma_n}(v_{m+1,n} - v_{m-1,n})^2.$$

If we have furthermore $v \in H$, then there exists a constant $C > 0$ such that for any $s \in N$, we have:

$$\sum_{m=0}^{s}\frac{1}{\gamma_m}(v^2_{m,-1} + v^2_{m,0}) \leq Cs^2|v|_{1,\hat{Q}},$$

where C depends neither on v nor on s.

Proof See Lemma 3.14 and Lemma 3.17 of [SS97] or see Lemma A.1. of [AC00].

Corollary 1 Suppose the continuous function $G : \mathbf{R}^2 \to [0, 1]$ satisfies

$$G(a, b) = \begin{cases} 1 & \text{for } (a, b) \in B \\ 0 & \text{for } (a, b) \in A, \end{cases}$$

then there exists a constant $C > 0$ which does not depend on k such that for all $v \in H$ which can be written of the form (4.5) we have:

$$\|\partial_x v^*\|^2_{0,\hat{Q}} \leq C\sqrt{k}|v|_{1,\hat{Q}},$$
$$\|\partial_y v^*\|^2_{0,\hat{Q}} \leq C\sqrt{k}\|\partial_y v\|.$$

Proof

According to the previous lemma, we can write

$$\|\partial_x v\|^2_{0,\hat{Q}} = 4\sum_{m=0}^{\infty}\sum_{n=0}^{\infty}\frac{\gamma_n}{\gamma_m}(v_{m,n+1} - v_{m,n-1})^2,$$

and similarly for v^*:

$$\|\partial_x v^*\|^2_{0,\hat{Q}} = 4\sum_{m=0}^{\infty}\sum_{n=0}^{\infty}\frac{\gamma_n}{\gamma_m}(v^*_{m,n+1} - v^*_{m,n-1})^2.$$

Since $v^*_{ij} = G\left(\frac{i}{k}, \frac{j}{k}\right) v_{ij}$ and $G(a,b)$ is respectively 0 and 1 in A and B, we deduce immediately that:

$$(v^*_{m,n+1} - v^*_{m,n-1}) = \begin{cases} v_{m,n+1} - v_{m,n-1} & \text{if } (m \leq k \text{ and } n \leq k-2) \\ 0 & \text{if } (m \geq k \text{ or } n \geq k+1). \end{cases}$$

Let us define the following index set:

$$I := \{0, ..., k\} \times \{k-1, k\}.$$

Let I^c stand for its complementary in $(\mathbf{N} \cup \{0\}) \times (\mathbf{N} \cup \{0\})$. We can therefore partition the sum in $\|\partial_x v^*\|^2_{0,\hat{Q}}$:

$$\|\partial_x v^*\|^2_{0,\hat{Q}} = 4\sum_{(m,n)\in I}\frac{\gamma_n}{\gamma_m}(v^*_{m,n+1} - v^*_{m,n-1})^2 + 4\sum_{(m,n)\in I^c}\frac{\gamma_n}{\gamma_m}(v_{m,n+1} - v_{m,n-1})^2.$$

Furthermore, for $n \geq k-1$, we have $v^*_{m,n+1} = 0$ because $G(\frac{m}{k}, \frac{n+1}{k}) = 0$. we haver therefore:

$$\|\partial_x v^*\|^2_{0,\hat{Q}} = 4\sum_{(m,n)\in I}\frac{\gamma_n}{\gamma_m}{v^*_{m,n-1}}^2 + 4\sum_{(m,n)\in I^c}\frac{\gamma_n}{\gamma_m}(v_{m,n+1} - v_{m,n-1})^2.$$

The second sum can be immediately estimated by $\|\partial_x v\|^2_{0,\hat{Q}}$, so we have:

$$\|\partial_x v^*\|^2_{0,\hat{Q}} \leq 4\sum_{(m,n)\in I}\frac{\gamma_n}{\gamma_m}{v^*_{m,n-1}}^2 + \|\partial_x v\|^2_{0,\hat{Q}}. \tag{4.9}$$

That means that we will need only to estimate the first sum:

$$4 \sum_{m=1}^{k} \sum_{n=k-1}^{k} \frac{\gamma_n}{\gamma_m} {v^*_{m,n-1}}^2.$$

On the other hand, it holds:

$$v^2_{m,n-1} \leq C \frac{1}{\gamma^2_{n-1}} \left[\sum_{j=0}^{\infty} \gamma_j (v_{m,j+1} - v_{m,j-1})^2 \right] + C(v^2_{m,-1} - v^2_{m,0}). \qquad (4.10)$$

Indeed,

$$v_{m,n-1} = (v_{m,n-1} - v_{m,n-3}) + (v_{m,n-3} - v_{m,n-5}) + \ldots + \begin{cases} (v_{m,1} - v_{m,-1}) + v_{m,-1} & \text{if } n \text{ even} \\ (v_{m,2} - v_{m,0}) + v_{m,0} & \text{if } n \text{ odd.} \end{cases}$$

We will consider only the case where n is even (the case when n is odd can be handled similarly)

$$v_{m,n-1} = \sum_{\substack{j=0, \\ j \text{ even}}}^{n-2} \frac{1}{\sqrt{\gamma_j}} \left[\sqrt{\gamma_j} (v_{m,j+1} - v_{m,j-1}) \right] + v_{m,-1}.$$

According to the Cauchy Schwartz inequality, we have:

$$v_{m,n-1} \leq \left(\sum_{\substack{j=0, \\ j \text{ even}}}^{n-2} \frac{1}{\gamma_j} \right)^{1/2} \left[\sum_{\substack{j=0, \\ j \text{ even}}}^{n-2} \gamma_j (v_{m,j+1} - v_{m,j-1})^2 \right]^{1/2} + v_{m,-1}. \qquad (4.11)$$

A simple proof by induction also shows that

$$\sum_{j=0}^{n-2} \frac{1}{\gamma_j} \leq \frac{C}{\gamma^2_{n-1}}. \qquad (4.12)$$

The fact that $(R+S)^2 \leq 2(R^2+S^2)$ together with the preceding inequalities (4.11) and (4.12) then imply that:

$$v^2_{m,n-1} \leq C \frac{1}{\gamma^2_{n-1}} \left[\sum_{\substack{j=0, \\ j \text{ even}}}^{n-2} \gamma_j (v_{m,j+1} - v_{m,j-1})^2 \right] + C v^2_{m,-1} \ .$$

The other case where n is odd can be treated similarly, so we skip the deductions but state only the final result:

$$v_{m,n-1}^2 \leq C\frac{1}{\gamma_{n-1}^2}\left[\sum_{\substack{j=1,\\ j \text{ odd}}}^{n-2} \gamma_j (v_{m,j+1} - v_{m,j-1})^2\right] + C v_{m,0}^2 \ .$$

Therefore, in both cases (n even or odd) we simply obtain the general inequality (4.10). Consequently, the following bound is true:

$$\sum_{m=1}^{k} \frac{1}{\gamma_m} v_{m,n-1}^2 \leq C\frac{1}{\gamma_{n-1}^2} \sum_{m=0}^{\infty}\sum_{j=0}^{\infty} \frac{\gamma_j}{\gamma_m}(v_{m,j+1} - v_{m,j-1})^2 + C \underbrace{\sum_{m=1}^{k} \frac{1}{\gamma_m}(v_{m,-1}^2 + v_{m,0}^2)}_{S}. \tag{4.13}$$

According to Lemma 12, we can deduce the next fact as follow:

$$\sum_{m=1}^{k} \frac{1}{\gamma_m} v_{m,n-1}^2 \leq C\frac{1}{\gamma_{n-1}^2} \|\partial_x v\|_{0,\hat{Q}} + Ck^2 |v|_{1,\hat{Q}}^2.$$

Consequently, by taking the sum we have the following estimate:

$$\begin{aligned}
\sum_{n=k-1}^{k}\sum_{m=1}^{k} \frac{\gamma_n}{\gamma_m} v_{m,n-1}^2 &\leq \sum_{n=k-1}^{k}\left[C\frac{\gamma_n}{\gamma_{n-1}^2}\|\partial_x v\|_{0,\hat{Q}} + C\gamma_n k^2 |v|_{1,\hat{Q}}^2\right] \\
&\leq C\left(\frac{\gamma_k}{\gamma_{k-1}^2} + \frac{\gamma_{k-1}}{\gamma_{k-2}^2}\right)\|\partial_x v\|_{0,\hat{Q}}^2 + Ck^2(\gamma_{k-1} + \gamma_k)|v|_{1,\hat{Q}}^2 \\
&\leq C\frac{1}{\gamma_k}\|\partial_x v\|_{0,\hat{Q}}^2 + Ck|v|_{1,\hat{Q}}^2 \leq C_1 k |v|_{1,\hat{Q}}^2,
\end{aligned}$$

because of the definition of $\gamma_k = (2k+1)^{-1}$.

Combining this last inequality with (4.9), we obtain simply:

$$\|\partial_x v^*\|_{0,\hat{Q}}^2 \leq C_1 k |v|_{1,\hat{Q}}^2 + \|\partial_x v\|_{0,\hat{Q}}^2;$$

therefore we deduce simply the conclusion, i. e.

$$\|\partial_x v^*\|_{0,\hat{Q}} \leq C_2\sqrt{k}|v|_{1,\hat{Q}}.$$

We can repeat the same proof for the partial derivative with respect to y. The difference is that, the term S which we see in the relation (4.13) vanishes in that case because of Lemma 9 which says that $v_{-1,m} = v_{0,m} = 0 \quad \forall m = -1, 0, ...$

Theorem 14 Let k be a fixed integer which is greater or equal to 2. Then, there exists a linear operator $\pi_k : H \to H$ which satisfies the following three relations:

(D1) For all $v \in H$, we have:

$$\begin{aligned} (\partial_x(v - \pi_k v), q)_{\hat{Q}} &= 0, \quad \forall q \in P_{k-1}(\hat{Q}), \quad \text{and} \\ (\partial_y(v - \pi_k v), q)_{\hat{Q}} &= 0, \quad \forall q \in P_{k-1}(\hat{Q}); \end{aligned}$$

(D2) $\pi_k v \in Q_{k+1,k}$;

(D3) There exists a positive constant C independent of k such that:

$$\begin{aligned} \|\partial_x \pi_k v\|_{0,\hat{Q}} &\leq C\sqrt{k}|v|_{1,\hat{Q}} \\ \|\partial_y \pi_k v\|_{0,\hat{Q}} &\leq C\sqrt{k}\|\partial_y v\|_{0,\hat{Q}}. \end{aligned}$$

for all $v \in H$.

Proof See [AC00] where the authors use the previous results to deduce this theorem. Because the set of all polynomials is dense in the Sobolev space $H^1(\hat{Q})$, and all polynomials can be written in the form (4.5).

4.1.3 The considered mesh and further results

We will work on the domain $\hat{Q} = (-1, 1) \times (-1, 1)$. Now we would like to give some explanations about the mesh. Like in the case of $Q_2 - Q_0$, we would like to consider a stripped mesh that we recall briefly: $\mathcal{T}_x$ is again any discretization of $(-1, 1)$. The final mesh $\mathcal{T}$ on $\hat{Q}$ is then:

$$\mathcal{T} = \{T : T = (-1, 1) \times T_x,\ T_x \in \mathcal{T}_x\}. \tag{4.14}$$

Most of the following results are the same or use the same techniques as in the case of $Q_2 - Q_0$, so we are not going to prove them in detail any more, we are only telling the results.

Definition 4 For all elements T of the mesh $\mathcal{T}$, we define the space:

$$H(T) := \{v \in H^1(T) : v \circ F_T \in H\}.$$

Let us fix an integer $k \geq 2$. We can then introduce the following function:

$$\pi_k^T : H(T) \to H(T) \cap Q_{k+1,k} \quad \text{with}$$
$$\pi_k^T v := (\pi_k(v \circ F_T)) \circ F_T^{-1}.$$

Corollary 2 Let T be any element of $\mathcal{T}$ and $k \geq 2$. Then for all $v \in H(T)$, we have:

$$|\pi_k^T v|_{1,T} \leq C\sqrt{k}|v|_{1,T},$$

where C is a positive constant which is independent of k and the element T.

The proof of this theorem is very much like that of Theorem 11 and so it will be omitted.

Theorem 15 (First main result) Let us consider a stripped mesh like in (4.14). Define the following spaces:

$$\begin{aligned} V_k &= \{u \in H_0^1(\hat{Q}) : u|_T \circ F_T \in Q_{k+1,k}(T)\ \forall T \in \mathcal{T}\} \\ Q_k &= \{p \in L_0^2(\hat{Q}) : p|_T \circ F_T \in P_{k-1}(T)\ \forall T \in \mathcal{T}\}. \end{aligned}$$

Then we have stability, i.e. there exists a positive constant C for which:

$$\inf_{0 \neq p_h \in Q_k} \sup_{0 \neq \mathbf{v}_h \in V_k^2} \frac{(\operatorname{div} \mathbf{v}_h, p_h)_{\hat{Q}}}{|\mathbf{v}_h|_{1,\hat{Q}} \|p_h\|_{0,\hat{Q}}} \geq C, \tag{4.15}$$

where the constant C depends neither on the aspect ratio nor on $\mathcal{T}$.

Proof

The goal of the proof is the construction of a Fortin operator. For any element T of $\mathcal{T}$, we define first the operator Π_k^T. This operator will be defined on $H(T)^2$ and it will be expressed componentwise by the π_k^T. More precisely, for any $\mathbf{v} = (v_1, v_2) \in H(T)^2$, we have:

$$\Pi_k^T \mathbf{v} := \left(\pi_k^T v_1, \pi_k^T v_2\right).$$

This last operator Π_k^T inherits the properties of π_k^T: among others we have:

$$\Big(\mathrm{div}(\mathbf{v} - \Pi_k^T \mathbf{v}), q\Big)_T = 0 \quad \forall\ q \in Q_k. \tag{4.16}$$

This relation is very much like that in Lemma 5 in the chapter about $Q_2 - Q_0$. We are now able to introduce an operator which is defined on the whole $H_0^1(\Omega)$. It will be in fact the Fortin operator that we will need. It is precisely:

$$\mathcal{B} : H_0^1(\hat{Q})^2 \to V_k,$$

which is defined elementwise by:

$$(\mathcal{B}\mathbf{v})|_T := \Pi_k^T(\mathbf{v}|_T) \quad \forall T \in \mathcal{T}.$$

Lemma 3.5 of [AC00] ensures that for any $\mathbf{v} \in H_0^1(\hat{Q})^2$, its image $(\mathcal{B}\mathbf{v})$ will be continuous on interelements, and so $(\mathcal{B}\mathbf{v})$ will be continuous on the whole domain $\hat{Q}$.

On the other hand, the relation (4.16) implies:

$$(\mathrm{div}\,\mathbf{v}, q)_{\hat{Q}} = (\mathrm{div}(\mathcal{B}\mathbf{v}), q)_{\hat{Q}} \quad \forall q \in Q_k.$$

Corollary 2 implies in particular the following boundedness:

$$|\mathcal{B}\mathbf{v}|_{1,\hat{Q}}^2 = \sum_{T\in\mathcal{T}} |\mathcal{B}\mathbf{v}|_{1,T}^2 = \sum_{T\in\mathcal{T}} |\Pi_k^T(\mathbf{v}|_T)|_{1,T}^2 \le Ck \sum_{T\in\mathcal{T}} |\mathbf{v}|_{1,T}^2 = C\,k|\mathbf{v}|_{1,\hat{Q}}^2.$$

According to the Fortin's lemma (see Lemma 3), we can conclude the theorem.

4.2 Stability in the corner macroelement

In this section, we intend to analyze the corner macroelement. Similarly to the case of $Q_2 - Q_0$, this $Q_{k+1,k} - P_{k-1}$ has a very difficult problem at the corner. A simple numerical experience can demonstrate that fact (See section 4.3). In the following discussion, we show two remedies to overcome that difficulty. The solution to this corner problem is to invoke p-version FEM. We recall that in the p-version FEM, one has the possibility to have different polynomial degree in each element. In other words, polynomial degrees are allowed to be different from one element to another.

4.2.1 Remedy 1 (Geometric tensor product mesh)

The first remedy that we can do is to invoke again the geometric tensor product meshes as we have done in the case of $Q_2 - Q_0$. We recall briefly this kind of mesh. Any geometric grading factor $\sigma \in (0,1)$ is first taken. The x-unit interval $(0,1)$ is first refined geometrically towards the origin. That means, it is subdivided into $n+1$ subintervals:

$$I_i = (x_{i-1}, x_i), i = 1, ..., n+1,$$

where

$$\begin{cases} x_0 &= 0\ , \\ x_i &= \sigma^{n+1-i}\ , \end{cases}$$

(n is any positive integer) .

We do the same for the y-unit interval. And the considered mesh is the resulting tensor product mesh. Like in the theory about $Q_2 - Q_0$, we will denote this resulting mesh by $\Delta^2_{n,\sigma}$ (see Figure 4.2).

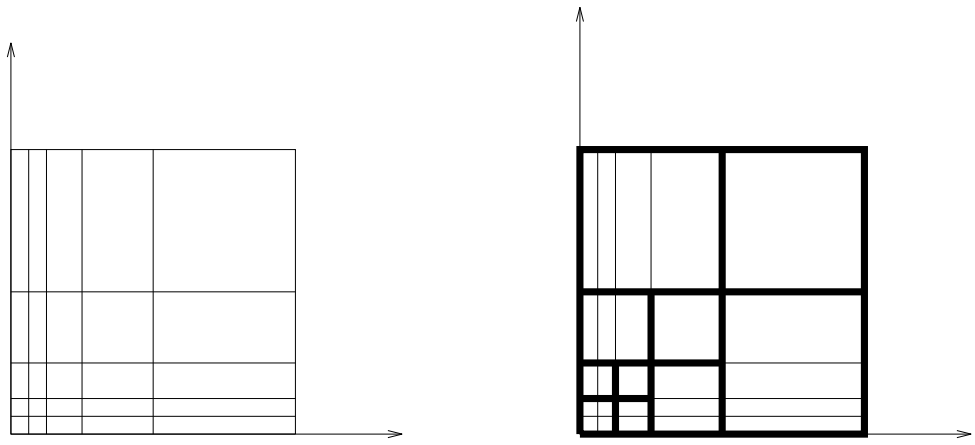

Figure 4.2: $\Delta^2_{n,\sigma}$ and the underlying macroelement.

We can directly state the following theorem:

Theorem 16 Define

$$\begin{aligned} V_{\sigma,n} &:= \{u \in H^1_0(\hat{Q}) : u|_T \in Q_{r,s}(T)\ \forall T \in \Delta^2_{n,\sigma}\} \\ P_{\sigma,n} &:= \{p \in L^2_0(\hat{Q}) : p|_T \in P_{k-1}(T)\ \forall T \in \Delta^2_{n,\sigma}\}, \end{aligned}$$

where

$$\begin{aligned}(r,s) &= (k+1,k) \quad \text{if } T \text{ is stretched in the } x\text{-direction}\,,\\ (r,s) &= (k,k+1) \quad \text{if } T \text{ is stretched in the } y\text{-direction}\,.\end{aligned}$$

Then we have stability, i.e. there exists a positive constant C for which:

$$\inf_{0\neq p_h\in P_{\sigma,n}} \sup_{0\neq \mathbf{v}_h\in V^2_{\sigma,n}} \frac{(\operatorname{div}\mathbf{v}_h, p_h)}{|\mathbf{v}_h|_{1,\Omega}\|p_h\|_{0,\Omega}} \geq C, \tag{4.17}$$

where C is independent of n and the aspect ratio of each element. C depends only on $\hat{Q}$ and the geometric grading factor σ.

Proof

The proof follows exactly the same lines as the proof of Theorem 12 which invokes a macroelement technique, so we do not need to repeat it. The only thing that we remark is that the space $\mathcal{L}^1(K)$ which we used in the case of $Q_2 - Q_0$ is still a subspace of $Q^2_{k+1,k}$ and $Q^2_{k,k+1}$ for $k \geq 2$. Consequently the reduced global stability (2.8) in Theorem 9 still holds here.

Remark 10 If the difference of polynomial degrees in the elements is not desirable then one has to take only $Q_{k+1,k+1}$ for all elements T in the definition of velocity space.

4.2.2 Remedy 2 (Varying corner domain)

The second solution to this corner problem is to use varying corner domain. That means that we adjust the size of the corner domain according to the desired aspect ratio.

For any positive number ρ, we define the domain $D_\rho = (0, 1+\rho)^2$. The mesh $\mathcal{T}_\rho$ will be then composed of (see Figure 4.3):

$$\begin{aligned}T_1 &= (0,\rho)^2\\ T_2 &= (\rho, 1+\rho)\times(0,\rho)\\ T_3 &= (\rho, 1+\rho)\times(\rho, 1+\rho)\\ T_4 &= (0,\rho)\times(\rho, 1+\rho).\end{aligned}$$

We admit the following polynomial degree partitioning:

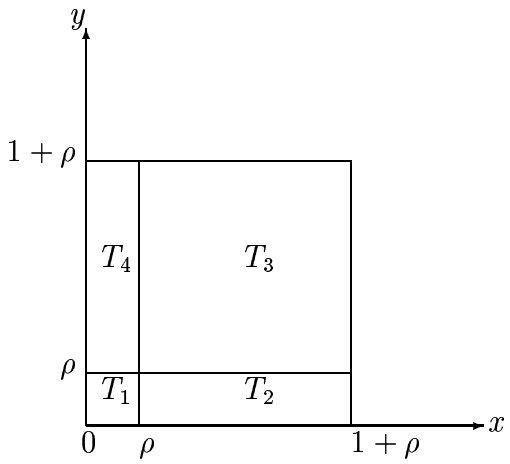

Figure 4.3: D_ρ and its discretization.

For the x variable, the degree on the element T_i is $k_x(i)$ which are:

$$k_x(1) = k, \quad k_x(2) = k+1, \quad k_x(3) = k+1, \quad k_x(4) = k.$$

We define the the y polynomial degrees similarly with:

$$k_y(1) = k, \quad k_y(2) = k, \quad k_y(3) = k+1, \quad k_y(4) = k+1.$$

We have then the following result:

Theorem 17 Define

$$\begin{aligned} V_\rho &:= \{u \in H_0^1(D_\rho) : u|_{T_i} \in Q_{k_x(i),k_y(i)}(T_i)\ \forall i = 1,2,3,4\} \\ Q_\rho &:= \{p \in L_0^2(D_\rho) : p|_{T_i} \in P_{k-1}(T_i)\ \forall i = 1,2,3,4\}, \end{aligned}$$

then we have stability, i.e. there exists a positive constant C which is independent of ρ and k such that

$$\inf_{0 \neq p_h \in Q_\rho} \sup_{0 \neq \mathbf{v}_h \in V_\rho^2} \frac{(\operatorname{div} \mathbf{v}_h, p_h)}{|\mathbf{v}_h|_{1,D_\rho} \|p_h\|_{0,D_\rho}} \geq C\sqrt{k} \min(1, k\sqrt{\rho}). \tag{4.18}$$

Remark 11 We do not prove this theorem because we are more interested in having more than just four elements. Readers who want to know the proof can see [AC00]. The theorem has not much value in the h-version because for a fixed k, the minimum in (4.18) will always be $k\sqrt{\rho}$ for sufficiently small ρ. But $k\sqrt{\rho}$ tends to zero with ρ, so we do not gain anything in this case. That means we are restricted to $\rho \geq Ck^{-3/2}$.

4.3 Numerical results

In this section, we report some numerical tests. It should be remarked that we have done two different tests that will be discussed independently in this section. It can be really seen that they are in accordance with our theoretical results.

4.3.1 Test 1

In this test 1, we compare the effect of high aspect ratio mesh to the pair $Q_k - P_{k-1}$ and the pair $Q_{k+1,k} - P_{k-1}$. As expected from the theory the latter is still stable on high aspect ratio mesh. The mesh that we consider is a very simple one. It consists of two rectangular elements only. We can see Figure 4.4 for a graphical illustration. Note that the mesh becomes anisotropic when the value of the positive parameter ρ becomes small. Because the value of the mesh aspect ratio is in fact:

$$\text{Aspect Ratio}=\frac{1}{\rho}.$$

The numerical result can be found in the next table (Table 4.1), where we considered both $Q_2 - P_1$ and $Q_{3,2} - P_1$ (that means $k = 2$):

This test 1 also emphasizes that although $Q_k - P_{k-1}$ is a very appreciated pair in the isotropic FEM, it generally fails to be stable in high aspect ratio mesh. Besides, test 1 also confirms our theoretical result about anisotropic stability of the pair $Q_{k+1,k} - P_{k-1}$ on stripped meshes.

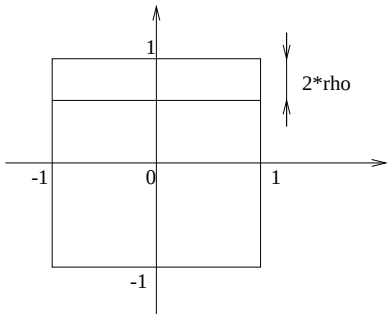

Figure 4.4: Grid 1: The investigated mesh for test 1.

The numerical outputs really show that for the values of ρ in the interval $[0.15, 0.5]$ the inf-sup constants for both pairs are still somewhat comparable,

ρ	aspect ratio	$Q_2 - P_1$	$Q_{3,2} - P_1$
0.50	2.000000	0.408248290	0.611386469
0.45	2.222222	0.403946910	0.605544640
0.40	2.500000	0.391232615	0.593358504
0.35	2.857142	0.370546843	0.579870918
0.30	3.333333	0.342321058	0.567487023
0.25	4.000000	0.306771156	0.558411238
0.20	5.000000	0.263797711	0.555452465
0.15	6.666666	0.212934335	0.562186852
0.10	10.00000	0.153265392	0.582152906
0.05	20.00000	0.083216624	0.614649130
0.01	100.0000	0.017902167	0.640500494
0.001	1000.000	0.001822100	0.645032131
0.00001	100000.0	1.82570e-05	0.645492612

Table 4.1: Results from grid 1: As predicted by the theory, the inf-sup constants for $Q_{3,2} - P_1$ is bounded (unlike those for $Q_2 - P_1$).

but in the range $\rho \in [0, 0.15]$, we can perfectly see the superiority (in terms of anisotropic stability) of the $Q_{3,2} - P_1$ pair over the $Q_2 - P_1$ pair. A graphical version of the numerical results are located in Figure 4.5 and Figure 4.6. They give a better aspect of the general behavior of the inf-sup constants. Finally, this test 1 shows that the increase of the velocity first polynomial degree is necessary in the anisotropic case, i.e. we never can expect an unconditional anisotropic stability for the $Q_k - P_{k-1}$ pair.

4.3.2 Test 2

In this test, we want to analyze again the corner mesh that we have considered in the pair $Q_2 - Q_0$. It is recalled in Figure 4.7. We test it with the $Q_{k+1,k} - P_{k-1}$ pair. The mesh tends to be anisotropic when the value of the positive constant a tends to zero. The results in the interval $a \in [0, 0.5]$ can be seen in Table 4.2.

It is very well seen that the dependence of the inf-sup constant on the aspect ratio is unavoidable for grid 2. Because the problem has a certain symmetry at ρ and at $1 - \rho$, the complete results (i.e. $a \in [0, 1]$), which is plotted in Figure 4.8 is already expected.

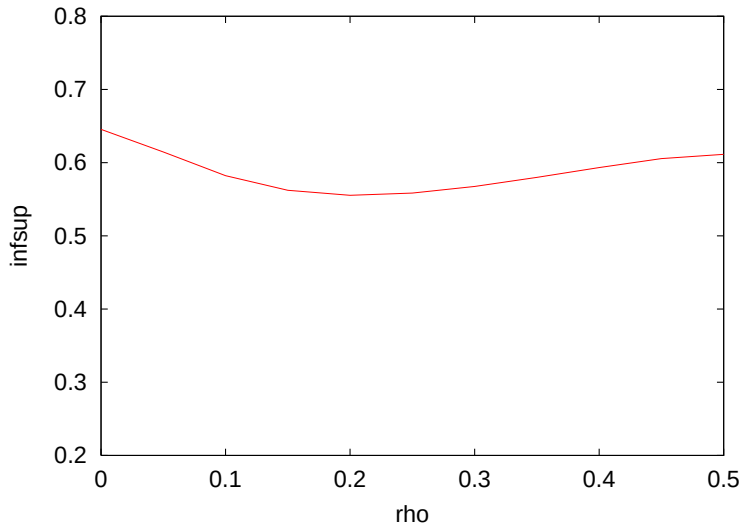

Figure 4.5: Results from grid 1: This graphs confirms our theoretical results about $Q_{k+1,k}/P_{k-1}$ stability on stripped meshes.

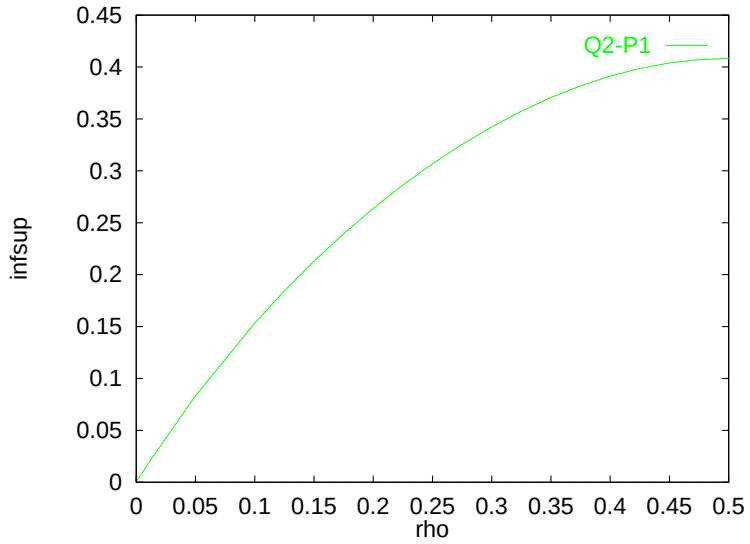

Figure 4.6: Results from Grid 1: This graphs shows the degradation of the $Q_2 - P_1$ pair on a high aspect ratio mesh.

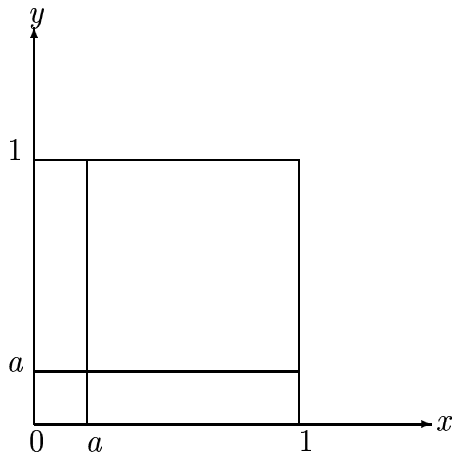

Figure 4.7: Grid 2: the investigated mesh for test 2.

a	aspect ratio	INF-SUP
0.5	1.000000	0.53554
0.4	1.500000	0.52764
0.3	2.333333	0.50975
0.2	4.000000	0.48835
0.15	5.666666	0.46562
0.1	9.000000	0.41889
0.05	19.00000	0.33467
0.0001	9999.000	0.01760
0.000001	999999.0	0.00176

Table 4.2: Results from grid 2: Unfortunately for the corner mesh even $Q_{3,2} - P_1$ is unstable.

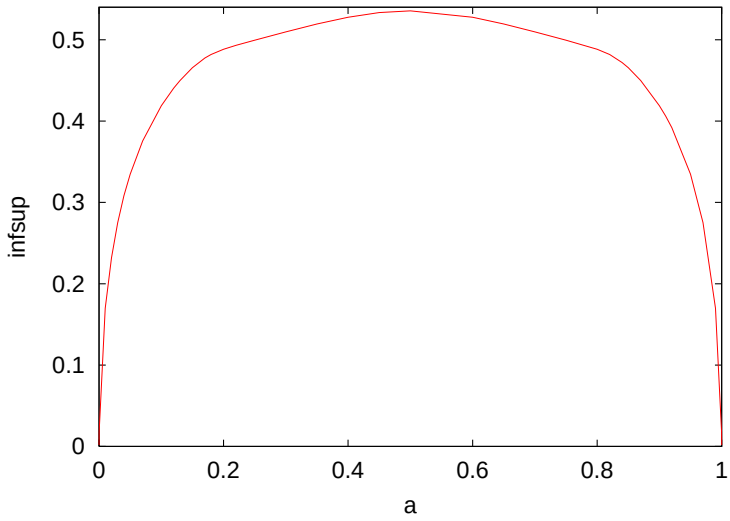

Figure 4.8: Results from grid 2.

Chapter 5

Stabilizations and application to $Q_1 - Q_1$

5.1 Abstract stabilization procedure

A stabilization method is generally used in order to be able to use a pair which is known to be unstable. Effectively, it is often applied when the velocity and the pressure discrete spaces are the same. For example $Q_1 - Q_1$ or $P_1 - P_1$. People also use a stabilization method in order to give some remedy to pairs which are practically easy to implement but which are unstable. An example of such a pair is the $Q_1 - Q_0$. In this chapter, we are not going to deal with all the interesting pairs which can be stabilized; but rather, we are giving some abstract theory which can be applied in practical problems and then we are applying it to the pair $Q_1 - Q_1$. Like in the previous discussions, we will be more interested in anisotropic grids.

5.1.1 Correction terms

The philosophy of stabilization is to modify the discrete variational formulation with a correction term so that the originally unstable pair will become suitable for the modified equation. Let V_h and Q_h be finite dimensional subspaces of the continuous velocity and pressure spaces. We will analyze the following modified stabilized discrete equation:

$$\begin{cases} (\nabla \mathbf{u}_h, \nabla \mathbf{v}_h) - & (p_h, \operatorname{div} \mathbf{v}_h) & = (\mathbf{f}, \mathbf{v}_h) & \forall \mathbf{v}_h \in V_h \\ (\operatorname{div} \mathbf{u}_h, q_h) + & c(p_h, q_h) & = 0 & \forall q_h \in Q_h. \end{cases} \tag{5.1}$$

First of all, we will see some assumption under which the stabilized discrete equation (5.1) is uniquely solvable because it does not look like the usual equations that were discussed in the previous chapters. But first, let us see the following topic which gives a generalization of Lax Milgram's lemma.

5.1.2 Generalized Lax-Milgram's lemma

Lemma 13 Let U be a Hilbert space. Let $a(\cdot,\cdot)$ be a bilinear form defined in U which satisfies the following assumptions:

(A1) There exists a positive constant C for which:

$$|a(u,v)| \leq C\|u\|.\|v\| \quad \forall u, v \in U \ .$$

(A2) There exists a positive constant α for which:

$$\sup_{0 \neq v \in U} \frac{a(u,v)}{\|v\|} \geq \alpha\|u\| \quad \forall u \in U \ .$$

(A3) For every $v \in U \setminus \{0\}$, there is $u \in U$ with:

$$a(u,v) \neq 0 \ .$$

Then, for each $f \in U^*$, the following problem has a unique solution:

$$\begin{cases} \text{Search for } u \in U \text{ with} \\ a(u,v) =< f, v > \quad \forall v \in U. \end{cases}$$

Proof

With the help of the $a(\cdot,\cdot)$, we can define a linear operator $A : U \to U^*$. For an element u of U, Au is defined by:

$$< Au, v >:= a(u,v) \quad \forall u, v \in U.$$

Because of the assumption (A1), the operator A is continuous. We can deduce from (A2) that A is a 1-to-1 mapping. Indeed, (A2) gives us:

$$\|Au\|_{U^*} \geq \alpha\|u\|;$$

therefore ker $(A) = \{0\}$.

That implies the evidence that A is bijective from U onto Ran (A).

Besides, (A2) implies also in particular that A has a continuous inverse. Consequently, $A(U)$ is a closed set. According to the closed range theorem, $A(U) = (\ker(A^*))^0$ (polar of the nullspace of the adjoint of A).

On the other hand, according to the assumption $(A3)$, we have:

$$\ker(A^*) = \{v \in U : a(u,v) = 0 \ \forall u \in U\} = \{0\}.$$

As a result, $(\ker(A^*))^0 = U^*$ which implies that A is bijective from U onto U^*.

Remark 12 The Lax Milgram's theorem is a particular case of the preceeding lemma because coercivity implies surely the assumption (A2).

5.1.3 Unique solvability theorem

Now we would like to prove the unique solvability of the stabilized problem (5.1). The previous lemma will be of so much use for the proof of the next theorem. We need however the following equivalent problem:

Definition 5 Let us first define the product space $R_h := V_h \times Q_h$. We can therefore introduce the following bilinear form $B : R_h \times R_h \to \mathbf{R}$ with:

$$B((\mathbf{u}_h, p_h); (\mathbf{v}_h, q_h)) := (\nabla \mathbf{u}_h, \nabla \mathbf{v}_h) - (\operatorname{div} \mathbf{v}_h, p_h) - (\operatorname{div} \mathbf{u}_h, q_h) - c(p_h, q_h). \tag{5.2}$$

Then the stabilized problem (5.1) is equivalent to the following one: search for $(\mathbf{u}_h, p_h) \in R_h$ with

$$B((\mathbf{u}_h, p_h); (\mathbf{v}_h, q_h)) = F((\mathbf{v}_h, q_h)) \quad \forall (\mathbf{v}_h, q_h) \in R_h,$$

where $F((\mathbf{v}_h, q_h)) :=< f, \mathbf{v}_h >$.

Theorem 18 Let us suppose that we have for all $p_h \in Q_h$:

$$\sup_{0 \neq \mathbf{v}_h \in V_h^2} \frac{(p_h, \operatorname{div} \mathbf{v}_h)}{\|\nabla \mathbf{v}_h\|_0} + \sqrt{c(p_h, p_h)} \geq \gamma \|p_h\|_0 \ , \tag{5.3}$$

then we have for all $(\mathbf{u}_h, p_h) \in R_h$:

$$\sup_{(\mathbf{v}_h,q_h)\in R_h} \frac{B\left((\mathbf{u}_h,p_h);(\mathbf{v}_h,q_h)\right)}{\|\nabla \mathbf{v}_h\|_0 + \|q_h\|_0} \geq C(\|\nabla \mathbf{u}_h\|_0 + \|p_h\|_0). \tag{5.4}$$

Proof

The proof is somewhat long and it will be divided into three parts.

Let us consider an arbitrary but fixed $(\mathbf{u}_h, p_h) \in R_h$,

Part 1:

According to (5.3), we have:

$$\sup_{0\neq \mathbf{v}_h\in V_h^2} \frac{(p_h, \operatorname{div} \mathbf{v}_h)}{\|\nabla \mathbf{v}_h\|_0} \geq \gamma \|p_h\|_0 - \sqrt{c(p_h,p_h)}. \tag{5.5}$$

Let us denote by $\mathbf{w}_h \in V_h^2$ the function where this supremum is attained. We can scale $\mathbf{w}_h$ in order to obtain $\|\nabla \mathbf{w}_h\|_0 = \|p_h\|_0$. We have now:

$$\begin{aligned} B\left((\mathbf{u}_h,p_h);(-\mathbf{w}_h,0)\right) &= -(\nabla \mathbf{u}_h, \nabla \mathbf{w}_h) + (\operatorname{div} \mathbf{w}_h, p_h) \\ &\geq -\|\nabla \mathbf{u}_h\|_0 \|\nabla \mathbf{w}_h\|_0 + \gamma \|p_h\|_0^2 - \|p_h\|_0 \sqrt{c(p_h,p_h)} \\ &= -\|\nabla \mathbf{u}_h\|_0 \|p_h\|_0 + \gamma \|p_h\|_0^2 - \|p_h\|_0 \sqrt{c(p_h,p_h)}. \end{aligned}$$

Let us now choose any $\epsilon \in (0, \gamma)$. We have simply the following two inequalities:

$$\begin{cases} \|\nabla \mathbf{u}_h\|_0 \|p_h\|_0 \leq \frac{1}{2\epsilon} \|\nabla \mathbf{u}_h\|_0^2 + \frac{\epsilon}{2} \|p_h\|_0^2 \\ \|p_h\|_0 \sqrt{c(p_h,p_h)} \leq \frac{\epsilon}{2} \|p_h\|_0^2 + \frac{1}{2\epsilon} c(p_h,p_h). \end{cases} \tag{5.6}$$

We can then deduce that:

$$B\left((\mathbf{u}_h,p_h);(-\mathbf{w}_h,0)\right) \geq -\frac{1}{2\epsilon}\|\nabla \mathbf{u}_h\|_0^2 - \frac{\epsilon}{2}\|p_h\|_0^2 + \gamma \|p_h\|_0^2 - \frac{\epsilon}{2}\|p_h\|_0^2 - \frac{1}{2\epsilon} c(p_h,p_h)$$

$$\geq -\frac{1}{2\epsilon}\|\nabla \mathbf{u}_h\|_0^2 + (\gamma - \epsilon)\|p_h\|_0^2 - \frac{1}{2\epsilon} c(p_h,p_h).$$

It follows then:

$$B\left((\mathbf{u}_h,p_h);(-\mathbf{w}_h,0)\right) \geq -C_5\|\nabla \mathbf{u}_h\|_0^2 + C_6\|p_h\|_0^2 - C_7 c(p_h,p_h). \tag{5.7}$$

And that result closes the first part.

Part 2:

$$B\left((\mathbf{u}_h, p_h); (\mathbf{u}_h, -p_h)\right) = \|\nabla \mathbf{u}_h\|_0^2 - (\operatorname{div} \mathbf{u}_h, p_h) + (\operatorname{div} \mathbf{u}_h, p_h) + c(p_h, p_h).$$

That means that we have:

$$B\left((\mathbf{u}_h, p_h); (\mathbf{u}_h, -p_h)\right) = \|\nabla \mathbf{u}_h\|_0^2 + c(p_h, p_h). \tag{5.8}$$

Part 3:

The third part of the proof consists of combining the results from the first and the second part. In fact, we are going to denote by $(v_h, q_h) := (u_h - \mu w_h, -p_h)$ where $\mu > 0$ will be specified later. Due to the relations (5.7) and (5.8), we have:

$$\begin{aligned} B\left((\mathbf{u}_h, p_h); (\mathbf{v}_h, q_h)\right) &= B\left((\mathbf{u}_h, p_h); (\mathbf{u}_h, -p_h)\right) + \mu B\left((\mathbf{u}_h, p_h); (-\mathbf{w}_h, 0)\right) \\ &\geq \|\nabla \mathbf{u}_h\|_0^2 + c(p_h, p_h) + \mu\left[-C_5\|\nabla \mathbf{u}_h\|_0^2 + C_6\|p_h\|_0^2 - C_7 c(p_h, p_h)\right] \\ &= (1 - \mu C_5)\|\nabla \mathbf{u}_h\|_0^2 + \mu C_6\|p_h\|_0^2 + (1 - \mu C_7)c(p_h, p_h). \end{aligned}$$

Now if we choose $0 < \mu < \min(C_5^{-1}, C_7^{-1})$, then:

$$B\left((\mathbf{u}_h, p_h); (\mathbf{v}_h, q_h)\right) \geq C\left(\|\nabla \mathbf{u}_h\|_0^2 + \|p_h\|_0^2\right). \tag{5.9}$$

On the other hand, we have:

$$\begin{aligned} \|\nabla \mathbf{v}_h\|_0 + \|q_h\|_0 &\leq \|\nabla \mathbf{u}_h\|_0 + \mu\|\nabla \mathbf{w}_h\|_0 + \|p_h\|_0 \\ &\leq \|\nabla \mathbf{u}_h\|_0 + (1 + \mu)\|p_h\|_0 \\ &\leq T(\|\nabla \mathbf{u}_h\|_0 + \|p_h\|_0). \end{aligned}$$

If we combine therefore this last relation with inequality (5.9), then we obtain:

$$\frac{B\left((\mathbf{u}_h, p_h); (\mathbf{v}_h, q_h)\right)}{\|\nabla \mathbf{v}_h\|_0 + \|q_h\|_0} \geq C(\|\nabla \mathbf{u}_h\|_0 + \|p_h\|_0).$$

That implies certainly that:

$$\sup_{(\mathbf{v}_h, q_h) \in R_h} \frac{B\left((\mathbf{u}_h, p_h); (\mathbf{v}_h, q_h)\right)}{\|\nabla \mathbf{v}_h\|_0 + \|q_h\|_0} \geq C(\|\nabla \mathbf{u}_h\|_0 + \|p_h\|_0),$$

which is the desired result.

Remark 13 The unique solvability of the stabilized equation (5.1) can then be deduced by applying Theorem 18 and the generalized Lax Milgram's theorem that we have discussed in Lemma 13.

5.2 Theoretical Results about $Q_1 - Q_1$

We will consider here the pair $Q_1 - Q_1$. This is appreciated by some practitioners because it has similar space for the velocity and the pressure. We have in fact:

$$\begin{array}{rcl} V_h & = & \{u \in H_0^1(\Omega)^2 : u|_T \in Q_1(T) \ \forall\, T \in \mathcal{T}_h\} \\ Q_h & = & \{p \in L_0^2(\Omega) : p|_T \in Q_1(T) \ \forall\, T \in \mathcal{T}_h\}. \end{array} \tag{5.10}$$

If we use this pair in the ordinary way then we will not have stability. Two stabilization procedures are known to be good in isotropic grids. For them the following stabilization terms are respectively added to the original equation:

$$\begin{array}{rcl} c_1(p,q) & = & \displaystyle\sum_T \mathrm{meas}(T)(\mathbf{grad}\, p, \mathbf{grad}\, q)_T \\ c_2(p,q) & = & \displaystyle\sum_T \mathrm{diam}(T)^2(\mathbf{grad}\, p, \mathbf{grad}\, q)_T \ . \end{array}$$

These stabilizations are however proved to lose accuracy as the mesh has high aspect ratio. For that discussion, see [Har91]. In the next discussion, we would like to analyze a stabilization which is good even in high aspect ratio meshes. It is precisely:

$$c(p,q) = \delta \sum_{T \in \mathcal{T}_h} \left\{ h_x(T)^2 (\partial_x p, \partial_x q)_T + h_y(T)^2 (\partial_y p, \partial_y q)_T \right\},$$

where $h_x(T)$ and $h_y(T)$ are respectively the widths of the rectangular element T along the x and the y axes and δ is a prescribed positive constant in $(0, 1]$.

We will introduce the following assumption about the mesh. The sizes of the elements are supposed to vary slowly in the sense that two neighboring elements do not have a very large difference in size. More precisely, if we denote by $\mathcal{N}(T)$ the set of all neighboring elements to T, then we assume the existence of a positive number ξ with:

$$\frac{1}{\xi} h_r(L) \le h_r(T) \le \xi h_r(L) \quad \forall L \in \mathcal{N}(T),\ r = x, y \ . \tag{5.11}$$

Note however that the aspect ratio of the mesh can be as large as needed. An example of such a mesh can be found in Figure(5.1) which may still become anisotropic. In this chapter, we always assume that (5.11) is valid.

The discussion of the following theorem can be found in [Bec95a] and [BR94].

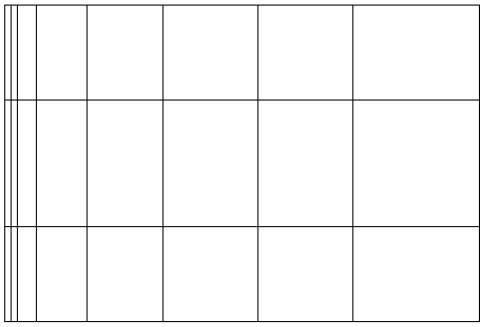

Figure 5.1: Mesh with slow change in sizes of elements.

Theorem 19 For the pair V_h, Q_h, we have the following generalized LBB condition:

$$\inf_{0\neq p_h\in Q_h}\left\{\sup_{0\neq \mathbf{v}_h\in V_h^2}\frac{(p_h,\operatorname{div}\mathbf{v}_h)^2}{\|\nabla\mathbf{v}_h\|_0^2\|p_h\|_0^2}+\frac{c(p_h,p_h)}{\|p_h\|_0^2}\right\}=\gamma_h^2\geq\gamma^2>0, \tag{5.12}$$

where γ depends neither on h nor on the aspect ratio.

Proof (Sketch only)

It will take more than ten pages to prove this theorem, so we will only give the main steps of the proof and readers who are interested in seeing the proof in full detail should read [Bec95a]:

For each given $p_h \in Q_h$, we can take its L_2-projection $\bar{p}_h$ into the space of piecewise constant space. We can prove that we have:

$$\|p_h-\bar{p}_h\|\leq\sum_{T\in\mathcal{T}_h}\left\{h_x(T)^2(\partial_x p,\partial_x q)_T+h_y(T)^2(\partial_y p,\partial_y q)_T\right\}.$$

With this piecewise constant function $\bar{p}_h$, one uses macroelement decomposition approach to prove the existence of $\mathbf{v}_h \in V_h$ with:

$$\frac{(\bar{p}_h,\operatorname{div}\mathbf{v}_h)}{\|\nabla\mathbf{v}_h\|_0\|\bar{p}_h\|_0}\geq\gamma-\frac{c_0(\bar{p}_h,\bar{p}_h)^{1/2}}{\|\bar{p}_h\|_0},$$

where

$$c_0(p,q):=\sum_{\Gamma}h_\Gamma^{\perp}\int_\Gamma[p]_\Gamma[q]_\Gamma ds,$$

in which $h_\Gamma^\perp$ stands for the mean of the widths (in the direction orthogonal to Γ) of all elements which are adjacent to the edge Γ.

After showing that:

$$c_0(\bar{p}_h, \bar{p}_h) \leq \sum_{T \in \mathcal{T}_h} \left\{ h_x(T)^2 (\partial_x p, \partial_x q)_T + h_y(T)^2 (\partial_y p, \partial_y q)_T \right\},$$

one can prove the conclusion of the theorem.

Remark 14 In matrix-vector language, the equation (5.1) takes the form:

$$\begin{pmatrix} A & \vdots & -B^T \\ \cdots & & \cdots \\ B & \vdots & C \end{pmatrix} \begin{pmatrix} \underline{u} \\ \cdots \\ \underline{p} \end{pmatrix} = \begin{pmatrix} \underline{b} \\ \cdots \\ 0 \end{pmatrix}.$$

Let us note by M the mass matrix related to the pressure basis functions that is we have: $\|p_h\|_0 = \underline{p}^T M \underline{p}$. Then, we have the following characterization of the generalized LBB condition (5.12).

Theorem 20 The generalized LBB condition (5.12) is related to the smallest eigenvalue of the following generalized eigenvalue problem:

$$(BA^{-1}B^T + C)\underline{p} = \lambda M \underline{p}. \tag{5.13}$$

Proof

In matrix-vector notation, the generalized LBB (5.12) gives:

$$\inf_{\underline{p}} \left\{ \sup_{\underline{u}} \frac{(\underline{p}^T B \underline{u})^2}{(\underline{u}^T A \underline{u})(\underline{p}^T M \underline{p})} + \frac{\underline{p}^T C \underline{p}}{\underline{p}^T M \underline{p}} \right\}.$$

If we make Cholesky factorizations $A = LL^T, \quad M = GG^T$ then it is equal to:

$$\inf_{\underline{p}} \left\{ \sup_{\underline{u}} \frac{(\underline{p}^T B \underline{u})^2}{[(L^T \underline{u})^T (L^T \underline{u})][(G^T \underline{p})^T (G^T \underline{p})]} + \frac{\underline{p}^T C \underline{p}}{(G^T \underline{p})^T (G^T \underline{p})} \right\}.$$

After putting $\underline{w} = L^T \underline{u}$ and $\underline{q} = G^T \underline{p}$, we obtain:

$$\inf_{\underline{q}} \left\{ \frac{1}{\underline{q}^T \underline{q}} \sup_{\underline{w}} \frac{(\underline{w}^T L^{-1} B^T G^{-T} \underline{q})^2}{\underline{w}^T \underline{w}} + \frac{\underline{q}^T G^{-1} C G^{-T} \underline{q}}{\underline{q}^T \underline{q}} \right\} =$$

$$\inf_{\underline{q}} \left\{ \frac{1}{\underline{q}^T \underline{q}} (L^{-1} B^T G^{-T} \underline{q})^T (L^{-1} B^T G^{-T} \underline{q}) + \frac{\underline{q}^T G^{-1} C G^{-T} \underline{q}}{\underline{q}^T \underline{q}} \right\} =$$

$$\inf_{\underline{q}} \left\{ \frac{1}{\underline{q}^T \underline{q}} \underline{q}^T G^{-1} (B A^{-1} B^T + C) G^{-T} \underline{q} \right\} = \lambda_{min} \left[G^{-1} (B A^{-1} B^T + C) G^{-T} \right]$$

.

And the eigenvalues of this last matrix are the generalized eigenvalues of (5.13) because: $\left[G^{-1} (B A^{-1} B^T + C) G^{-T} \right] \underline{q} = \lambda \underline{q}$ implies:

$$(B A^{-1} B^T + C) \underline{p} = \lambda G G^T \underline{p} = \lambda M \underline{p} \ ,$$

where $\underline{p} = G^{-T} \underline{q}$.

Theorem 21 Let $(\mathbf{u}, p)$ be the solution of the continuous problem (1.15) and let $(\mathbf{u}_h, p_h)$ be the solution of the stabilized discrete problem (5.1). If we suppose that $(\mathbf{u}, p) \in (H_0^1(\Omega) \cap H^2(\Omega))^2 \times (L_0^2(\Omega) \cap H^1(\Omega))$, then we have:

$$\|\mathbf{u} - \mathbf{u}_h\|_1 + \|p - p_h\|_0 \leq C h (\|\mathbf{u}\|_2 + \|p\|_1).$$

Proof see [Bec95b].

5.3 Numerical results

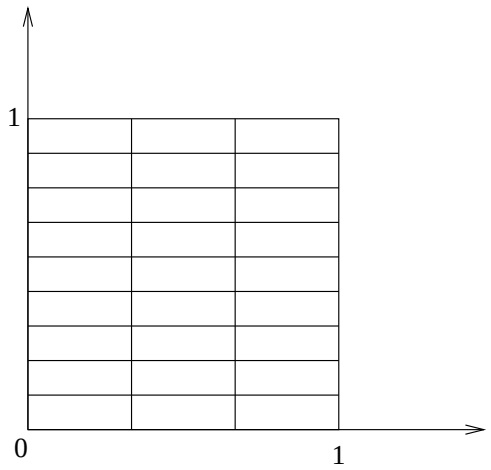

Figure 5.2: The investigated mesh for the stabilized $Q_1 - Q_1$ pair.

For the following numerical results, we take the rectangular domain $\Omega = [0,1] \times [0,1]$. The x-interval $[0,1]$ is first discretized into subintervals of number n_x and we do the same with the y-interval $[0,1]$ into n_y subintervals. The considered mesh for Ω is then the tensor product of those two discretizations. In Figure 5.2, we can find a graphical view of the mesh in which the number of x-intervals is $n_x = 3$ and that of the y-intervals is $n_y = 9$. The mesh dimensions $h_x(T) = 1/n_x$ and $h_y(T) = 1/n_y$ remain then the same for all elements T so we will only write h_x and h_y. We will call aspect ratio the quantity:

$$\text{Aspect Ratio} = \max\left\{\frac{h_y}{h_x}, \frac{h_y}{h_x}\right\}.$$

n_x	aspect ratio	(INF-SUP)^2
5	2.5	0.737652
10	5	0.433470
20	10	0.359642
50	25	0.339127
70	35	0.337216
100	50	0.336202
250	125	0.335383
500	250	0.335266
700	350	0.335247

Table 5.1: As predicted by the theory, we have an anisotropic stability for the stabilized $Q_1 - Q_1$.

5.3.1 Test 1: behavior of the inf-sup constants for various aspect ratio

In the first test, we fix the number of y-subintervals to be $n_y = 2$ and we vary the number of the x-subintervals n_x. We should note that the mesh becomes more and more anisotropic as n_x becomes larger. In these results, we have taken the value of the fixed parameter δ to be 1. The results have been tabulated in Table 5.1. As it is clearly seen, the (inf-sup)^2 constants tend to a positive limit which is approximately equal to $\lim \approx 0.335247$ as the aspect ratio becomes high. It is to be noted that between the values $n_x = 5$ until $n_x = 20$, the inf-sup constants decrease quickly, but from there on, it is already close to the limit case.

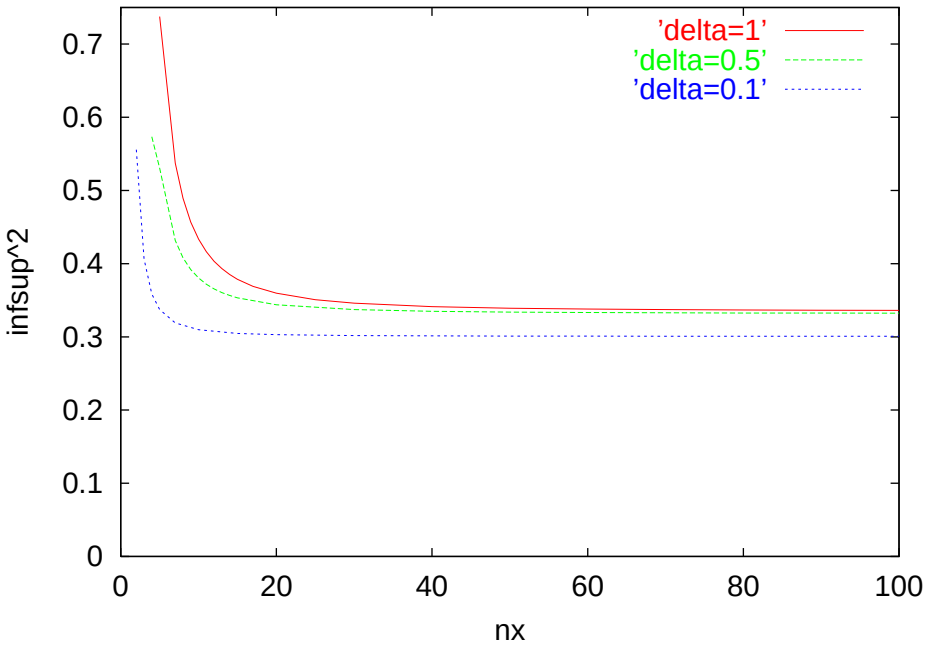

Figure 5.3: Numerical results confirms our theory. Here we see the inf-sup constants in function of n_x for different δ.

5.3.2 Test 2: Similar behavior for other values of δ

In the second test, we still take the mesh in test 1, but we investigate three different values of the parameter δ. They are $\delta = 0.1$, then $\delta = 0.5$ and finally $\delta = 1$. The outputs are gathered graphically in Figure 5.3. We can see that all of these three delta's give a stability which is good anisotropically. The limiting cases are displayed the following data:

$$\begin{array}{lll} \delta = 0.1 & \ldots\ldots\ldots & (\text{inf-sup}^2) \approx 0.300742 \\ \delta = 0.5 & \ldots\ldots\ldots & (\text{inf-sup}^2) \approx 0.331883 \\ \delta = 1.0 & \ldots\ldots\ldots & (\text{inf-sup}^2) \approx 0.335247\ . \end{array}$$

5.3.3 Test 3: investigation of the influence of the parameter δ

As we have seen in the previous numerical tests, any prescribed fixed value of $\delta \in (0, 1]$ seems to give an anisotropic stability. The purpose of the third test is to analyze which value of δ is the best choice. To that end, we consider two meshes: a mesh with a low aspect ratio and a mesh with a high one. In the document [Har91], the author took a certain exact solution and made a simulation, and then he has shown that the interval $[0.1, 1]$ is a good choice for δ. We want to investigate as well the interval domain $\delta \in [0.1, 1]$. In our numerical test, the mesh with low aspect ratio has $n_x = 5$ and $n_y = 5$ in which the aspect ratio is equal to 1 and the stabilization terms $c_1(p, q)$ and $c(p, q)$ are the same, up to a constant factor. As for the high aspect ratio mesh, we have taken: $n_x = 100$ and $n_y = 2$ where the aspect ratio is 50. The numerical results are displayed in the next tables (see Figure 5.4 and Figure 5.5).

We can affirm from those data that in both cases, the choice $\delta = 1$ is the best. The second conclusion is that the changes in inf-sup values are more accentuated in the low aspect ratio mesh than in the high aspect ratio mesh. In the high aspect ratio grid we have always $(\text{inf-sup})^2 \approx 0.3\ldots$. Even from the curves in Figure5.3, we already can draw that conclusion.

δ	inf-sup^2
0.1	0.31445926
0.2	0.40698448
0.3	0.47028211
0.4	0.52197184
0.5	0.56975413
0.6	0.61539042
0.7	0.65972945
0.8	0.70322738
0.9	0.74615009
1	0.78866258

Figure 5.4: Low aspect ratio.

δ	inf-sup^2
0.1	0.3008277
0.2	0.3212331
0.3	0.3274751
0.4	0.3305198
0.5	0.3323456
0.6	0.3335788
0.7	0.3344797
0.8	0.3351754
0.9	0.3357358
1	0.3362022

Figure 5.5: High aspect ratio.

Chapter 6

Nonconforming anisotropic pairs

6.1 The Crouzeix-Raviart/P_0 pair

The Crouzeix-Raviart element is the most famous finite element which uses a nonconforming discrete velocity space. The investigation of its behavior in anisotropic meshes has been completely detailed in [ANS00] and [ANS99] on which the following theory is based. Before giving any theorem and result, we need to define and introduce different notations.

6.1.1 The discrete spaces

Let us consider a mesh $\mathcal{T}_h$ composed of tetrahedral elements. We do not require any uniformity condition to the mesh. That means that all elements of $\mathcal{T}_h$ are allowed to have an arbitrary aspect ratio. We want to analyze in this section that the aspect ratio of the mesh does not influence at all the stability result. We will denote by $\partial\mathcal{T}_h$ the set of all faces of elements in the mesh $\mathcal{T}_h$. We approximate the velocity and the pressure in the following discrete spaces:

$$\begin{aligned} V_h &:= \left\{ \mathbf{v}_h \in L^2(\Omega)^3 : \ \mathbf{v}_h|_T \in (P_1)^3 \, \forall T \in \mathcal{T}_h, \text{ and } \int_F [\mathbf{v}_h] = 0 \ \forall F \in \partial\mathcal{T}_h \right\} , \\ Q_h &:= \left\{ q_h \in L^2_0(\Omega) : \ q_h|_T \in P_0 \quad \forall T \in \mathcal{T}_h \right\}, \end{aligned}$$

where $[\mathbf{v}_h]$ stands for the jump of $\mathbf{v}_h$ across the face F if F is an internal face. And it is equal to $\mathbf{v}_h$ itself if F is a boundary face.

Remark 15 We are effectively in disposition of nonconforming finite elements because the discrete velocity space is not a subspace of its continuous counterpart. In other words, we have:

$$V_h \not\subset H_0^1(\Omega)^3 .$$

6.1.2 Modification of the discrete variational equation

As a consequence to the nonconformity, we need also to modify the discrete variational problem into: search for $(\mathbf{u}_h, p_h) \in V_h \times Q_h$ such that

$$\left\{ \begin{array}{lll} a_h(\mathbf{v}_h, \mathbf{u}_h) + b_h(\mathbf{v}_h, p_h) & = & (\mathbf{f}, \mathbf{v}_h) \qquad \forall \mathbf{v}_h \in V_h \\ b_h(\mathbf{u}_h, q_h) & = & 0 \qquad\quad \forall q_h \in Q_h \ , \end{array} \right.$$

with:

$$a_h(\mathbf{u}, \mathbf{v}) = \sum_{T \in \mathcal{T}_h} \sum_{j=1}^{3} \int_T \mathbf{grad}\, u_j \cdot \mathbf{grad}\, v_j \quad \text{and} \quad b_h(\mathbf{v}, q) = -\sum_{T \in \mathcal{T}_h} \int_T q \,\mathrm{div}\, \mathbf{v}.$$

We are going to define as well the following mesh dependent norm which is defined elementwise:

$$\|v\|_{1,h}^2 = \sum_{T \in \mathcal{T}_h} |v|_{1,T}^2 \ .$$

6.1.3 Main result

Now, we are able to tell our main result which is summarized in the next theorem. The proof of Theorem 22 is concise and elegant, so we are repeating it here. It can be found in [ANS00].

Theorem 22 In any anisotropic grid $\mathcal{T}_h$ (see subsection 6.1.1), there exists a positive constant γ which does not depend on h and the aspect ratio of the mesh such that

$$\inf_{0 \neq q_h \in Q_h} \sup_{0 \neq \mathbf{u}_h \in V_h} \frac{b_h(\mathbf{u}_h, q_h)}{\|\mathbf{u}_h\|_{1,h} \|p_h\|_0} \geq \gamma \ ,$$

Proof

We need to introduce the Crouzeix-Raviart interpolant $I_h : H_0^1(\Omega)^3 \to V_h$ which is defined by:

$$\int_F \mathbf{u} = \int_F I_h \mathbf{u} \quad \forall\, F \text{ face of } T \quad \forall\, T \in \mathcal{T}_h. \tag{6.1}$$

Let q_h be an arbitrary element of Q_h. According to the continuous inf-sup condition, there exists (see Remark 1.4. of [GR86]) $\mathbf{v} \in H_0^1(\Omega)^3$ such that:

$$\operatorname{div} \mathbf{v} = -q_h, \quad \text{and} \quad |\mathbf{v}|_{1,\Omega} \leq C \|q_h\|_{0,\Omega} \ . \tag{6.2}$$

With the help of (6.1) and partial integrations, we deduce:

$$\begin{aligned} b_h(I_h\mathbf{v}, q_h) &= -\sum_{T\in\mathcal{T}_h} \int_T q_h \operatorname{div} I_h\mathbf{v} = -\sum_{T\in\mathcal{T}_h} q_h \int_T \operatorname{div} I_h\mathbf{v} \\ &= -\sum_{T\in\mathcal{T}_h} q_h \sum_{F\subset\partial T} \int_F I_h\mathbf{v} = -\sum_{T\in\mathcal{T}_h} q_h \sum_{F\subset\partial T} \int_F \mathbf{v} \\ &= -\sum_{T\in\mathcal{T}_h} q_h \int_T \operatorname{div} \mathbf{v} = -\sum_{T\in\mathcal{T}_h} \int_T q_h \operatorname{div} \mathbf{v} \ . \end{aligned}$$

If we combine this last relation with (6.2) then we have:

$$b_h(I_h\mathbf{v}, q_h) = \|q_h\|_{0,\Omega}^2 \ . \tag{6.3}$$

Lemma 3.1 of [ANS99] gives

$$|I_h\mathbf{v}|_{1,T} \leq C_1 |\mathbf{v}|_{1,T} \ . \tag{6.4}$$

The use of (6.3), (6.4) and (6.2) gives then:

$$b_h(I_h\mathbf{v}, q_h) \geq \gamma \|I_h\mathbf{v}\|_{1,h} \|q_h\|_{0,\Omega} \ ,$$

which implies the desired stability (The aspect ratio of the mesh is nowhere involved).

6.2 The $\tilde{Q}_1 - P_0$ pairs

In this section, we will consider mainly the variants of $\tilde{Q}_1 - P_0$. Those pairs of elements have been investigated by Rannacher and Turek in [RT92]. The FEATFLOW solver uses also these kinds of elements (see [Tur99]). There are two versions, the parametric rotated $\tilde{Q}_1 - P_0$ and the nonparametric one. We will be more interested in the nonparametric version but we need to recall the parametric version first. Some numerical results will be also provided in order to confirm the theory.

6.2.1 Brief recall about the parametric version of $\tilde{Q}_1 - P_0$

Let us discretize $\Omega \subset \mathbf{R}^2$ by the mesh $\mathcal{T}_h$ which is composed of quadrilaterals. We will denote by $\partial\mathcal{T}_h$ the set of all edges of $\mathcal{T}_h$ and by $\partial_0\mathcal{T}_h$ the set of all edges which are on the boundary of Ω. We consider the reference element $\hat{T} = [0,1]^2$. For each quadrilateral T, we introduce the one-to-one transformation $\psi_T : \hat{T} \to T$ which is given by:

$$\psi_T \begin{pmatrix} \hat{x} \\ \hat{y} \end{pmatrix} = \begin{pmatrix} \alpha_1 + \beta_1\hat{x} + \gamma_1\hat{y} + \delta_1\hat{x}\hat{y} \\ \alpha_2 + \beta_2\hat{x} + \gamma_2\hat{y} + \delta_2\hat{x}\hat{y} \end{pmatrix}. \tag{6.5}$$

We note that the transformation ψ_T becomes affine only in the case that T is a parallelogram. With the help of this transformation, we can define, for each quadrilateral T, the set:

$$\tilde{Q}_1(T) := \left\{ q \circ \psi^{-1} : \; q \in \mathrm{span}(1, \hat{x}, \hat{y}, \hat{x}^2 - \hat{y}^2) \right\}. \tag{6.6}$$

We can choose between the following two spaces for the discrete velocity space:

$$V_h^{(a)} := \Big\{ v \in L^2(\Omega) : v|_T \in \tilde{Q}_1(T) \; \forall T \in \mathcal{T}_h, \text{ and } \int_e [v] = 0 \; \forall e \in \partial\Omega \text{ and } \int_e v = 0 \; \forall e \in \partial_0\Omega \Big\}, \text{or}$$

$$V_h^{(b)} := \Big\{ v \in L^2(\Omega) : v|_T \in \tilde{Q}_1(T) \; \forall T \in \mathcal{T}_h, \text{ and } F_e(v) = 0 \; \forall e \in \partial\Omega \text{ and } v(m_e) = 0 \; \forall e \in \partial_0\Omega \Big\}.$$

In the above definition, we denoted by m_e the midpoint of the edge e and by $F_e(v)$ the jump at the midpoint m_e for two elements which are separated by e.

The first choice means that we demand that the integrals of the function over an edge of two adjacent elements are the same, whereas the second choice means that the values at the midpoints are the same.

The discrete pressure space is very simple, it is the piecewise constant space:

$$Q_h := \left\{ p \in L_0^2(\Omega) : p|_T \text{ is constant } \forall\, T \in \mathcal{T}_h \right\}.$$

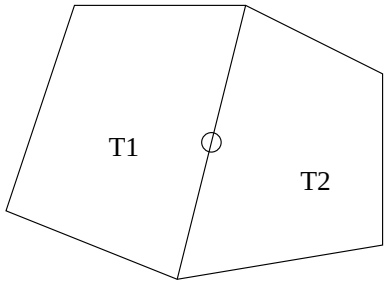

Figure 6.1: Two adjacent quadrilaterals, the common edge and its midpoint.

6.2.2 The nonparametric version

For the nonparametric version of the rotated $\tilde{Q}_1 - P_0$, we do not need to introduce the parameterization (6.5). For each quadrilateral element $T \in \mathcal{T}_h$, we introduce:

$$\tilde{Q}_1(T) := \text{span}(1, w, z, w^2 - z^2), \tag{6.7}$$

where (w, z) is the local coordinate system obtained by the direction connecting the midpoints of opposite edges of T. A graphical illustration can be seen in Figure 6.2.

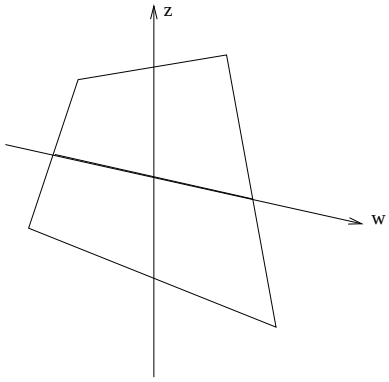

Figure 6.2: The local coordinates of T.

With the help of the nonparametric $\tilde{Q}_1(T)$ which is defined in the relation (6.7), we can define the velocity spaces in a similar fashion as in the parametric counterpart. The pressure space remains unchanged.

Our first remark is to note that we are really dealing with a nonconforming FEM in our case because the discrete velocity space is not a subspace of its continuous counterpart, i.e. we have:

$$V_h^{(i)} \not\subset H_0^1(\Omega) \qquad i = a, b.$$

Due to this fact, we need to modify our discrete variational formulation. It will be defined piecewise: we have to search for $(\mathbf{u}_h, p_h) \in V_h^2 \times Q_h$ with:

$$\left\{ \begin{array}{lll} a_h(\mathbf{v}_h, \mathbf{u}_h) & -b_h(\mathbf{v}_h, p_h) = (\mathbf{f}, \mathbf{v}_h) & \forall \mathbf{v}_h \in V_h^2 \\ b_h(\mathbf{u}_h, q_h) & = 0 & \forall q_h \in Q_h \ , \end{array} \right.$$

with:

$$a_h(\mathbf{v}, \mathbf{u}) = \sum_{T \in \mathcal{T}_h} (\nabla \mathbf{v}, \nabla \mathbf{u})_T \quad \text{and} \quad b_h(p, \mathbf{v}) = \sum_{T \in \mathcal{T}_h} (p, \operatorname{div} \mathbf{v})_T.$$

We introduce also the mesh dependent norm: $\|\mathbf{v}\|_h = a_h(\mathbf{v}, \mathbf{v})^{1/2}$.

Before we state our main result that had been discussed in [BR94], let us mention the following very simple lemma

Lemma 14 Let T be any rectangle. For the nonparametric version, a polynomial $v \in \tilde{Q}_1(T)$ is completely determined if we know the four integrals at its boundaries:

$$\int_{e_i} v, \quad i = 0, 1, 2, 3.$$

Proof

The coefficients $\alpha, \beta, \gamma, \delta$ of

$$v = \alpha + \beta x + \gamma y + \delta(x^2 + y^2)$$

will be the solution of a linear system whose 4×4 matrix will be regular.

Remark 16 In the next theorem, we will be more interested in the integral version, i.e. we take the space $V_h = V_h^{(a)}$. It should be remarked that, we do not have generally stability for the midpoint oriented version, i.e. for the space $V_h^{(b)}$. For the midpoint oriented version, we require a certain condition on the mesh in order to ensure stability. More precisely, shapes of

elements must not be very far from parallelogram. In Figure 6.3, the mesh of a rectangular domain is composed of two quadrilaterals. Both elements of the mesh may be distorted to be far from parallelogram shape if the parameter a tends to zero. We can see [RT92] for such a discussion. We report here the proof of Theorem 23 which can be seen in [BR94].

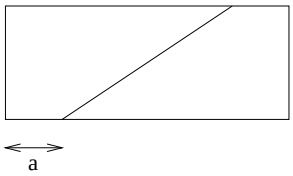

Figure 6.3: Elements which may be distorted far from parallelogram shape.

Theorem 23 (Main result) The nonparametric version of the rotated $\tilde{Q}_1 - P_0$ pair gives a stable pair on *any* rectangular tensor product mesh, i.e.: there exists a positive number γ such that

$$\inf_{0 \neq p_h \in Q_h} \sup_{0 \neq \mathbf{u}_h \in V_h^2} \frac{b_h(p_h, \mathbf{u}_h)}{\|\mathbf{u}_h\|_h \|p_h\|_0} \geq \gamma \ ,$$

where the constant γ depends neither on the mesh aspect ratio nor on the meshwidth h. It depends uniquely on the domain Ω.

Proof

Let p_h be a function in Q_h. According to the continuous inf-sup condition, we can find a function $\mathbf{v} \in H_0^1(\Omega)^2$, such that :

$$(p_h, \operatorname{div} \mathbf{v}) \geq \gamma \|p_h\|_0 |\mathbf{v}|_1 \ .$$

According to Lemma 14, we can define $\mathbf{v}_h \in V_h^2$ with the following property:

$$\int_e \mathbf{v}_h ds = \int_e \mathbf{v} ds \qquad \forall e \in \partial \mathcal{T}_h \ .$$

We have therefore by partial integration:

$$(p_h, \operatorname{div} \mathbf{v}_h)_T = (p_h, \operatorname{div} \mathbf{v})_T \quad \forall T \in \mathcal{T}_h \ .$$

Consequently, we have:

$$\begin{aligned} b_h(p_h, \mathbf{v}_h) &= \sum_{T\in\mathcal{T}_h} (p_h, \operatorname{div} \mathbf{v}_h)_T = \sum_{T\in\mathcal{T}_h} (p_h, \operatorname{div} \mathbf{v})_T \\ &= (p_h, \operatorname{div} \mathbf{v})_\Omega \geq \gamma \|p_h\|_0 |\mathbf{v}|_1 \ . \end{aligned} \tag{6.8}$$

On the other hand, we have for each $T \in \mathcal{T}_h$:

$$\begin{aligned} |\mathbf{v}_h|^2_{1,T} &= \int_T \nabla \mathbf{v}_h \nabla \mathbf{v}_h d\mathbf{x} \\ &= -\int_T \Delta \mathbf{v}_h \mathbf{v}_h d\mathbf{x} + \int_{\partial T} \mathbf{v}_h \nabla \mathbf{v}_h \cdot \mathbf{n}\, ds \\ &= -\int_T \Delta \mathbf{v}_h \mathbf{v} d\mathbf{x} + \int_{\partial T} \mathbf{v} \nabla \mathbf{v}_h \cdot \mathbf{n}\, ds \ . \end{aligned} \tag{6.9}$$

The last equality is obtained due to the facts that $\Delta \mathbf{v}_h$ vanishes on T and $\nabla \mathbf{v}_h \cdot \mathbf{n}$ is constant on horizontal and vertical edges.

Another application of the partial integration formula to the expression in (6.9) gives :

$$|\mathbf{v}_h|^2_{1,T} = \int_T \nabla \mathbf{v}_h \nabla \mathbf{v} d\mathbf{x}.$$

The application of the Cauchy Schwarz inequality with the above expression then implies:

$$|\mathbf{v}_h|^2_{1,T} \leq |\mathbf{v}|_{1,T} |\mathbf{v}_h|_{1,T}.$$

We have then the piecewise H^1-stability:

$$|\mathbf{v}_h|_{1,T} \leq |\mathbf{v}|_{1,T} \quad \forall T \in \mathcal{T}_h. \tag{6.10}$$

The combination of (6.8) and (6.10) then gives:

$$b_h(p_h, \mathbf{v}_h) \geq \gamma \|p_h\|_0 \|\mathbf{v}_h\|_h \ .$$

Remark 17 This theorem seems to still hold for general non-rectangular meshes. The proof becomes however more intricate because $\nabla \mathbf{v}_h \cdot \mathbf{n}$ is not any more necessarily constant on edges which are neither horizontal nor vertical.

Remark 18 This pair of elements seems to be very good in terms of stability. It should be remarked that it is used in the FEATFLOW flow solver. For further information about it, we can see [Tur99]. One problem of this pair is the absence of a posteriori error estimator (for the time being).

Remark 19 For a rectangular element T, instead of using the space in (6.7), it is possible to introduce the space:

$$G(T) = \text{span}(1, x_S, x_L, x_L^2)\,,$$

where x_S and x_L are the variables corresponding to the short and the long edges of T respectively. In the case of Figure 6.4, the variable x_S is y and x_L is x.

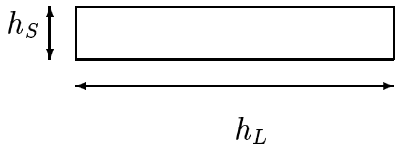

Figure 6.4: $x_S = y$ and $x_L = x$.

In the document [ANS99], it is shown that this kind of space has also a very nice property in anisotropic meshes.

6.3 Numerical Results

For the numerical test, we examine again the corner mesh that we have already taken into consideration in the $Q_2 - Q_0$ pair in which we did not have stability (see Figure 6.5).

We would like to analyze the stability in this mesh for the pair $V_h^{(a)} - Q_h$. We vary the value of the parameter a and observe the behavior of the inf-sup constant. It is clear that the more a approaches the value zero, the more anisotropic the mesh becomes.

Let us take a look at Table 6.1. We take into consideration the values of a which are in $(0, 0.5]$. It can be very well seen that the inf-sup constants are all greater than the minimum value $\min \approx 0.8451542$. This minimum value is obtained at the point $a = 0.5$. The inf-sup becomes greater and greater as the value of a tends to 0. This numerical result really confirms our theoretical results which affirms that the inf-sup constants are bounded away from zero independently of the aspect ratio. The complete result can be found in Figure 6.6. It is shown that the inf-sup tends in limit to 1.0 as the aspect ratio tends to infinity.

In the graphical version (see Figure 6.6) of the previous numerical results, it is perfectly seen that the minimum value is gotten at the point $a = 0.5$ where

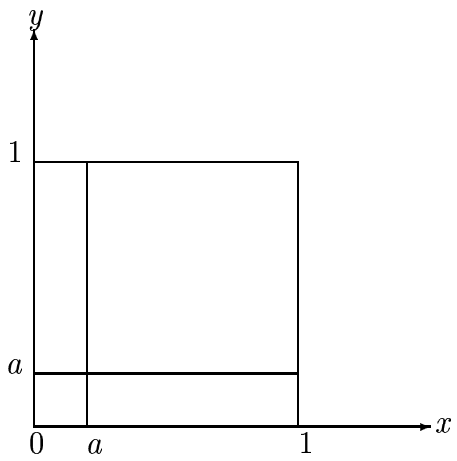

Figure 6.5: The examined domain and its grid.

a	aspect ratio	INF-SUP
0.50	1.0000000	0.8451542
0.45	1.2222222	0.8464723
0.40	1.5000000	0.8504910
0.35	1.8571429	0.8573804
0.30	2.3333333	0.8673588
0.25	3.0000000	0.8806305
0.20	4.0000000	0.8973415
0.15	5.6666666	0.9175699
0.10	9.0000000	0.9413527
0.01	99.000000	0.9934209
0.00001	99999.000	0.9999933

Table 6.1: As predicted by the theory, we have an inf-sup constant which is bounded away from zero for $V_h^{(a)}$.

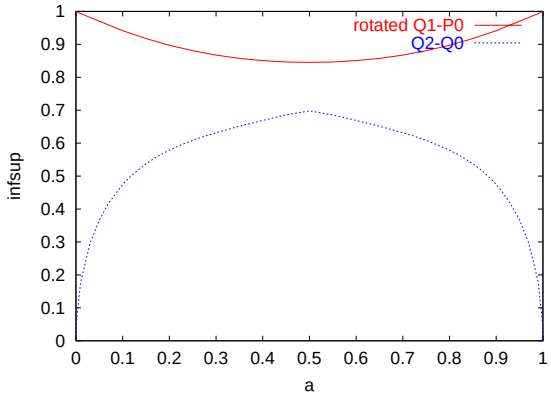

Figure 6.6: This graphs compares the $Q_2 - Q0$ pair with the rotated $\tilde{Q}_1 - P_0$ on the corner mesh. As predicted from the theory, the $\tilde{Q}_1 - P_0$ is stable

we have four elements of the same size. The symmetry of the graph is also predictable because of the symmetry of the mesh for $a = \sigma$ and $a = 1 - \sigma$. In the same figure (Figure 6.6), we compare the pair $Q_2 - Q_0$ and the rotated $\tilde{Q}_1 - P_0$ in the corner mesh, it is very well seen that the latter pair resists high aspect ratio mesh as it is stated by the previous theory.

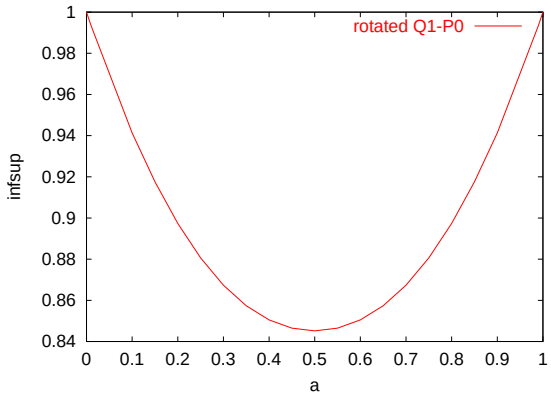

Figure 6.7: The midpoint version V_h^b gives also stability in this corner mesh.

All those numerical results were obtained for the integral version, i.e. $V_h^{(a)}$. Now we would like to say a few words for the "midpoint" version $V_h^{(b)}$. Although, in the general case, it gives instability, we have stability for this particular corner mesh. We have in fact a similar result as for its "integral" counterpart as Figure 6.7 demonstrates.

Chapter 7

Further results

7.1 The MINI element

7.1.1 Brief facts from the isotropic case

In this section, we will recall the proof(sketch, the detail can be seen in the book [Bra97]) for the isotropic case, in which the uniformity of the mesh is used (boundedness of the aspect ratio). Afterward it will be shown with the help of some numerical test that the dependence of the inf-sup constant on the aspect ratio of the element is in general unavoidable. First of all we need to define precisely the discrete pair of spaces. But before doing that, let us recall the definition of barycentric coordinates.

Definition 6 Let us consider any triangle T with vertices $\mathbf{a_1}$, $\mathbf{a_2}$, $\mathbf{a_3}$. The barycentric coordinates of a point $\mathbf{x} \in \mathbf{R}^2$ are $\lambda_1 = \lambda_1(\mathbf{x})$, $\lambda_2 = \lambda_2(\mathbf{x})$, $\lambda_3 = \lambda_3(\mathbf{x})$ which are defined by:

$$\begin{array}{ll} \lambda_i \in \mathcal{P}_1 & i = 1, 2, 3 \text{ and} \\ \lambda_i(\mathbf{a_j}) = \delta_{ij} & i, j = 1, 2, 3. \end{array}$$

Two important properties of the barycentric coordinates are:

$$\begin{array}{l} \lambda_1 + \lambda_2 + \lambda_3 = 1 \ , \\ T = \{\mathbf{x} \in \mathbf{R}^2 : \ 0 \leq \lambda_i(\mathbf{x}) \leq 1, \ i = 1, 2, 3\} \ . \end{array}$$

Now, we can define the discrete spaces. The velocity discrete space is:

$$\begin{aligned} V_h &:= [\mathcal{M}^1 \oplus B_3]^2 \ , \qquad \text{where} \\ \mathcal{M}^1 &= \{v \in H_0^1(\Omega) : v|_T \in \mathcal{P}_1 \text{ for all} T \in \mathcal{T}_h\} \\ B_3 &= \{v \in C^0(\bar{\Omega}) : v|_T \in \text{span}\{\lambda_1\lambda_2\lambda_3\} \quad \forall T \in \mathcal{T}_h\}. \end{aligned}$$

And for the pressure we have the following space:

$$Q_h := \{p \in L_0^2(\Omega) : p|_T \in \mathcal{P}_1 \quad \forall T \in \mathcal{T}_h\} \ .$$

Theorem 24 Suppose that the mesh $\mathcal{T}_h$ is uniformly regular with parameter κ, i.e.

$$h \leq \kappa\rho(K) \quad \forall K \in \mathcal{T}_h.$$

Then the MINI element satisfies the inf-sup condition. That is: There exists a constant $\beta = \beta(\Omega, \kappa) > 0$

$$\inf_{0 \neq p \in Q_h} \sup_{0 \neq \mathbf{v} \in V_h} \frac{(\text{div}\, \mathbf{v}, p)}{|\mathbf{v}|_{1,\Omega} \|p\|_{0,\Omega}} \geq \beta > 0 \ .$$

Proof (Sketch)

Consider the following bilinear form which is defined on $H_0^1(\Omega) \times H_0^1(\Omega)$:

$$a(u, v) := (\nabla u, \nabla v)_{0,\Omega} + (u, v)_{0,\Omega} \ .$$

First we would like to define a projection

$$\Pi_1 : H_0^1(\Omega) \longrightarrow \mathcal{M}^1.$$

For a given $u \in H_0^1(\Omega)$, $a(u, \cdot)$ gives a continuous linear functional on $\mathcal{M}^1$. Therefore, Lax Milgram's theorem ensures the existence of a unique $\Pi_1(u)$ which satisfies:

$$a(\Pi_1(u), v) = a(u, v) \quad \forall v \in \mathcal{M}^1 \ .$$

We have therefore:

$$\|\Pi_1(u)\|_1^2 = a(\Pi_1(u), \Pi_1(u)) \leq a(u, u) = \|u\|_1^2 \ . \tag{7.1}$$

And the usual error estimation gives:

$$\|\Pi_1(u) - u\|_0 \leq C_2 h \|u\|_1 \ . \tag{7.2}$$

Now we define a second mapping $\Pi_2 : L_2(\Omega) \longrightarrow B_3$ with:

$$\int_T (\Pi_2 v - v) dx = 0 \quad \forall T \in \mathcal{T}_h \ .$$

We have therefore:

$$\|\Pi_2(u)\|_0 \leq C_3 \|u\|_0 \ . \tag{7.3}$$

We are now able to define the following projection:

$$\Pi_h v := \Pi_1 v + \Pi_2(v - \Pi_1 v) \ .$$

Applying the formula of Green and taking into account the fact that the gradient of pressure is piecewise constant, we can obtain:

$$(\mathrm{div}\,(v - \Pi_h v), q_h)_{0,\Omega} = 0 \quad \forall q_h \in Q_h \ .$$

We are now willing to estimate the projection Π_h in which we will use the inverse inequality. It ought to be remarked that the inverse inequality considerably depends on the fact that the mesh presents some uniformity. We have in fact:

$$\begin{aligned}
\|\Pi_h v\|_1 &\leq \|\Pi_1 v\|_1 + \|\Pi_2(v - \Pi_1 v)\|_1 \\
&\leq \|\Pi_1 v\|_1 + C_4(\kappa) h^{-1} \|\Pi_2(v - \Pi_1 v)\|_0 \quad \text{(inverse inequality)} \\
&\leq \|v\|_1 + C_4(\kappa) h^{-1} C_3 \|v - \Pi_1 v\|_0 \quad \text{(because of (7.1) and (7.3))} \\
&\leq \|v\|_1 + C_4(\kappa) C_3 C_2 \|v\|_1 \ . \qquad \text{(because of (7.2))}
\end{aligned}$$

And applying the Fortin's lemma (see Lemma 3) gives the desired result. We can see clearly that the inf-sup constant depends on the uniformity parameter.

7.1.2 Anisotropic instability

Now we will show that in the general case the dependence of the inf-sup on the uniformity parameter cannot be avoided in the case of the MINI element. That fact is extremely important in the analysis of anisotropic mesh. Let us take the domain Ω to be the unit square $\Omega = (-1, 1)^2$.

In the triangulation of Ω, we have chosen the method as illustrated in Figure 7.1. Let us denote by $N + 1$ the number of nodes which are located in the positive y-axis. That means, $N + 1$ is the number of nodes in the y-segment $(0, 1)$. For instance, in Figure 7.1, the values of N are 2 and 5.

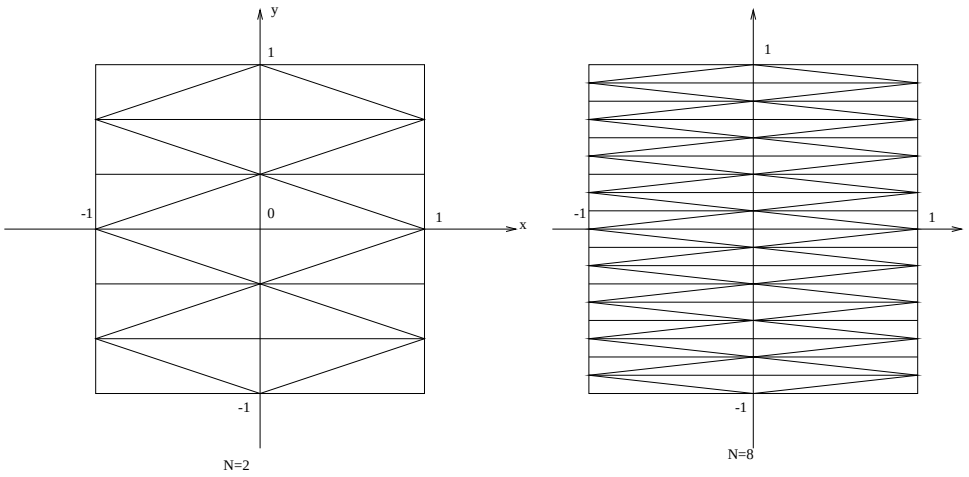

Figure 7.1: Mesh for N=2 and N=5.

It can be seen that the domain Ω does not depend on N, but as N grows the mesh becomes more and more anisotropic since the length of elements along the x axis is always equal to 1, whereas the one along the y axis is $\frac{1}{N+1}$. We have effectively:

$$\Omega = \Omega_h \text{ for every mesh width } h \ .$$

Our goal is to analyze the inf-sup constants of this mesh in function of N.

The analysis deals with varying the value of N and investigating the behavior of the inf-sup for each N. After doing some tests, it can be remarked that the inf-sup of the mesh tends to zero as N grows. A graphical illustration of that can be found in the next scheme (Figure 7.2).

In the graphical illustration of these data, please note that the y-axis has a logarithmic scaling; the curve declines much more quickly in reality.

7.2 Taylor Hood Element

This is one of the most famous elements which are used in the Stokes problem. A convergence result about it was already detailed by Bercovier and Pironneau in [BP79]. In 1984, Verfürth has given the stability proof of this pair of elements in [Ver84]. In this section we want to analyze the stability of this pair in the anisotropic case. First, it is better to recall the definition of this pair precisely:

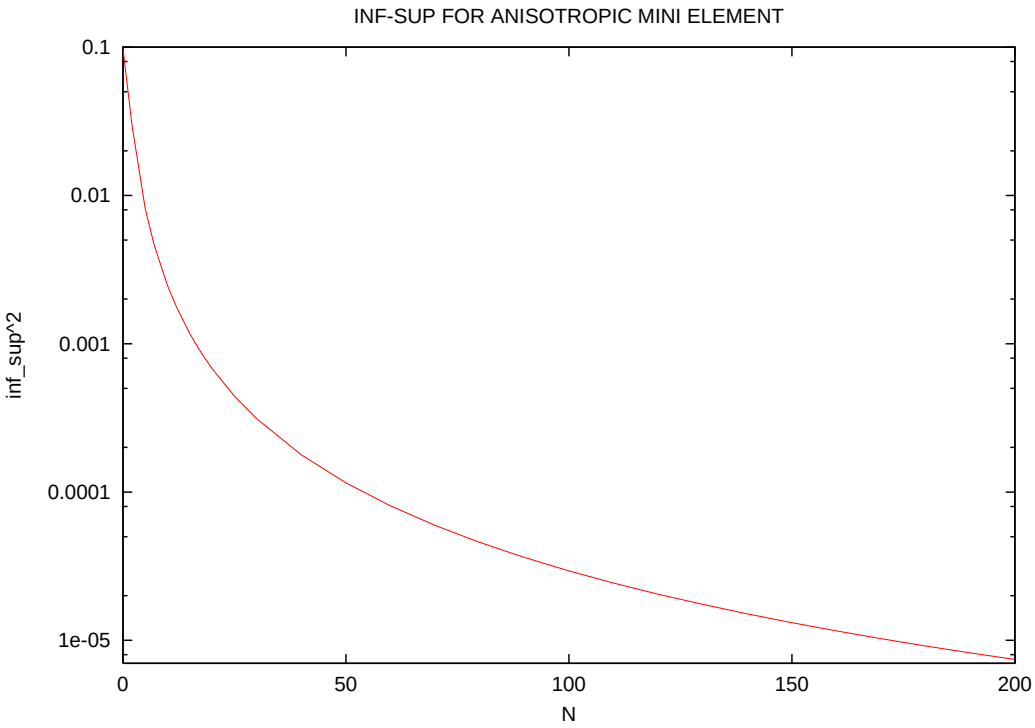

Figure 7.2: Squared of the Inf-Sup constants.

$$\begin{aligned} V_h &= \{v \in H_0^1(\Omega) : v|_T \in \mathcal{P}_2(T) \quad \forall T \in \mathcal{T}_h\} \\ Q_h &= \{v \in L_0^2(\Omega) : v|_T \in \mathcal{P}_1(T) \quad \forall T \in \mathcal{T}_h\} \ . \end{aligned}$$

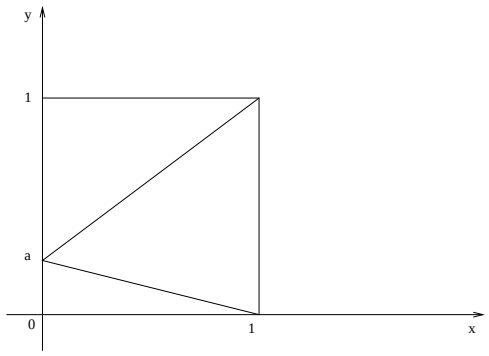

Figure 7.3: Grid 1.

Test 1:

A simple grid composed of three elements like in Figure 7.3 was implemented. The parameter a can vary and the behavior of the inf-sup constants in function of a was investigated. In the following table (Table 7.1), one can find the results. The aspect ratio of the mesh is tending to infinity as the value of the parameter a approaches zero. It is seen that the Taylor Hood element does not have anisotropic stability in general because the inf-sup quantity tends to zero with the value of a. We will see however in the next discussion that under some hypothesis on the mesh, we can have stability even on high aspect ratio meshes.

Test 2:

A further numerical test was done with the mesh in Figure 7.5 in which we have first a mesh composed of rectangle then each rectangle is divided into two triangles. This mesh was already used to test the MINI element. The curve in Figure 7.6 indicates that we have stability independently of the aspect ratio. We can deduce that in some sense the Taylor Hood element behaves better than the MINI element.

Test 3:

An idea which might come suddenly is that if we have any rectangular tensor product mesh, and then if each rectangle is halved in order to have two triangles, then we can expect anisotropic stability. But that idea does not

values of a	aspect ratio	(INF-SUP)^2
0.1	10	0.02665448567
0.01	100	0.00360538266
0.001	1000	0.00037350553
0.0001	10^4	0.00003748500
0.00001	10^5	0.00000374985
0.000001	10^6	0.00000037499
0.0000001	10^7	0.00000003749
0.00000001	10^8	0.00000000375

Table 7.1: Numerical results of Taylor Hood wit Grid 1.

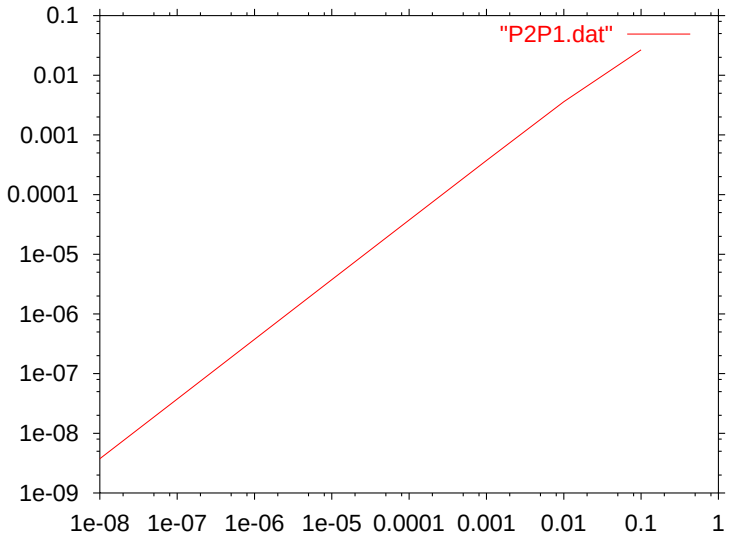

Figure 7.4: Graphical Version for the result from Grid 1.

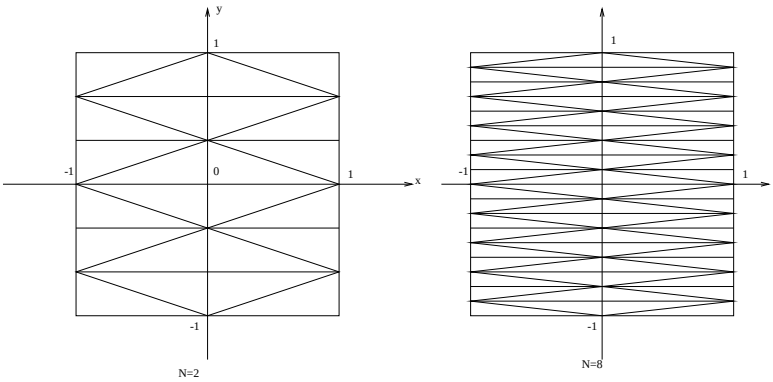

Figure 7.5: Grid 2.

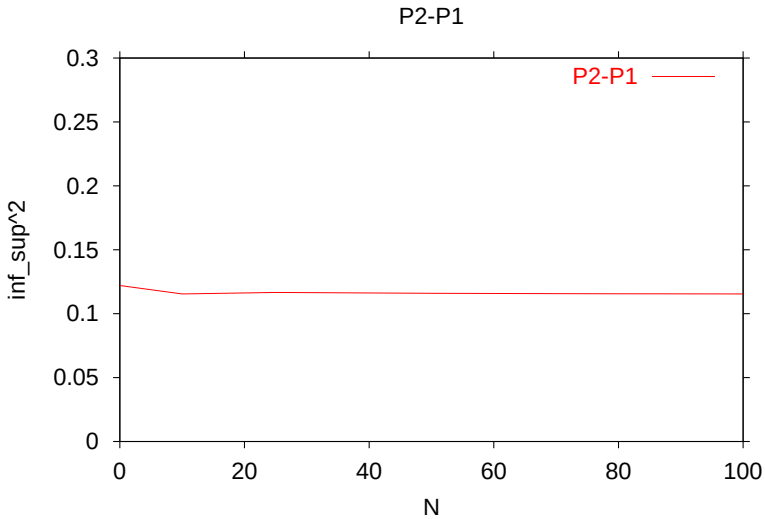

Figure 7.6: Numerical result for Grid 2 using Taylor Hood pair.

generally lead to an anisotropic stability as the simple mesh in Figure 7.7 shows. For the grid number 3, we have first a rectangular tensor product mesh composed of four rectangles, then each of the four is divided into two similar triangles to have the final grid 3. The mesh parameter s controls our aspect ratio. We investigate this mesh for the Taylor Hood element in which the parameter s ranges in the interval $(0, 0.5]$. We are again in the case where the mesh aspect ratio tends to infinity when the parameter s tends to zero. The outcomes have been plotted in Figure 7.8. The dependence of the inf-sup on the aspect ratio is in fact unavoidable in this case.

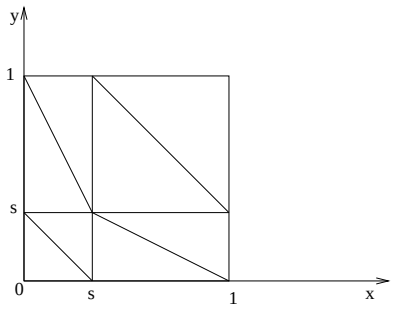

Figure 7.7: Grid 3.

No theoretical proof about the anisotropic stability of the Taylor Hood pair is known yet (as far as I know). Yet, many steps of the proof in ([BP79]) can still be kept for meshes like grid 2 (see Figure 7.5). The real hardship is the absence of something like *global* inverse inequality in the anisotropic case. It is to be remarked anyway that there is a proof of the Taylor Hood stability in the isotropic case which uses only *local* inverse inequalities. That means an inverse inequality which only considered piecewise. The problem in the generalization of that proof is the fact that the uniformity of the mesh is used repeatedly. And that fact does not seem to be avoidable. We can conclude that the Taylor Hood pair is a pair which is almost anisotropically stable because in some meshes it demonstrates itself to be stable independently of the aspect ratio. In the next section we will consider some way to make this stable even in a mesh like grid 1 and grid 3.

7.3 The $\mathcal{P}_2^+ - \mathcal{P}_1$ pair

An usual way to stabilize an almost stable pair is to integrate a bubble function to the discrete velocity space. That way, the velocity space has more

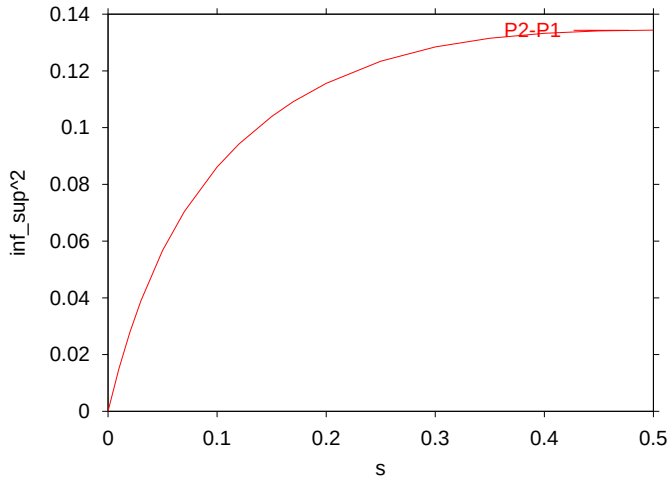

Figure 7.8: Numerical results for Grid 3 using Taylor Hood pair.

dimension and it makes the inf-sup constant behave better. In this section, the velocity will be approximated with the help of quadratic polynomials enriched with bubbles and the pressure is approximated with piecewise linear polynomials. The $\mathcal{P}_2^+ - \mathcal{P}_1$ is an improvement of the Taylor Hood pair. We will see in this section that all the meshes, in which the Taylor Hood pair was anisotropically unstable, will still give stability for this improved pair. Now, we are going to define in a precise way the discrete spaces. The discrete space for the velocity is:

$$\begin{aligned} V_h &:= [\mathcal{M}^2 \oplus B_3]^2 \qquad \text{in which} \\ \mathcal{M}^2 &= \{v \in H_0^1(\Omega) : v|_T \in \mathcal{P}_2 \,\text{for all}\, T \in \mathcal{T}_h\} \\ B_3 &= \{v \in C^0(\bar{\Omega}) : v|_T \in \text{span}\{\lambda_1\lambda_2\lambda_3\} \quad \forall T \in \mathcal{T}_h\}, \end{aligned}$$

where λ_1, λ_2, and λ_3 are the barycentric coordinates.

And for the pressure we have the following discrete space:

$$Q_h := \{p \in L_0^2(\Omega) : p|_T \in \mathcal{P}_1 \quad \forall T \in \mathcal{T}_h\} .$$

The grid 2 has not any more been implemented because it was stable for the Taylor Hood equation, so logically, it must still be stable for the $\mathcal{P}_2^+ - \mathcal{P}_1$ pair. We will be more interested in the grid 1 and grid 3.

Test 1:

For the grid 1, we have again investigated the interval $a \in (0, 0.5]$. We clearly see in Table 7.2 that in this interval, the inf-sup is bounded away from zero by

values of a	aspect ratio	INF-SUP
0.50	2.000000	0.56413486
0.40	2.500000	0.55957379
0.30	3.333333	0.55350091
0.25	4.000000	0.55234160
0.20	5.000000	0.55339623
0.14	7.142857	0.55888988
0.10	10.00000	0.56631249
0.01	100.0000	0.61072136
0.001	1000.000	0.62629093
0.0001	10000.00	0.63062465
0.00001	100000.0	0.63189003
0.000001	10000000	0.63227810

Table 7.2: Numerical results of $\mathcal{P}_2^+ - \mathcal{P}_1$ with Grid 1.

some minimum value which is approximately min ≈ 0.55234160. This value is obtained for the value of a equal to 0.25. The inf-sup declines first in the domain from $a = 0.000$ to 0.25, then it increases permanently in the domain 0.25 to 0.5. When the mesh is very anisotropic, that is a tends to zero or 1, then the inf-sup is tending to some positive limit which is approximately equal to lim ≈ 0.63227810. In Table 7.2, we have only given the value for $a \in (0, 0.5]$. In the interval $a \in [0.5, 1)$, we have symmetrical results. The plot of the whole numerical result can be seen in the next curve (Figure 7.9) where a ranges in the whole interval $(0, 1)$. As a conclusion, we can say that we have still anisotropic stability in for the pair $\mathcal{P}_2^+ - \mathcal{P}_1$ from the grid 1.

Test 2:

We have also implemented the grid number 3 for this pair $\mathcal{P}_2^+ - \mathcal{P}_1$. And the result is positive. That means, we have stability independent of the aspect ratio. The numerical result can be clearly seen in the next figure(Figure 7.10). Remark that the curve has a symmetry about the line $s = 0.5$. That fact is clearly already expected. The minimum value is obtained at about $s \approx 0.24$ and at $s \approx 0.76$ where the value is about (inf-sup)$^2 \approx 0.26968961$. That shows that adding bubble really makes the Taylor Hood element stable (At least in this mesh). When the mesh is very anisotropic (that is the value of s approaches 0 or 1), then the (inf-sup)^2 tends to a finite limit which is approximately equal to lim ≈ 0.27610469 whereas it tends to zero for the Taylor Hood pair. This approach of stabilization using bubble was already used frequently in isotropic cases (see for example [GR86] and [BF91]), and

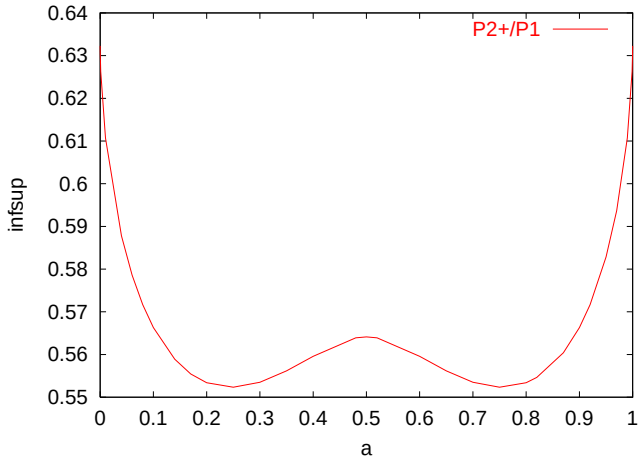

Figure 7.9: Numerical results for Grid 1 using $\mathcal{P}_2^+ - \mathcal{P}_1$.

here it seems also that it is still a good method.

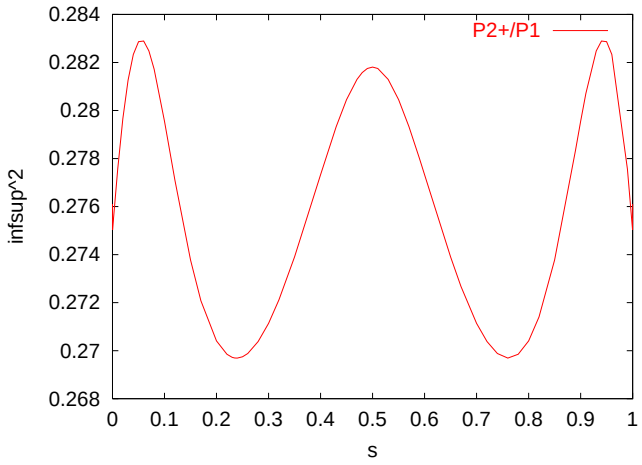

Figure 7.10: Numerical results for Grid 3 using $\mathcal{P}_2^+ - \mathcal{P}_1$.

Last word about $\mathcal{P}_2^+ - \mathcal{P}_1$:

Those numerical tests shows perfectly well that the incorporation of bubble functions to the velocity space really improves stability. We can say that the $\mathcal{P}_2^+ - \mathcal{P}_1$ is anisotropically a good pair (At least for grid 1, grid 2 and grid 3). Those computational results are very promising in the sense that this pair will probably be stable on all meshes. Anyway we cannot affirm that this

pair is generally anisotropically stable unless some theoretical proof is found. But so far, such a proof remains unknown.

Chapter 8

Summary and open problems

The Stokes problem is a good application of the general abstract saddle point problem. The efficiency of an element pair can be quantified by the LBB-condition:

$$\inf_{0\neq p_h\in Q_h}\sup_{0\neq \mathbf{u}_h\in V_h}\frac{(\operatorname{div}\mathbf{u}_h,p_h)}{|u_h|_{1,\Omega}\|p_h\|_{0,\Omega}}\geq\gamma. \tag{8.1}$$

The desired property of an element pair is the the fact that the inf-sup constant has a positive lower bound. For anisotropic meshes, we want that the inf-sup constants do not tend to zero when the aspect ratios become large.

The macroelement techniques deal with grouping some neighboring elements. These techniques demonstrate themselves to be very useful in the theoretical proofs of LBB conditions. And they have been applied to the pairs Q_2-Q_0 and $Q_{k+1,k}-P_{k-1}$. We have seen in particular that those pairs have reference stability in any stripped mesh. Counterexamples demonstrated however the corner problem to which some remedies have been given, namely the use of geometric tensor product meshes and adjusting the corner domain size in accordance to the mesh aspect ratio.

A stabilization procedure has been used to adapt the Q_1-Q_1 pair in anisotropic meshes. Numerical as well as analytical results have shown that adding the correction term

$$c(p,q)=\delta\sum_{T\in\mathcal{T}_h}\left\{h_x(T)^2(\partial_x p,\partial_x q)_T+h_y(T)^2(\partial_y p,\partial_y q)_T\right\}$$

really makes this pair good on high aspect ratio discretizations.

All the meshes that were discussed here require some little conditions on the mesh in order to be stable in anisotropic meshes except the Crouzeix-Raviart/P_0 pair and the nonparametric rotated $\tilde{Q}_1 - P_0$ pair. They provide nonconforming finite elements. The former is stable in any mesh composed of tetrahedral elements and the latter in any rectangular mesh.

We cannot generally expect stability from the MINI element in anisotropic grids, as a numerical counterexample has shown. The Taylor-Hood element behaves better than the MINI element. Still, it demonstrates itself to lose stability in some stretched grids. The use of bubble functions can improve the stability of a pair. The numerical evidence from the examination of the $P_2^+ - P_1$ pair shows that fact more clearly.

Open problems:

The future works that we still intend to perform are multiple. First, we would like to analyze the three dimensional extensions of the results which were investigated in 2D in this document. Furthermore, we propose to keep on finding (numerically or not) pairs which are stable in anisotropic meshes. Besides, we will strive for searching some theoretical proofs to numerically good pairs like $P_2^+ - P_1$ which has been investigated in this material. Some of the pairs that we have seen here are perfect in terms of stability, but they suffer from the absence of a-posteriori error estimators; for example the rotated $\tilde{Q}_1 - Q_0$ pair. We want therefore to investigate that problem more deeply.

Bibliography

[AC00] M. Ainsworth and P. Coggins. The stability of mixed *hp*-Finite Element Methods for Stokes flow on high aspect ratio elements. *SIAM J. Numer. Anal.*, 38:1721–1761, 2000.

[ANS99] T. Apel, S. Nicaise, and J. Schöberl. Crouzeix-Raviart type finite elements on anisotropic meshes. Preprint 99-10, SFB 393, TU Chemnitz, 1999.

[ANS00] T. Apel, S. Nicaise, and J. Schöberl. A non-conforming finite element method with anisotropic mesh grading for the Stokes problem in domains with edges. Preprint 00-11, SFB 393, TU Chemnitz, 2000.

[Ape99] T. Apel. Anisotropic finite elements: Local estimates and applications. Preprint 99-03, SFB 393, TU Chemnitz, 1999.

[Bec95a] R. Becker. An adaptive finite element method for the incompressible Navier-Stokes equations on time-dependent domains. *Ph.D. Thesis, University of Heidelberg*, 1995.

[Bec95b] R. Becker. An adaptive finite element method for the Stokes equations including control of the iteration error. *ENUMATH*, 1995.

[BF91] F. Brezzi and M. Fortin. *Mixed and Hybrid Finite Element Methods.* Springer, New York, 1991.

[BIC00] K. J. Bathe, A. Iosilevich, and D. Chapelle. An inf-sup test for shell finite elements. *Computers & Structures*, 75:439–456, 2000.

[BP79] M. Bercovier and O. Pironneau. Error estimates for finite element method solution of the Stokes problem in the primitive variables. *Numer. Math.*, 33:211–224, 1979.

[BR94] R. Becker and R. Rannacher. Finite Element Solution of the Incompressible Navier-Stokes Equations on Anisotropically Refined Meshes. Preprint 94-31, University of Heidelberg, 1994.

[Bra97] D. Braess. *Finite Elemente*. Springer, Berlin, 1997.

[CB93] D. Chapelle and K. J. Bathe. The Inf-Sup test. *Computers & Structures*, 47:537–545, 1993.

[GR86] V. Girault and P.-A. Raviart. *Finite Element Methods for Navier-Stokes Equations*. Springer, Paris, 1986.

[Gri85] P. Grisvard. *Elliptic Problems in Nonsmooth Domains*. Pitman Advanced Publishing Program, Massachusetts, 1985.

[Har91] J. Harig. Eine robuste und effiziente Finite Elemente Methode zur Lösung der inkompressiblen 3D Navier-Stokes Gleichungen auf Vektorrechnern. Preprint 91-18, Heidelberg University, 1991.

[Kun97] G. Kunert. Error estimation for anisotropic tetrahedral and triangular finite element meshes. Preprint 97-16, SFB 393, TU Chemnitz, 1997.

[Mal81] D. S. Malkus. Eigenproblems associated with the discrete LBB-condition for incompressible finite elements. *Internat. J. Eng. Sci.*, 19:1299–1310, 1981.

[Mav97] D. J. Mavriplis. Directional Coarsening and Smoothing for anisotropic Navier-Stokes problem. *Electron. Trans. Numer. Anal.*, 6:182–197, 1997.

[NW99] F. Nocedal and S. Wright. *Numerical Optimization*. Springer, Berlin, 1999.

[RT92] R. Rannacher and S. Turek. Simple nonconforming quadrilateral Stokes element. *Num. Meth. Part. Diff. Eqns.*, 8:97–111, 1992.

[SS97] D. Schötzau and C. Schwab. Mixed *hp*-fem on anisotropic meshes. Report 97-2, Seminar für Angewandte Mathematik, ETH Zürich, 1997.

[SSS97] D. Schötzau, C. Schwab, and R. Stenberg. Mixed *hp*-fem on anisotropic meshes II: Hanging nodes and tensor products bounds of boundary layer meshes. Report 97-14, Seminar für Angewandte Mathematik, ETH Zürich, 1997.

[Ste84] R. Stenberg. Analysis of mixed finite element methods for the Stokes problem: a unified approach. *Math. Comp.*, 42:9–23, 1984.

[Ste90] R. Stenberg. Error analysis of some finite element methods for the Stokes problem. *Math. Comp.*, 54:495–508, 1990.

[Tur99] S. Turek. *Efficient Solvers for Incompressible Flow Problems.* Springer Verlag, Berlin, 1999.

[Ver84] R. Verfürth. Error estimates for a mixed finite element approximation of the Stokes equations. *R.A.I.R.O.*, 18:175–182, 1984. no 2.

[WG89] Z. X. Wang and D. R. Guo. *Special functions.* World Scientific Publishing, 1989.

[Zdr97] M. M. Zdravkovich. *Flow around circular cylinders.* Oxford University Press, Oxford, 1997.

THESES

1. Macroelement techniques are precious analytical tools for the investigations of LBB conditions especially in anisotropic meshes. They allow in particular the reduction of the initial problem into smaller problems which are easier to analyze.

2. The $Q_2 - Q_0$ and the $Q_{k+1,k} - P_{k-1}$ pairs possess reference stability in any stripped mesh independently of the aspect ratio. A numerical test shows that a certain corner macroelement leads however to instability. The remedies to the corner instability are the use of geometric tensor product meshes or p-version on a special varying corner domain.

3. Stabilization techniques consist of altering the discrete variational equation with the help of some correction terms in order that some initially unstable pair gets appropriate for the corrected equation. Thanks to this method, the $Q_1 - Q_1$ pair can behave satisfactorily in anisotropic meshes as analytical and numerical investigations show.

4. The nonconforming Crouzeix-Raviart/P_0 pair is unconditionally stable in any mesh composed of tetrahedral elements. The same hold for the integral version of the nonparametric $\tilde{Q}_1 - P_0$ pair in any rectangular mesh. Numerical experiences confirm that fact.

5. The MINI element is good in isotropic meshes but a counterexample demonstrates that it is not generally stable in anisotropic discretizations. The Taylor-Hood element presents stability in some anisotropic meshes. Yet, it becomes unstable in other ones. The $P_2^+ - P_1$ pair which is the Taylor-Hood pair enriched with bubbles, is numerically satisfactory in terms of stability.